ENTROPY GENERATION AND THERMAL PERFORMANCE OF A PULSATING HEAT PIPE

A Thesis

presented to

the Faculty of the Graduate School

at the University of Missouri-Columbia

In Partial Fulfillment

of the Requirements for the Degree

Master of Science

---

by

SEJUNG KIM

Dr. Yuwen Zhang, Thesis Supervisor

DECEMBER 2012

The undersigned, appointed by the dean of the Graduate School, have examined the [thesis or dissertation] entitled

ENTROPY GENERATION AND THERMAL PERFORMANCE

OF A PULSATING HEAT PIPE

presented by Sejung Kim,

a candidate for the degree of master of science,

and hereby certify that, in their opinion, it is worthy of acceptance.

Professor Yuwen Zhang

Professor Chung-Lung Chen

Professor Stephen Montgomery-Smith

ACKNOWLEDGEMENTS

I would like to express the deepest appreciation to my advisor, Dr. Zhang for his continued support and teaching throughout the project. Without his guidance and persistent help this thesis would not have been possible. I would also like to appreciate the members of my thesis committee, Dr. Chen and Dr. Montgomery-Smith for taking time to provide helpful suggestions and comments.

I would also like to thank all my colleagues, Hamid R. Seyf, Nazia Afrin, Yijin Mao, Yunpeng Ren , Pengfei Ji, and Daofei Li. It is thankful for everything and really good time to work with them.

I would like to express my gratitude to my parents, Young-seung Kim and Hyo-Sook Ahn, who support and give me the strength that I need to complete this work. I would not been able to finish my master's degree. Most importantly, I would like to thank my wonderful wife, Minsun who stand by me and support me in the difficult time and believed me even when I did not believe in myself. Without all the love, sacrifice and devotion I have received these 2 years from her, I would have never been finished to successfully reach my study.

There are many people and others I should mention. I would also like to thank them for praying and encouraging me. I really want to say them: Thank you all.

Above all, I would like to thank Almighty God who made this thesis possible and an unforgettable experience with good people for me

TABLE OF CONTENTS

LIST OF FIGURES

LIST OF TABLE

NOMENCLATURES

A	Area, m^2
A_H	Amplitude of heating section
A_C	Amplitude of cooling section
c_p	Specific heat at constant pressure, J/kg-K
c_v	Specific heat at constant volume, J/kg-K
d	Diameter of heat pipe, m
f	Frequency, Hz
g	Gravity, m/s^2
$h(h_{lsen}, h_{lv})$	Convection heat transfer coefficient of liquid slug, W/m^2-K
$k\ (K)$	Thermal conductivity, W/m^2-K
K	Loss coefficient
L	Length, m
L_p	Length of liquid slug, m
m	Mass of vapor plugs, kg
$\dot{m}$	Mass flow rate, kg/s
Nu	Nusselt number
p	Vapor pressure, Pa
Q	Heat capacity, kJ
$Q_{in,v1}$	Evaporation heat transfer rate of left vapor plug, W
$Q_{out,v1}$	Condensation heat transfer rate of left vapor plug, W
$Q_{in,v2}$	Evaporation heat transfer rate of right vapor plug, W
$Q_{out,v2}$	Condensation heat transfer rate of right vapor plug, W
$Q_{in,s,l}$	Sensible heat transfer into liquid slug, W
$Q_{out,s,l}$	Sensible heat transfer out of liquid slug, W
r	Curvature radius of bend, mm

R	Gas constant of vapor, kJ/kg-K
Re	Reynolds number
RN	Random number
s	Specific entropy, kJ/kg-K
S	Entropy, kJ/K
t	Time, s
T	Temperature of liquid slug, K
v_p	Velocity of liquid slug, m/s
x_p	Displacement of liquid slug, m

Greek symbols

α	Thermal diffusivity, m^2/s
γ	Ratio of specific heats
Δ	Difference
ρ	Density, kg/m^3
σ	Standard deviation
ω	Angular frequency
ϕ	Phase angle (shift) and Volume fraction
π	Ratio of a circle's circumference
ε	Normal distribution
μ	Mean value
τ_p	Shear stress, N/m^2

Subscripts

0	Initial condition
B	Bend
c(C)	Condensation(Cooling section)

e(H)	Evaporation(Heating section)
eff	Effective nanofluid
f	Base fluid
l	Liquid
p	Nanoparticle
v	Vapor plug
W	Wall

ABSTRACT

A U-shaped pulsating heat pipe is an excellent heat transfer performance device. This study has been investigated step by step.

a) The entropy generation is based on the second law of thermodynamics. In the present study, the entropy generation in a U-shaped Pulsating Heat Pipe (PHP) is numerically investigated. The following five parameters, which are vapor mass, liquid temperature, latent heat, sensible heat, and friction, determine the entropy generation. The results show that the entropy generation is significantly affected by the initial temperature in the PHP. Particularly, the variation of the vapor mass is a primary factor of the entropy generation. On the other hand, the amplitude of the entropy generation is barely related with the pressure loss at the bend in the PHP. However, the frequency of the entropy generation with the pressure loss is faster than that without the pressure loss at the bend.

b) Pulsating heat pipe is a two-phase heat transfer device that transfers heat from heating section to cooling section via oscillatory liquid-vapor two-phase flow. The temperatures of heating and cooling sections are extremely important parameters, and play significant roles for the performance of pulsating heat pipes. The objective of this work is to study the effects of fluctuations of heating and cooling section temperatures on the oscillatory flow, temperature and pressure of the vapor plugs, as well as latent and sensible heat transfer of a pulsating heat pipe. The fluctuations of wall temperatures include a periodic component and a random component. The periodic component is characterized by the amplitude and frequency, while the random component is described by the standard deviation. The performance of the pulsating heat pipe is evaluated at various amplitudes, frequencies and standard deviations of the fluctuations.

c) A numerical study is performed to investigate heat transfer performance and effect of nanofluids on a pulsating heat pipe (PHP). Pure water is employed as the base fluid while Al_2O_3 with two different particle sizes, 38.4 and 47 nm, is used as nanoparticle. Different parameters including displacement of liquid slug, vapor temperature and pressure, liquid slug temperature distribution, as well as sensible and latent heat transfer in evaporator and condenser are calculated numerically and compared with the ones for pure water as working fluid. The results show that nanofluid has significant effect on heat transfer enhancement of the system and with increasing volume fraction and decreasing particles diameter the enhancement intensifies.

CHAPTER 1 INTRODUCTION

1.1 Background

Problems of cooling electronic devices such as desktop and laptop computers are accounted for a significant proportion in design. This is because the products could have a malfunction when the important part like CPU generates a lot of heat. In addition, the smaller the size of the electronics is, the greater the importance of heat removal becomes. More heat must be removed out of the area as the size of the area becomes reduced with the same amount of heat. The field of heat transfer has been evolved a lot as the electronics industries have been growing. Many researchers began to develop a two-phased control device, with rising interest in heat transfer. In the 1990's, Akachi [1] has registered a patent for a new type of heat pipe called the pulsating heat pipe (PHP). The features of PHP are that, unlike the conventional heat pipe, there is no wick structure and this leads to much lower costs.

1.2 Fundamental of the U-shaped Pulsating Heat Pipe on this Thesis

Figure 1 shows the configuration of the U-shaped PHP under consideration. The evaporator and the condenser are located in the top and the bottom of the U-shaped PHP, respectively; the vapor plugs 1 and 2 are located on the left and the right sides as shown in the Fig. 1 (a), respectively. There is a liquid slug between the two vapor plugs, and the two ends of the PHP are sealed. With pressure at the bend considered empirically [18], the U-shaped PHP can be considered as an equivalent straighten heat pipe in the modeling (see Fig. 1(b)). The displacement of liquid slug is represented by x_p, which can be negative or positive when the liquid slug moves to the left side or the right side. The driving force of the oscillatory flow is the pressure difference between the two vapor plugs. The liquid slug is considered to be incompressible, and the vapor is assumed to behavior like ideal gas. The heat conduction of the liquid slug is assumed to be one dimension along the axial direction.

1.3 Analysis and Modeling of Pulsating Heat Pipes

In the past two decades, applications of heat pipe were focused on the purpose of cooling an electronic system. The research on the heat pipe begun in 1960's as several scientists started the invention of the conventional heat pipe. Trefethen [2] grafted the idea of the heat pipe onto his space program. Grover *et al.* [3, 4] revealed that the sodium heat pipe is very effective in the heat transport with the high performance. They represented the experimental results by using the working fluids such as sodium, silver, and lithium in the stainless steel heat pipe with the screen wick. The results produced the development of the heat pipe as the effective thermal device. Also, Leefer [5] and Judge [6] led the research on the heat pipe and showed that the maximum operating temperature of the heat pipe can be as high as 1,650°C. Dobson *et al*. [7] showed that the motion of the PHP with the open-end mathematically. They assumed the heat transfer coefficient between the wall and the vapor, and ignored the effect of the surface tension and the heat transfer of the surrounding liquid. Cai *et al*. [8] visualized the processes of the heat transfer and the motion of the working fluid by using the plastic or the glass PHP. They also showed that the pulsating motion takes place better if the working fluid has the low latent heat. Hosoda *et al*. [9] computed the temperature and the pressure of the PHPs by solving the momentum and the energy equations in the two-dimensional two-phase flow. Zhang and Faghri [10] considered the thin film evaporation and condensation and showed that the heat transfer of PHP is dominated by the sensible heat regardless of the surface tension. Groll *et al*. [11] presented the generation and the collapse of the vapor bubble due to the total fixed volume of the PHP. Rittidech *et al*. [12] investigated the energy thrift as an air pre-heater using the open-looped copper PHP. They used variable conditions such as 60 degree, 70 degree and 80 degree of temperature in heating section and 3.3 m/s of gas velocity with water and R-123 as the working fluid. The result was that the heat transfer rate increased a little when the heat section temperature climbed from 60 degree to 80 degree. Similarly, the heat transfer rate using R-123 was more increased than the one using water. Shao and Zhang [18] analyzed the movement and the effect of liquid, vapor and heat

transfer with constant temperatures of the heating and the cooling section in the U-shaped PHP. Kim *et al*. [13] also analyzed the effect of entropy generation at the initial vapor temperatures of 70 degree and 20 degree. Likewise, the temperatures in the heating and the cooling section appeared to affect the heat transfer of the PHPs. On the other hand, the entropy is generated by the thermodynamic cycle when the working fluid moves in the PHP. The entropy generation is also caused by the friction loss and the heat transfer of the working fluid [14]. Furthermore, the entropy generation is directly related with the irreversible process, and the quantity of the entropy generation is determined by the entropy and the lost work during the process. Al-Zaharnah [15] conducted the research on the effect of the wall temperature and the Reynolds number on the entropy distribution in the pipe system. Moreover, Al-Zaharnah *et al*. [16] studied the effect of the fluid viscosity on the entropy generation for each different wall temperature. It was presented that the rate of the entropy generation is increased by the high temperature of the pipe wall. Sahin *et al*. [17] researched the effect of the developing laminar viscous fluid flow on the entropy generation in the circular pipe. They showed that the entropy generation increases near the wall and decreases gradually toward the axial direction.

Thermal conductivity and viscosity are the key properties of nanofluids that have been reported more in the last decade. Many theoretical models are presented in the literature for calculating thermal conductivity and viscosity of nanofluids. However, there are no reliable theoretical model for prediction of anomalous viscosity and effective thermal conductivity of nanofluids. The viscosity and thermal conductivity data of nanofluids are still contradictory in various research publications. Therefore, it is still unclear to choose the best models to use for viscosity and thermal conductivity of nanofluids. The convectional models for thermal conductivity [26, 27] cannot describe accurately the thermal conductivity of nanofluids because they do not consider the effect of temperature and some of enhancement mechanisms such as effect of nanoparticle clustering, Brownian motion [24, 28], the nature of heat transport in nanoparticles, and molecular-level layering of the liquid at the liquid/particle interface [29]. The

conventional understanding of the effective thermal conductivity of mixtures is useful for larger-size solid/fluid systems. These theories originates from continuum formulations which assume diffusive heat transfer in both fluid and solid phases and typically involve only the particle size/shape and volume fraction. Experimental results showed that thermal conductivity of nanofluids depends on different parameters including volume fraction, surface area, temperature, thermal conductivity of nanoparticles and base fluid, shape of nanoparticles and etc. Based on the traditional models, some dynamical models have been proposed to address random motion of nanoparticles. Khanafer and Vafai [21] analyzed thermophysical characteristics of nanofluids and their role in heat transfer enhancement. Based on pertinent experimental data, they developed some general correlations in terms of temperature, thermophysical properties of base fluid, volume fraction and particle diameter for calculating effective thermal conductivity and viscosity as well as density of nanofluids. Their models appeared to be accurate and comprehensive so in this paper we used these models for calculating effective properties of nanofluids.

1.4 Thesis Objectives

As I mentioned above so far, many studies of PHPs had investigated the effect of heat transfer by testing experiments and using computer programs. Some studies have focused on characterizing the heat transfer performance. Other studies have approached theoretically by the details of the modeling such as different working fluids, random wall temperature and different volume fractions and nanoparticle diameters of nanofluids.

The objective of this study is to examine the entropy generation and thermal performance of a U-shaped pulsating heat pipe. All simulations of this study are figured out to investigate the entropy generations with the initial temperature, the effect of the pressure loss at the bend on the entropy generation, random noise of wall temperature and volume fractions and nanoparticle diameters of nanofluids.

1.4.1 Entropy Generation with Initial Temperature and Pressure Loss at Bends

The entropy generation is based on the second law of thermodynamics. In the present study, the entropy generation in a U-shaped Pulsating Heat Pipe (PHP) is numerically investigated. The following five parameters, which are vapor mass, liquid temperature, latent heat, sensible heat, and friction, determine the entropy generation. The results show that the entropy generation is significantly affected by the initial temperature in the PHP. In the present study, the entropy generation will be numerically analyzed with considering two vapor plugs, a liquid slug, evaporation and condensation in the PHP. The effects of initial temperature and the pressure loss in the bend on the entropy generation in the PHP will also be studied.

1.4.2 Random Noise of Wall Temperature

Most researchers had investigated the heat transfer in PHPs based on the assumption that the heating and cooling section temperatures are constant. However, heating and cooling section temperatures are usually not constant in the real operation as it can fluctuate by changing of heating load, cooling condition or even oscillation of liquid slugs. Effects of fluctuations of heating and cooling section temperatures on the performance of a PHP are investigated in this paper. Effects of amplitude, frequency and standard deviation of the temperature fluctuations on the performance of the PHP are investigated.

1.4.3 Volume Fractions and Particle Diameters of Nanofluids.

It appears that there is no theoretical model for predicting the thermal performance of PHPs with nanofluid as working fluid. Clearly, it is necessary to do further research to determine the effect of nanofluids on different parameters including displacement of liquid slug, vapor temperature and pressure, liquid slug temperature distribution, as well as sensible and latent heat transfer in evaporator and condenser. Therefore, the objective of this paper is to conduct a theoretical analysis predicting the heat transfer enhancement of PHPs and investigating the effect of nanoparticles volume concentration and size on thermal performance of the system.

CHAPTER 2 ANALYSIS FO ENTROPY GENERATION IN A PULSATING HEAT PIPE

2.1 Physical Model

2.1.1 Problem Description

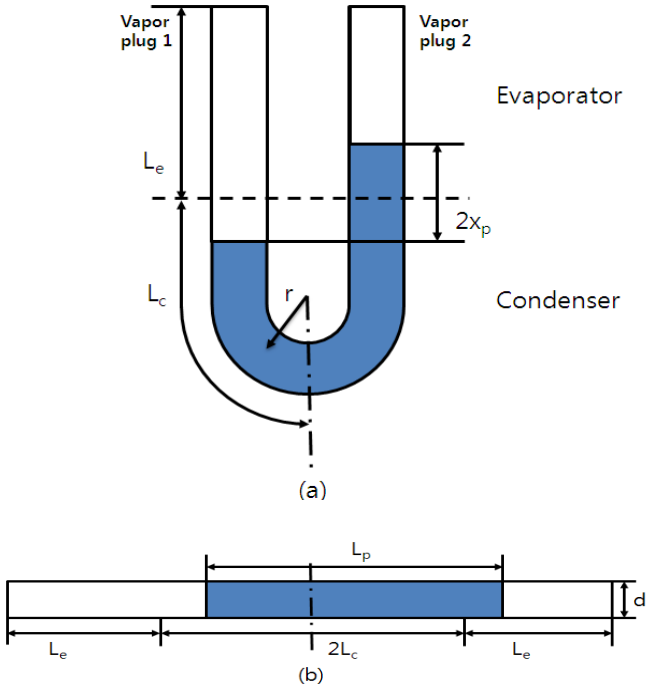

Figure 1 Configureation of pulsatign heat pipe

Figure 1 shows the configuration of the U-shaped PHP [18]. The evaporator and the condenser are located in the top and the bottom of the U-shaped PHP, and the vapor plug 1 and the vapor plug 2 are displayed in the left side and the right side as shown in the Fig. 1 (a), respectively. There is also liquid slug between two vapor plugs, and the end of the U-shaped PHP is already sealed. Figure 1 (b) is considered as the straighten heat pipe, not the U-shaped one. L_p indicates the length of the liquid slug, and L_e and L_c demonstrate the lengths of the evaporator and the condenser, respectively. Furthermore, the displacement of liquid slug is indicated by x_p, and the diameter of heat pipe and the radius of the bend are presented by d and r, respectively. x_p can be negative or positive when the liquid slug moves the left side or the right side, depending on the movement of the liquid slug.

The following assumptions are made in order to investigate the entropy generation in the U-shaped PHP:

1) The pressure drop in the vapor due to the friction is neglected.

2) The vapor plug is assumed to be always in the saturation condition and behave as an ideal gas.

3) The entropy is assumed to be generated by the heat transfer and the friction.

4) The liquid is assumed to be incompressible, and the sub-cooling in the liquid is considered.

2.1.2 Governing Equations for Pulsating Flow

The acceleration of the liquid slug is related with pressure, gravity and shear stress. Thus, the momentum equation is [18]:

$$AL_p\rho_l\frac{d^2x_p}{dt^2}=[(p_{v1}-p_{v2})-\Delta p_b]A-2\rho_l gAx_p-\pi dL_p\tau_p \tag{1}$$

where Δp_b is the pressure loss at the bend [19] (Rohsenow et al., 1985):

$$\Delta p_b=\begin{cases}K\rho_l\dfrac{v_p{}^2}{2} & v_p>0\\ -K\rho_l\dfrac{v_p{}^2}{2} & v_p<0\end{cases} \tag{2}$$

and τ_p is the shear stress:

$$\tau_p=c_l\rho\upsilon^2/2\ ,\quad c_l=\begin{cases}16/\mathrm{Re}, & \mathrm{Re}\le 2200\\ 0.078\,\mathrm{Re}^{-0.2}, & \mathrm{Re}>2200\end{cases} \tag{3}$$

The energy equations of the two vapor plugs are [18]:

$$\frac{d(m_{v1}c_vT_{v1})}{dt}=c_pT_{v1}\frac{dm_{v1}}{dt}-p_{v1}\frac{\pi}{4}d^2\frac{dx_p}{dt} \tag{4}$$

$$\frac{d(m_{v2}c_vT_{v2})}{dt}=c_pT_{v2}\frac{dm_{v2}}{dt}+p_{v2}\frac{\pi}{4}d^2\frac{dx_p}{dt} \tag{5}$$

The vapor plug can be assumed to be an ideal gas. Thus, the equation of state can be presented by:

$$p_{v1}(L_e + x_p)\frac{\pi}{4}d^2 = m_{v1}RT_{v1} \tag{6}$$

$$p_{v2}(L_e - x_p)\frac{\pi}{4}d^2 = m_{v2}RT_{v2} \tag{7}$$

Considering the initial conditions, the masses and the temperatures of the two vapor plugs can be obtained:

$$m_{v1} = \frac{\pi d^2 p_0}{4RT_0}\left(\frac{p_{v1}}{p_0}\right)^{\frac{1}{\gamma}}(L_e + x_p) \tag{8}$$

$$m_{v2} = \frac{\pi d^2 p_0}{4RT_0}\left(\frac{p_{v2}}{p_0}\right)^{\frac{1}{\gamma}}(L_e - x_p) \tag{9}$$

$$T_{v1} = T_0\left(\frac{p_{v1}}{p_0}\right)^{\frac{(\gamma-1)}{\gamma}} \tag{10}$$

$$T_{v2} = T_0\left(\frac{p_{v2}}{p_0}\right)^{\frac{(\gamma-1)}{\gamma}} \tag{11}$$

where T_0 and P_0 are the initial temperature and the pressure, respectively.

2.1.3 Latent and sensible heat transfer

The heat transfer in the PHP means that the heat moves from the evaporator to the condenser. There are two types of the heat transfer in the PHP. One is the latent heat due to the phase change of the working fluid, and the other is the sensible heat because of the heat transfer between the wall and the liquid slug. The heat transfer rates in the two vapors are related with the mass flux, and can be obtained by:

$$Q_{in,v1} = \dot{m}_{evp,v1}h_{lv} \tag{12}$$

$$Q_{out,v1} = \dot{m}_{con,v1} h_{lv} \tag{13}$$

$$Q_{in,v2} = \dot{m}_{evp,v2} h_{lv} \tag{14}$$

$$Q_{out,v2} = \dot{m}_{con,v2} h_{lv} \tag{15}$$

The temperature distribution of the liquid slug can be obtained by solving the energy equation:

$$\frac{1}{\alpha_l}\frac{dT_l}{dt} = \frac{d^2T_l}{dx_p^2} - \frac{h_{lsen}\pi d}{k_l A}(T_l - T_w) \tag{16}$$

The initial and boundary conditions for Eq. (16) are:

$$T = T_0, \;\; t = 0, \;\; 0 < x_p < L_p \tag{17}$$

$$T = T_{v1}, \;\; x_p = 0 \tag{18}$$

$$T = T_{v2}, \;\; x_p = L_p \tag{19}$$

The sensible heat transfer in and out of the liquid slug can be obtained by integrating the heat transfer over the length of the liquid slug.

$$Q_{in,s,l} = \begin{cases} \int_{L_p - x_p}^{L_p} \pi dh(T_e - T_l)dx_l, \; x_p > 0 \\ \int_0^{|x_p|} \pi dh(T_e - T_l)dx_l, \; x_p < 0 \end{cases} \tag{20}$$

$$Q_{out,s,l} = \begin{cases} \int_0^{-x_p} \pi dh(T_l - T_c)dx_l, \; x_p > 0 \\ \int_{|x_p|}^{L_p} \pi dh(T_l - T_c)dx_l, \; x_p < 0 \end{cases} \tag{21}$$

where the sensible heat transfer coefficient can be obtained from $h = Nuk_l / d$ [23].

2.1.4 Entropy Generation of Two Vapor Plugs

The entropy is generated when the liquid slug becomes the vapor plug due to the evaporation in the PHP. According to the second law of thermodynamics, the rate entropy generation due to phase change can be calculated by:

$$\frac{dS_v}{dt} = \sum \dot{m}_{in} s_v - \sum \dot{m}_{out} s_v \tag{22}$$

The entropy generation in the vapor plug 1 is

$$\frac{d(m_{v1} s_{v1})}{dt} = s_{v1} \frac{dm_{v1}}{dt} \tag{23}$$

since the change of specific entropy with respect to time is zero, i.e., $ds_{v1}/dt = 0$. Thus, the entropy generation in the vapor plug 1 is:

$$\frac{dS_{v1}}{dt} = s_{v1} \frac{dm_{v1}}{dt} \tag{24}$$

Similarly, the entropy generation in the vapor plug 2 is

$$\frac{dS_{v2}}{dt} = s_{v2} \frac{dm_{v2}}{dt} \tag{25}$$

Therefore, the equations of the entropy generation in the vapor plug 1 and 2 can be rearranged as:

$$S_{v1} = m_{v1} s_{v1} \tag{26}$$

$$S_{v2} = m_{v2} s_{v2} \tag{27}$$

Also, these equations can be written as following because the entropy of the two vapor plugs is equal in the reference state.

$$S_{v1} = m_{v1} s_0 \tag{28}$$

$$S_{v2} = m_{v2} s_0 \tag{29}$$

Finally, the entropy generations in the two vapor plugs can be obtained by:

$$\Delta S_{v1} = (m_{v1} - m_{v1,0}) s_0 \tag{30}$$

$$\Delta S_{v2} = (m_{v2} - m_{v2,0}) s_0 \tag{31}$$

2.1.5 Entropy generation of liquid slug

Since the liquid phase is incompressible, the following entropy equation is valid:

$$Tds = c_p dT \tag{32}$$

$$\frac{ds}{dt} = \frac{c_p}{T} \frac{dT}{dt} \tag{33}$$

Integrating Eq. (33) yields

$$s_l = s_{l,0} + c_p \ln \frac{T_l}{T_0} \tag{34}$$

The entropy generation of the liquid slug can be obtained by integrating Eq. (34) over the length of the liquid slug:

$$S_l = \int_0^{m_l} s_l dm = \rho_l \frac{\pi}{4} d^2 \int_0^{L_p} s_{l,0} + c_p \ln \frac{T_l}{T_0} dx \tag{35}$$

$$S_l - S_{,l0} = \rho_l \frac{\pi}{4} d^2 c_p \int_0^{L_p} \ln \frac{T_l}{T_0} dx \tag{36}$$

$$\Delta S_l = \rho_l \frac{\pi}{4} d^2 c_p \int_0^{L_p} \ln \frac{T_l}{T_0} dx \tag{37}$$

The friction by the liquid slug is related to area, velocity and shear stress. The entropy generation due to the friction on the liquid slug can be gained by:

$$S_f - S_{f,0} = \Delta S_f = \tau_l \pi d v_p \int_0^{L_p} \frac{1}{T_l} dx \tag{38}$$

2.1.6 Entropy generation of latent heat and sensible heat in heating and cooling sections

When the working fluid is pulsating, the system is affected by the latent heat and the sensible heat. By using the latent heat from Eqs. (12)-(15), the entropy generations of the latent heat for the evaporation and the condensation are as follows:

$$\Delta S_{e,lat} = -\frac{Q_{e,lat}}{T_e} \text{ and } \Delta S_{c,lat} = \frac{Q_{c,lat}}{T_c} \tag{39}$$

The entropy generations of the sensible heat transfer are obtained by using the sensible heat from:

$$\Delta S_{e,sen} = \frac{Q_{e,sen}}{T_e} \text{ and } \Delta S_{c,sen} = \frac{Q_{c,sen}}{T_c} \tag{40}$$

As a result, the total entropy generation in the U-shaped PHP can be obtained by adding all the terms of the entropy generation.

$$\dot{S}_{tot,gen} = \Delta S_{v1} + \Delta S_{v2} + \Delta S_l + (\Delta S_{e,lat} + \Delta S_{e,sen}) + (\Delta S_{c,lat} + \Delta S_{c,sen}) + \Delta S_f \tag{41}$$

2.2 Numerical Application

The iteration method and the implicit finite difference method are used to solve the physical model of the vapor plugs and the liquid slug numerically. Also, the equation of the heat conduction is solved by TDMA (Tridiagonal Matrix Algorithm) in order to get the temperature distribution of the liquid slug. The numerical procedures to obtain the entropy generation are as follows:

1) Temperatures of the two vapor plugs, T_{v1} and T_{v2}, are assumed, and the thermal and physical properties of the liquid slug are calculated according to T_l.
2) The vapor pressures, p_{v1} and p_{v2}, are solved by Eqs. (10) and (11).
3) The displacement of the liquid slug, x_p, is calculated by Eq. (1).

4) The new masses of the two vapor plugs, m_{v1} and m_{v2}, are obtained by accounting for the change of the vapor masses from Eqs. (8) and (9).

5) The pressures of the two vapor plugs, p_{v1} and p_{v2}, are calculated by Eqs. (6) and (7).

6) T_{v1} and T_{v2} are solved by Eqs. (9) and (10).

7) T_{v1} and T_{v2} are compared, which are obtained in step 6, with the assumed values in the step 1. If the differences meet the small tolerance, go to the step 8; otherwise, the above procedures are repeated the steps 2-6 until a converged solution is obtained.

8) The temperature distribution of the liquid slug is solved by Eq. (16) and then the sensible heat is calculated.

9) The latent heat is obtained by Eqs. (12)-(15).

10) The entropy generations in the vapor 1 and 2, ΔS_{v1} and ΔS_{v2}, are calculated by Eqs. (30) and (31).

11) The entropy generations of the liquid slug and the friction, ΔS_l and ΔS_f, are calculated by Eqs. (37) and (38).

12) The entropy generations of the latent heat and the sensible heat, $\Delta S_{e,lat}$, $\Delta S_{e,sen}$, $\Delta S_{c,lat}$ and $\Delta S_{c,sen}$, are calculated by Eqs. (39) and (40). The sensible heat and the latent heat are obtained from the step 8 and 9.

13) The total entropy generation of the U-shaped PHP is calculated by Eq. (41).

2.3 Results and Discuss

The following parameters are used in the numerical calculation, which are obtained from Zhang *et al* [18]: L_e=0.1m, L_c=0.1m, L_p=0.2m, d=3.34mm, T_e=123.4℃, T_c=20℃, and $h_e = h_c = 200\text{W/m}^2\text{K}$, $\Delta t = 1\times10^{-4}$.

2.3.1 The effect of the entropy generation with the initial temperature.

When the initial temperatures in the U-shaped PHP are 70°C and 20 °C, respectively, the entropy generations with the initial temperature are shown in Figs. 2-8. Figure 2 (a) shows the entropy generations with time in the vapor plugs 1. Although the value of the entropy generation is supposed to be positive, the entropy generation in the vapor plug 1 has the negative value because the initial mass is larger than the new mass. The entropy generation in the vapor plug 1 with the initial temperature of 20 °C shows the relatively large amplitude and the constant pattern with time. Unlike the initial temperature of 20°C, the entropy generation in the vapor plug 1 with the initial temperature of 70 °C presents the relatively small amplitude. Also, the amplitude and the frequency of the entropy generation in the vapor plug 2 with the initial temperature of 20 °C are relatively larger than those with the initial vapor temperature of 70 °C as shown in Fig. 2 (b). The reason of this phenomenon is that the difference between the initial and the current masses at 20 °C is relatively larger than those at 70 °C. Figure 3 presents the entropy generations of the liquid slug with time when the initial temperatures are 70 °C and 20 °C. The entropy generations at the initial temperatures of 70°C and 20°C maintain about 0.146 kJ/K and 0.194 kJ/K, respectively. The entropy generation of the liquid slug is almost uniform without the difference of amplitude and not significantly affected by the initial temperature.

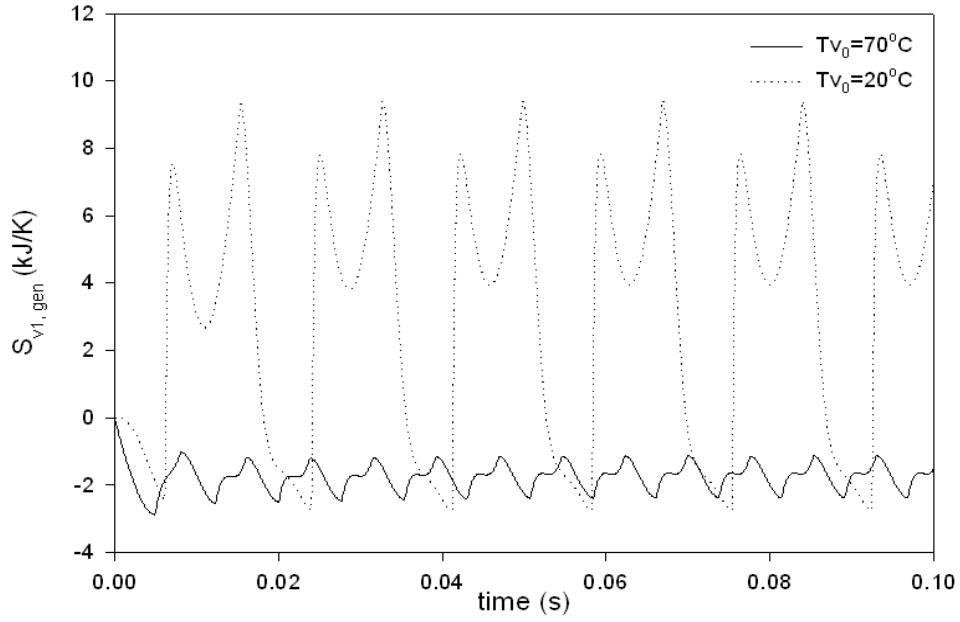

(a) Vapor plug 1

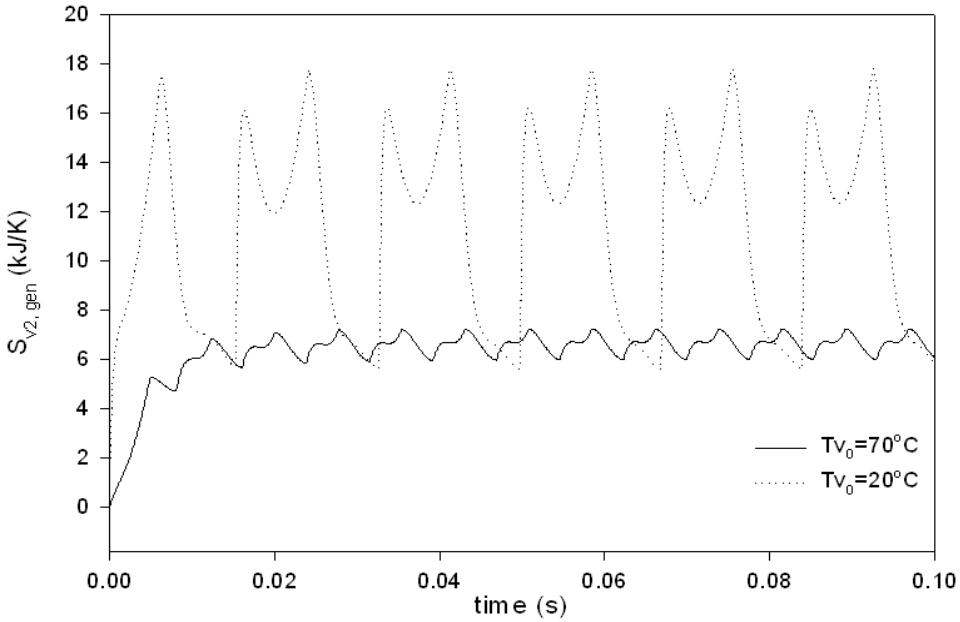

(b) Vapor plug 2

Figure 2 Entropy generation in two vapor plugs

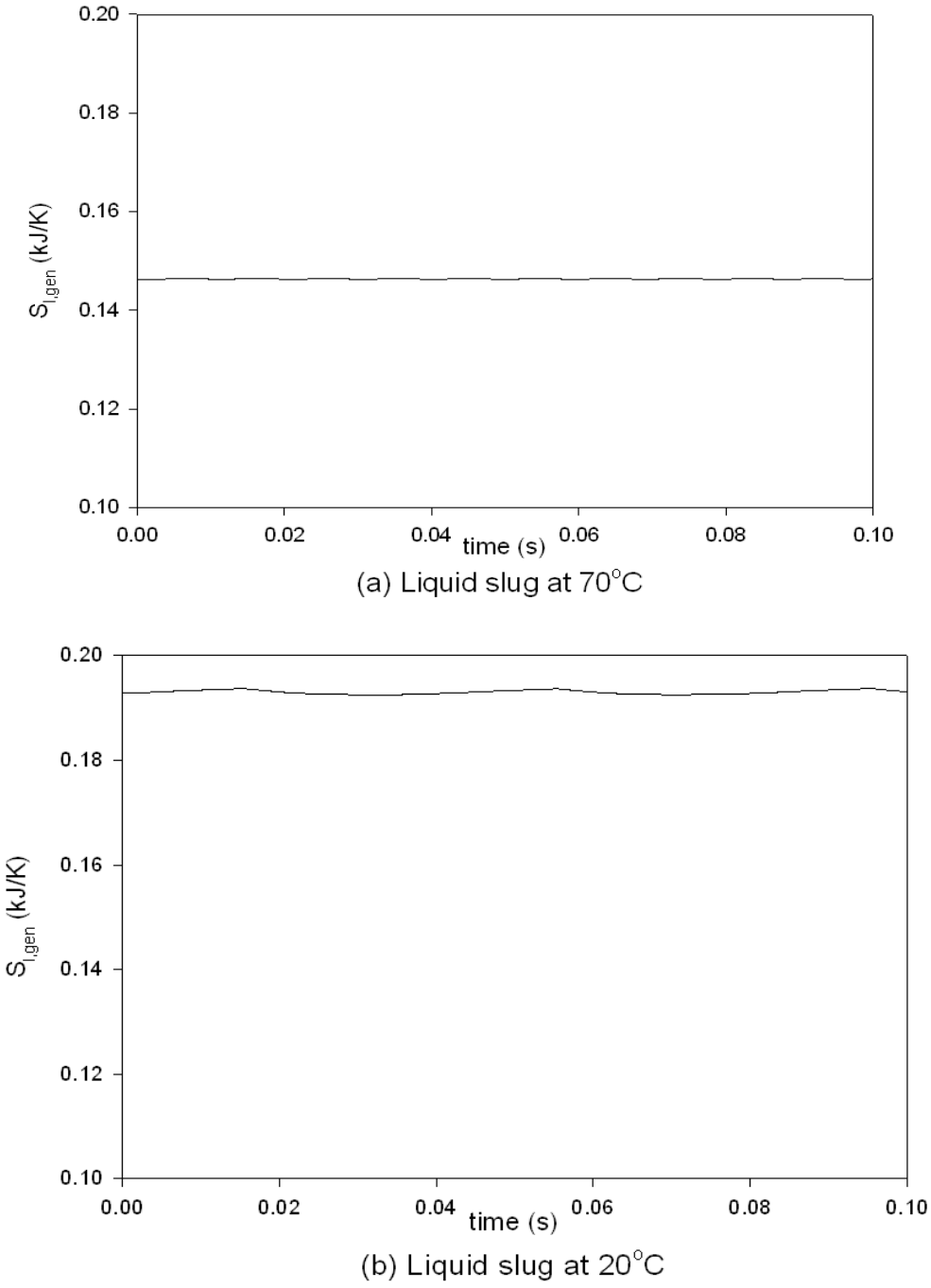

Figure 3 Entropy generation in liquid slugs

The entropy generations with time are shown in Figs. 4 and 5 due to the latent heat in the vapor plugs 1 and 2, respectively. Figures 4 (a) and 5 (a) represent the entropy generations in the evaporation, and the entropy generations in the vapor plugs 1 and 2 increase sharply with the regular intervals at the initial temperature of 20°C because of the noticeable difference in

temperature. The amplitude and the frequency at the initial temperature of 70^{o}C are steady, and the entropy generation with time is almost the same in the cycle. Also, the frequency at the initial temperature of 20^{o}C is longer than that at the initial temperature of 70^{o}C in the maximum entropy generation. Figures 4 (b) and 5 (b) show the entropy generations with time in the vapor plugs 1 and 2 when the vapor plug enters into the cooling section. Unlike the evaporation process, the entropy generation at the initial temperature of 70^{o}C is higher than that at the initial temperature of 20^{o}C because the difference between the cooling section's temperature and the initial temperature of 70oC is larger than that with the initial temperature of 20^{o}C. However, the frequency at the initial temperature of 20^{o}C is longer than that at the initial vapor temperature of 70oC. Figure 6 shows the entropy generation due to the sensible heat at the initial temperatures of 70^{o}C and 20^{o}C. When the liquid slug is pulsated, the entropy generation is related with the sensible heat as well as the latent heat. As seen from Fig. 6 (a), the graph at the initial temperature of 70^{o}C presents the entropy generation of the constant period and shape when the sensible heat transfers into the liquid slug. However, the change of the entropy generation at the initial temperature of 20^{o}C is gradually decreased with increasing time because the sensible heat is sensitive to the temperature difference. On the other hand, the entropy generation in the cooling section at the initial vapor temperature of 70^{o}C is larger than that at the initial temperature of 20^{o}C as shown in Fig. 6 (b). The amplitude of the entropy generation at the initial temperature of 70^{o}C is gradually decreased because the difference of temperature is reduced with increasing time. However, there is a little change in the entropy generation at the initial temperature of 20^{o}C.

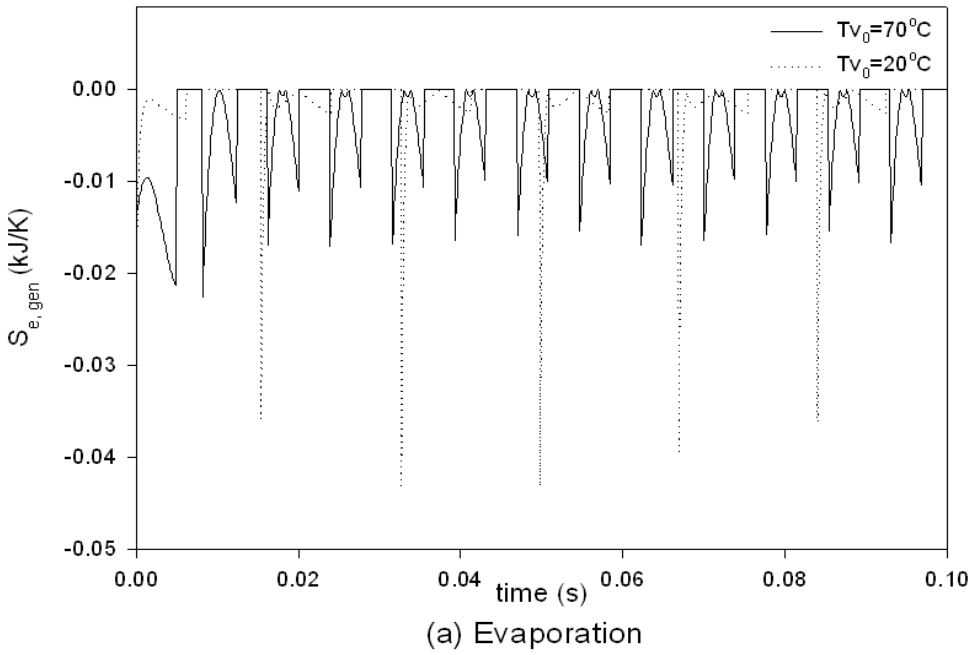

(a) Evaporation

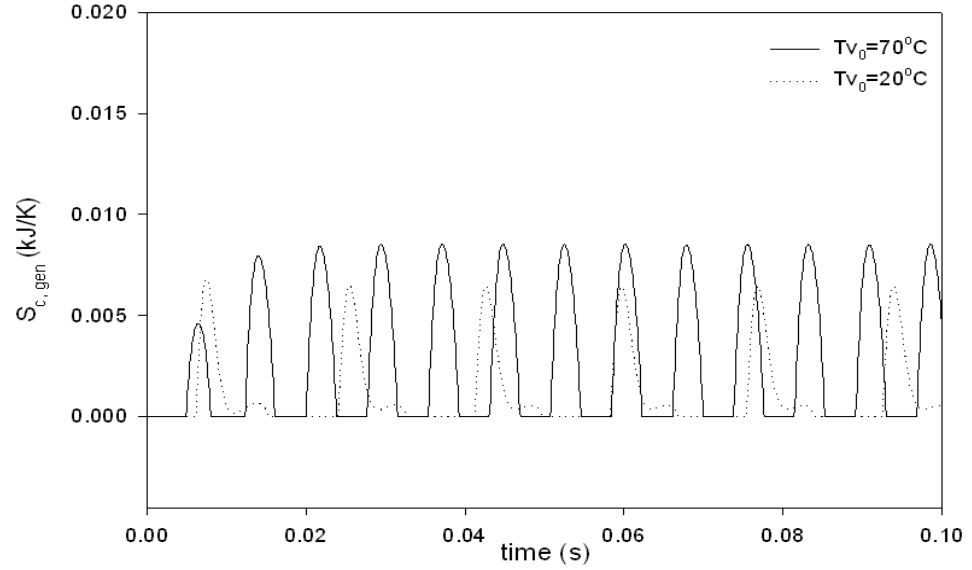

(b) Condensation

Figure 4 Entropy generation due to latent heat in vapor plug 1

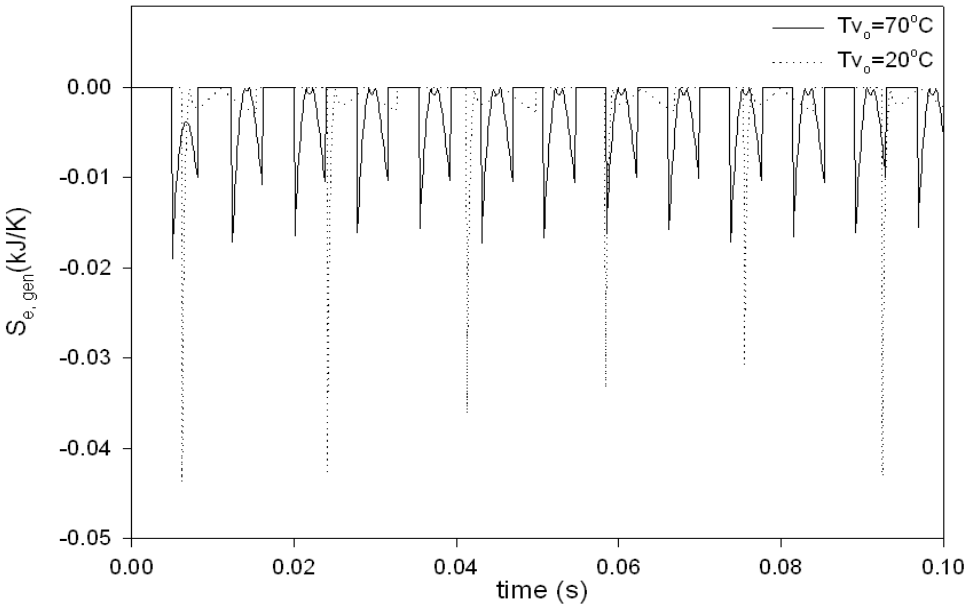

(a) Evaporation

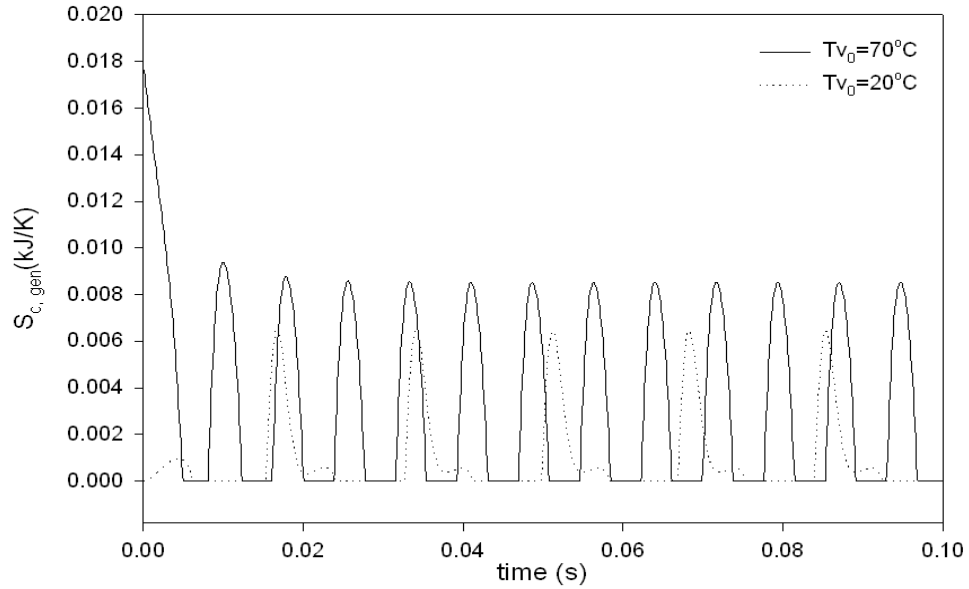

(b) Condensation

Figure 5 Entropy generation due to latent heat transfer in vapor plug 2

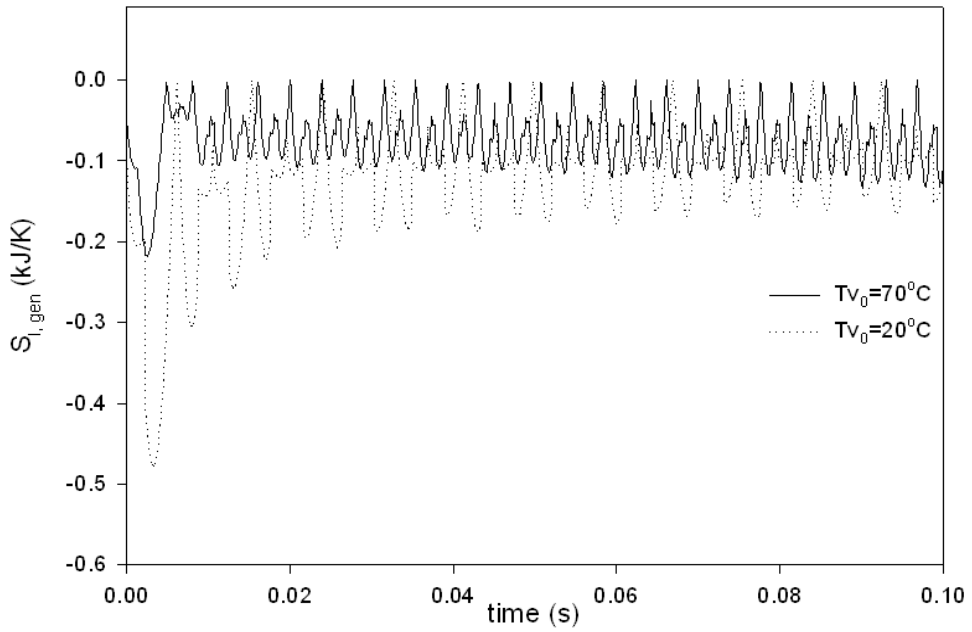

(a) Sensible heat transferred into the liquid slug

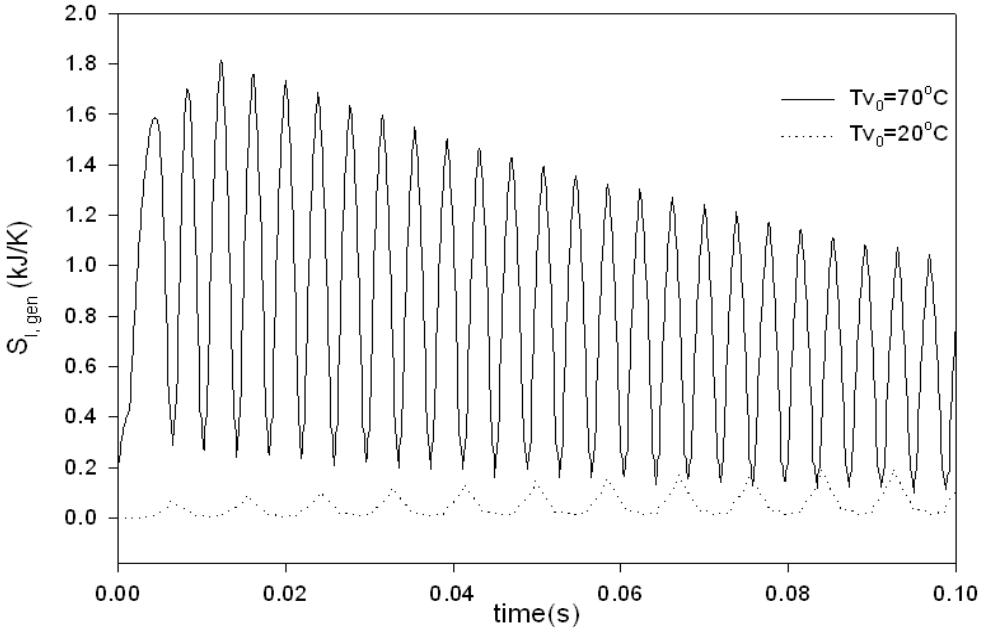

(b) Sensible heat transferred out of the liquid slug

Figure 6 Entropy generation due to sensible heat in liquid slug

Figure 7 presents the entropy generation due to the friction of the liquid slug at the initial temperatures of 70°C and 20°C. There is a little difference in the entropy generation because the velocity of the liquid slug is not nearly affected by the initial temperature. The values of the

entropy generation due to the friction are very small, which have the order of approximately 10-12 kJ/K. Therefore, since the friction of the liquid slug does not affect the entropy generation, it can be ignored.

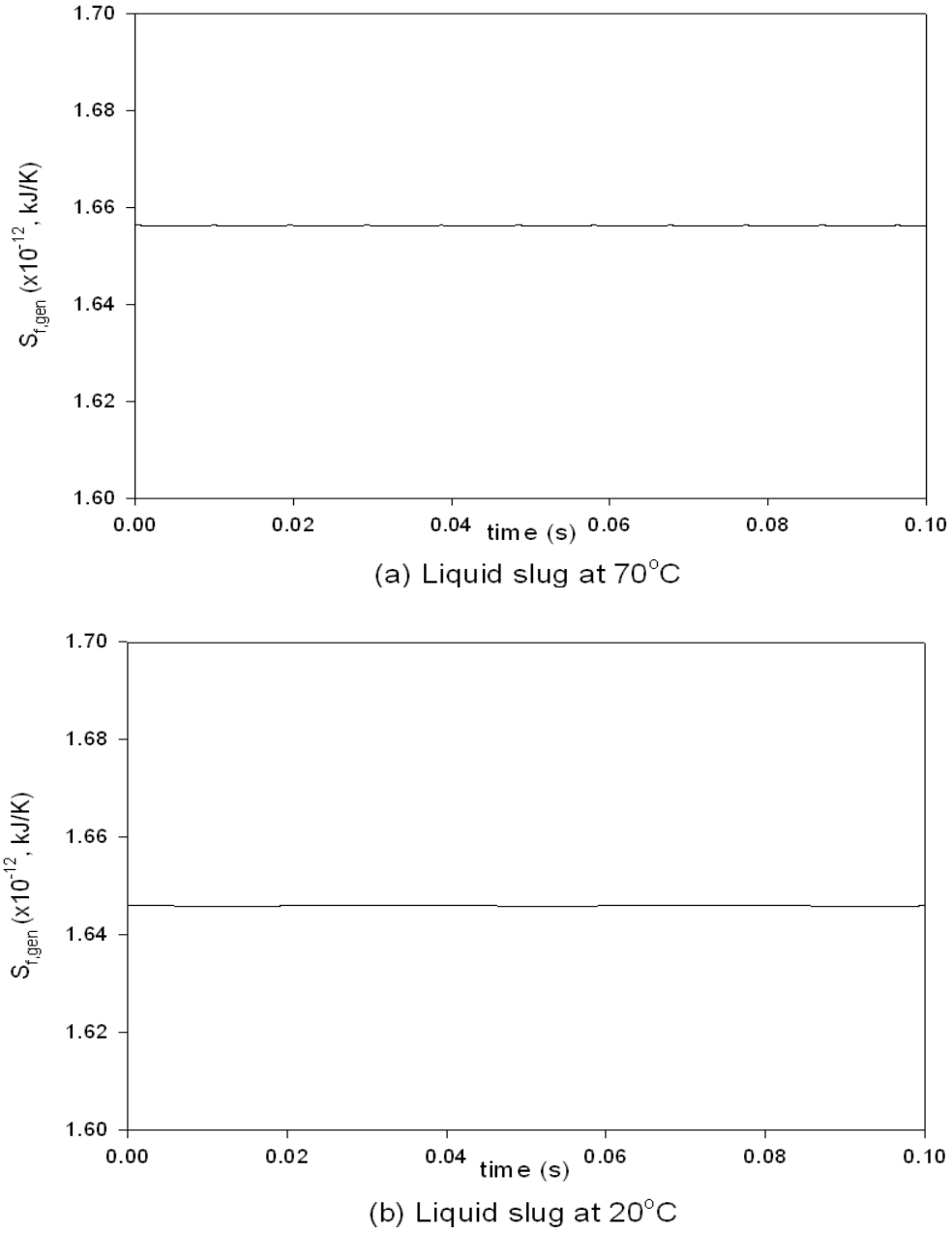

Figure 7 Entropy generation due to friction in liquid slug

Figure 8 shows the above mentioned entropy generations at the initial temperatures of 70°C and 20°C. The change in the vapor plugs 1 and 2 is noticeably larger than the others in the

entropy generation. In addition, the value of the entropy generation at the initial temperature of 20°C is higher than that at the initial temperature of 70°C. As a result, the initial vapor temperature has a significant effect on the change of the entropy generation in the U-shaped PHP.

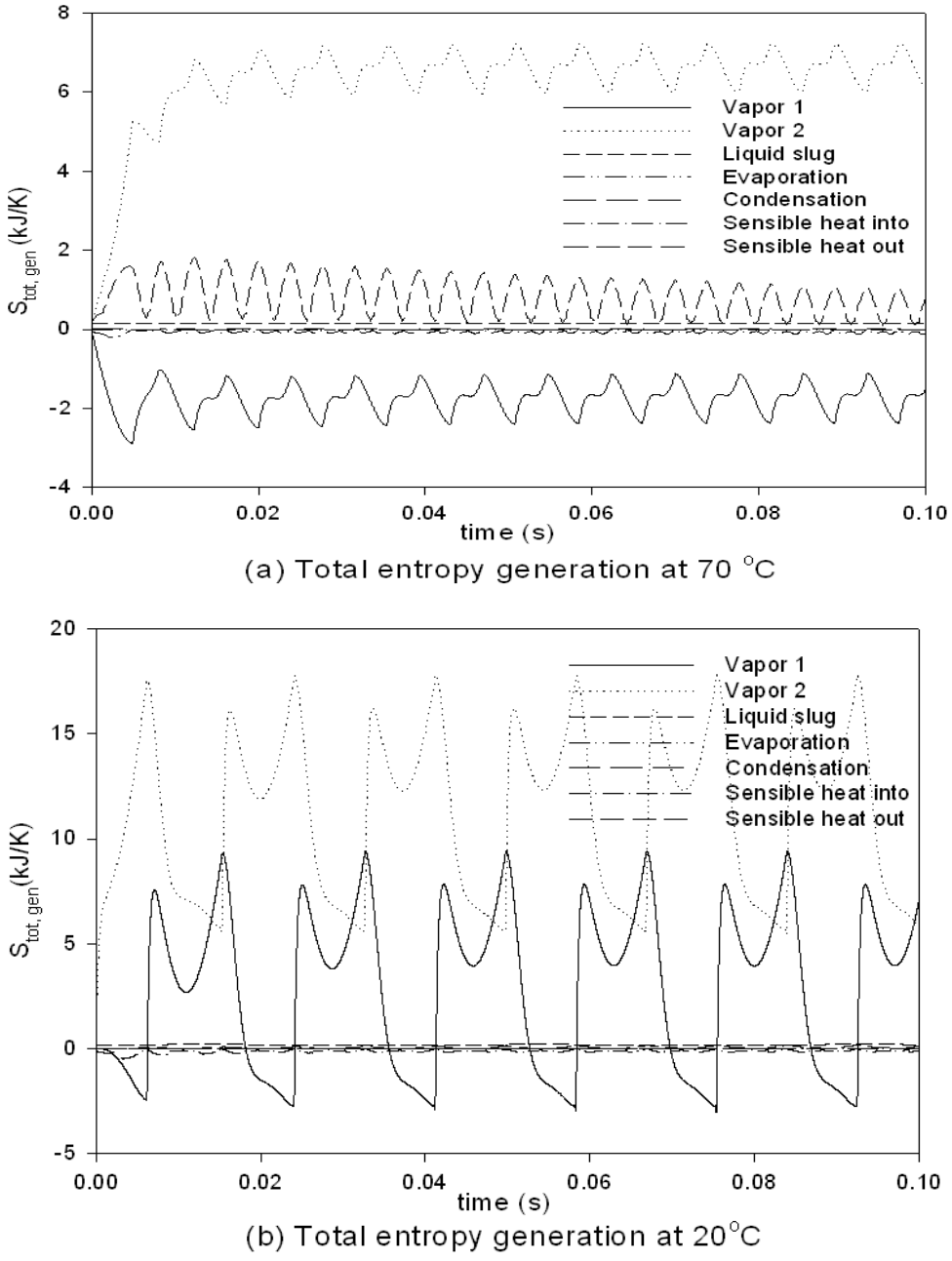

Figure 8 Total entropy generation at different initial temperatures

2.3.2 The effect of the pressure loss at the bend on the entropy generation

Figures 9-19 demonstrate the effect of the pressure loss at the bend on the entropy generation. The pressure loss coefficient of 0.31 is used in the calculations when the curvature radius (r) of the bend is 5.83mm as shown in Fig. 1 [18]. Figures 9 and 10 show the entropy generations with or without the pressure loss at the bend in the vapor plugs 1 and 2, respectively. In the startup stage, the entropy generations have the same frequency. However, in the final stage, the frequency of the entropy generation with the pressure loss is faster than that without the pressure loss. The reason is that the pressure drop prevents the liquid slug from moving in the PHP. Thus, the pressure loss at the bend has a significant effect on the frequency, while it does not affect the amplitude of the entropy generation. Unlike the cases for the two vapor plugs, Figure 11 shows the entropy generation of the liquid slug with time, and there is a little difference of the entropy generation with or without pressure loss at the bend. The amplitude difference is about 0.004 kJ/K, and the frequency difference is almost constant. Figures 12-15 show the entropy generations due to the evaporation and the condensation with or without the pressure loss in the vapor plugs 1 and 2, respectively. In other words, they present the effect of the latent heat on the entropy generation with or without the pressure loss. The frequencies of the entropy generations due to the evaporation and the condensation in the two vapor plugs are similar to those as shown in Figs. 4 and 5. The entropy generation in the startup stage is almost constant regardless of the existence of the pressure loss at the bend. However, the frequencies with the pressure loss are still faster than those without the pressure loss in the final stage.

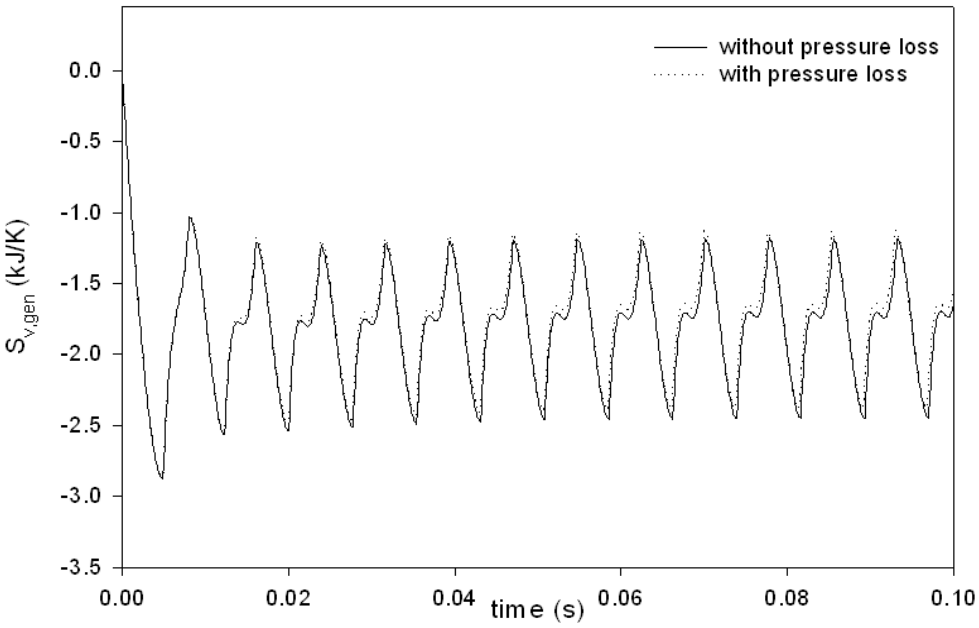

(a) Startup stage

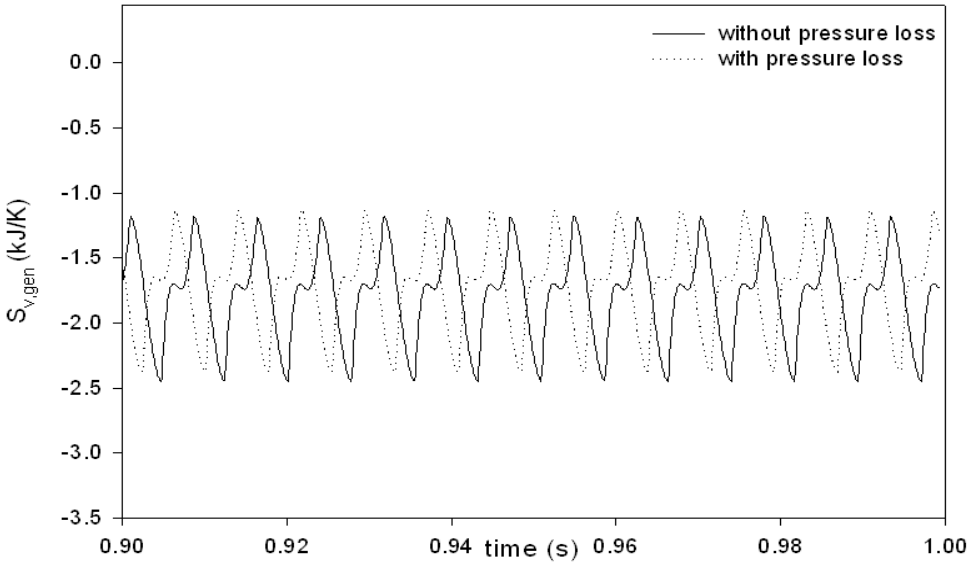

(b) Final stage

Figure 9 Entropy generation with or without pressure loss at bend in the vapor plug 1

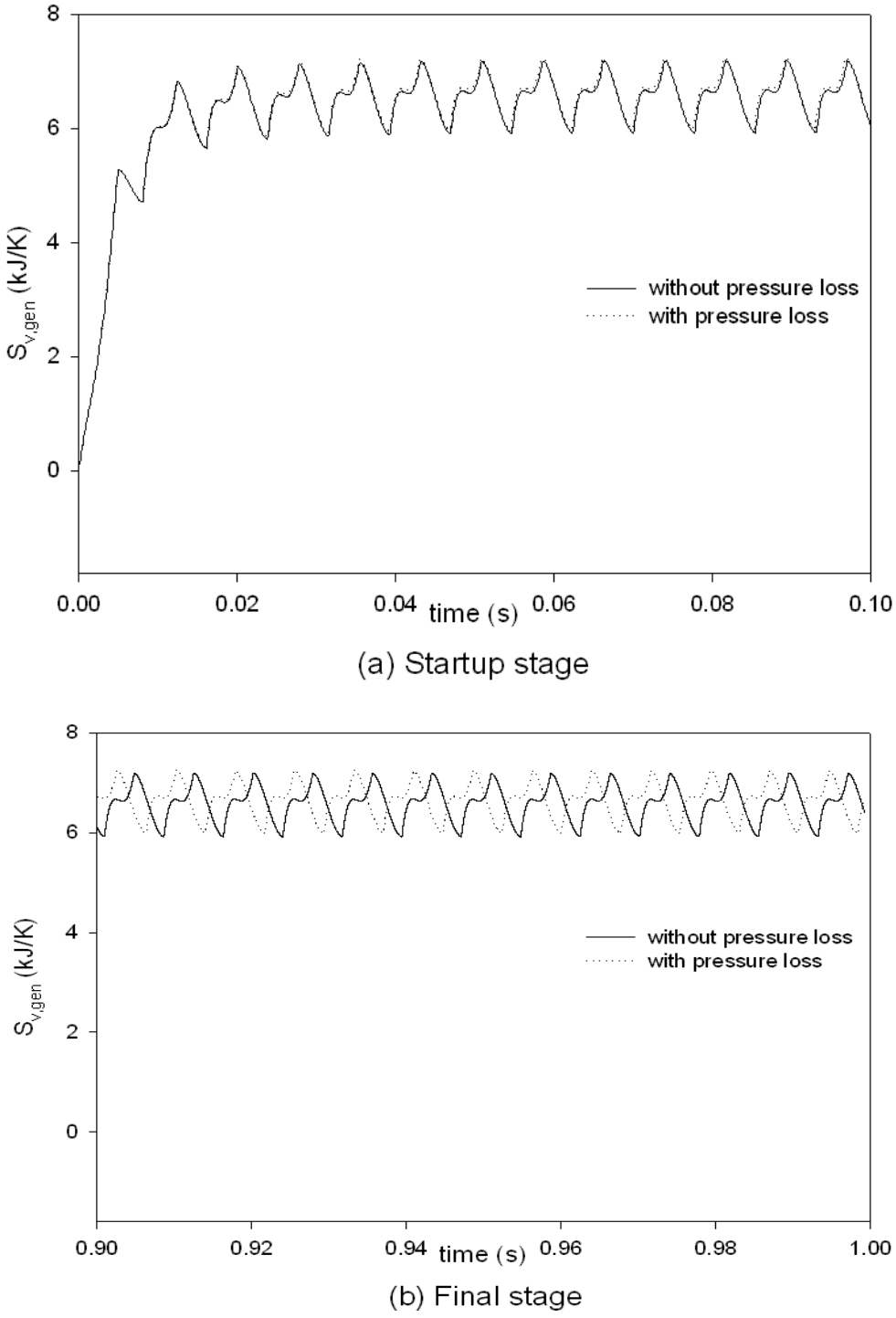

Figure 10 Entropy generation with or without pressure loss at bend in the vapor plug 2

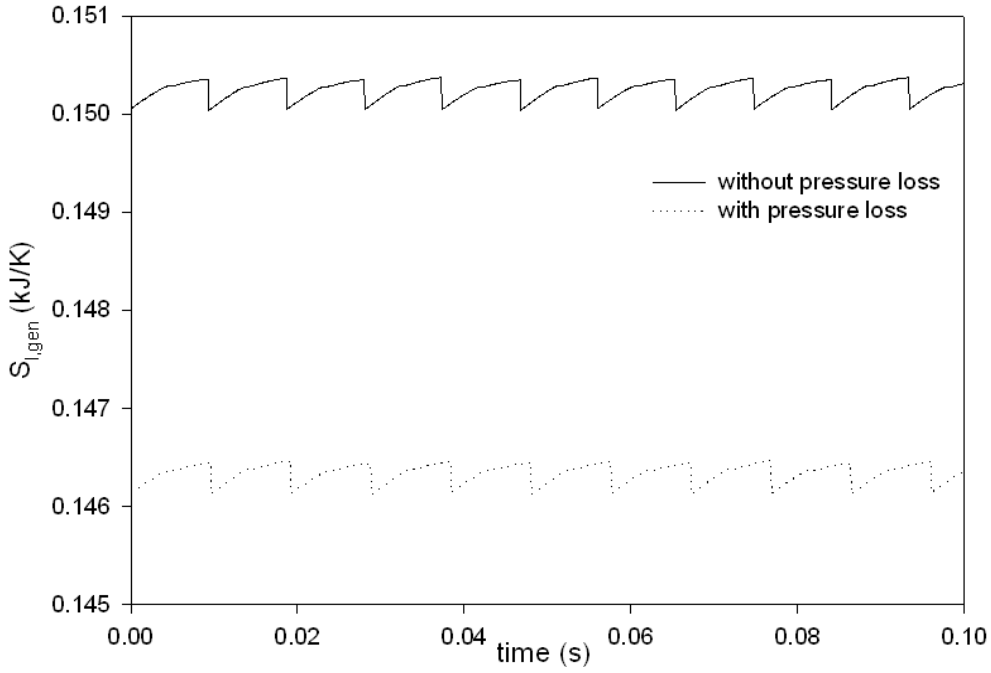

Figure 11 Entropy generation with or without pressure loss at bend in the liquid slug

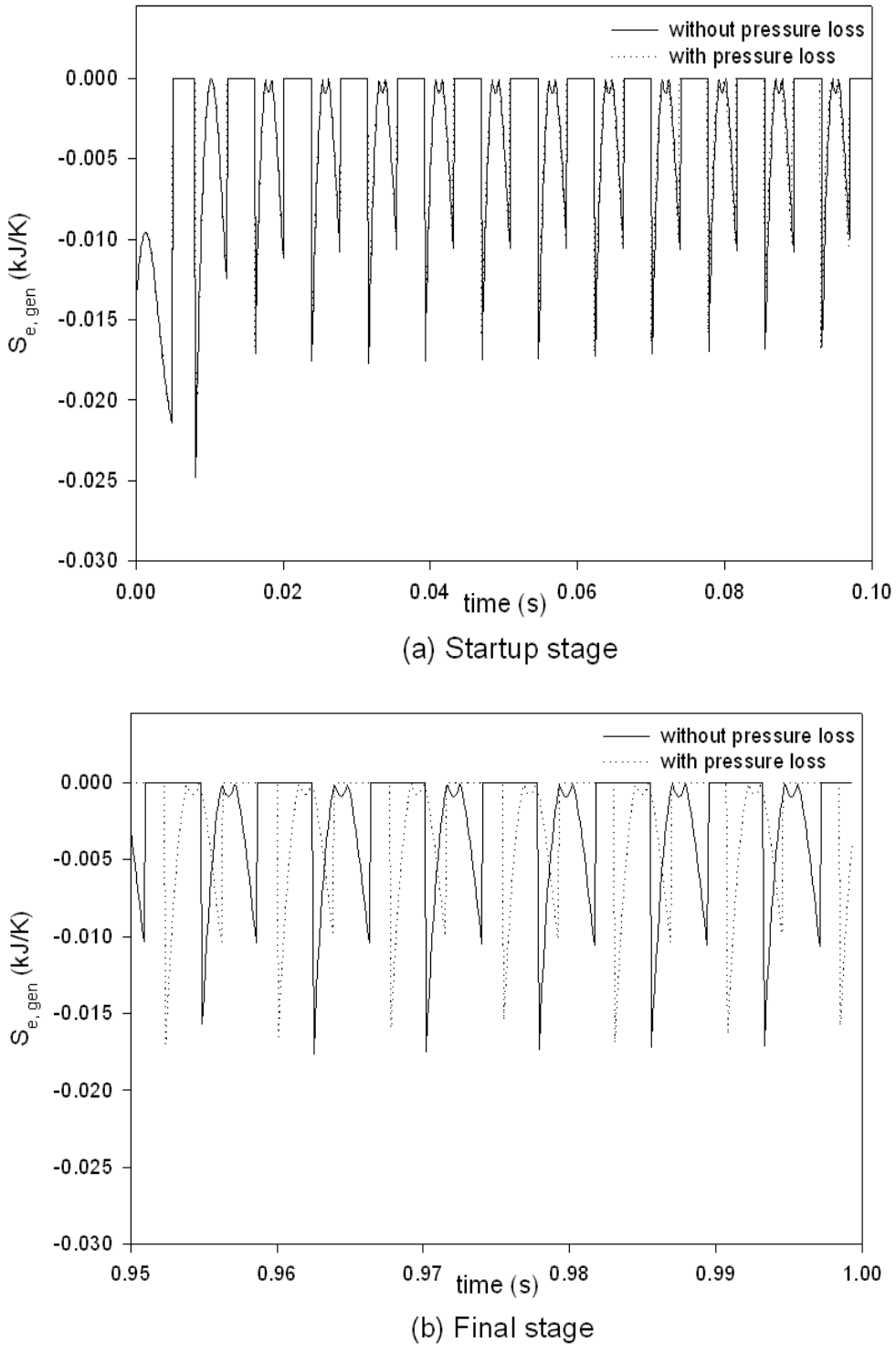

Figure 12 Entropy generation due to evaporation with or without pressure loss in vapor plug 1

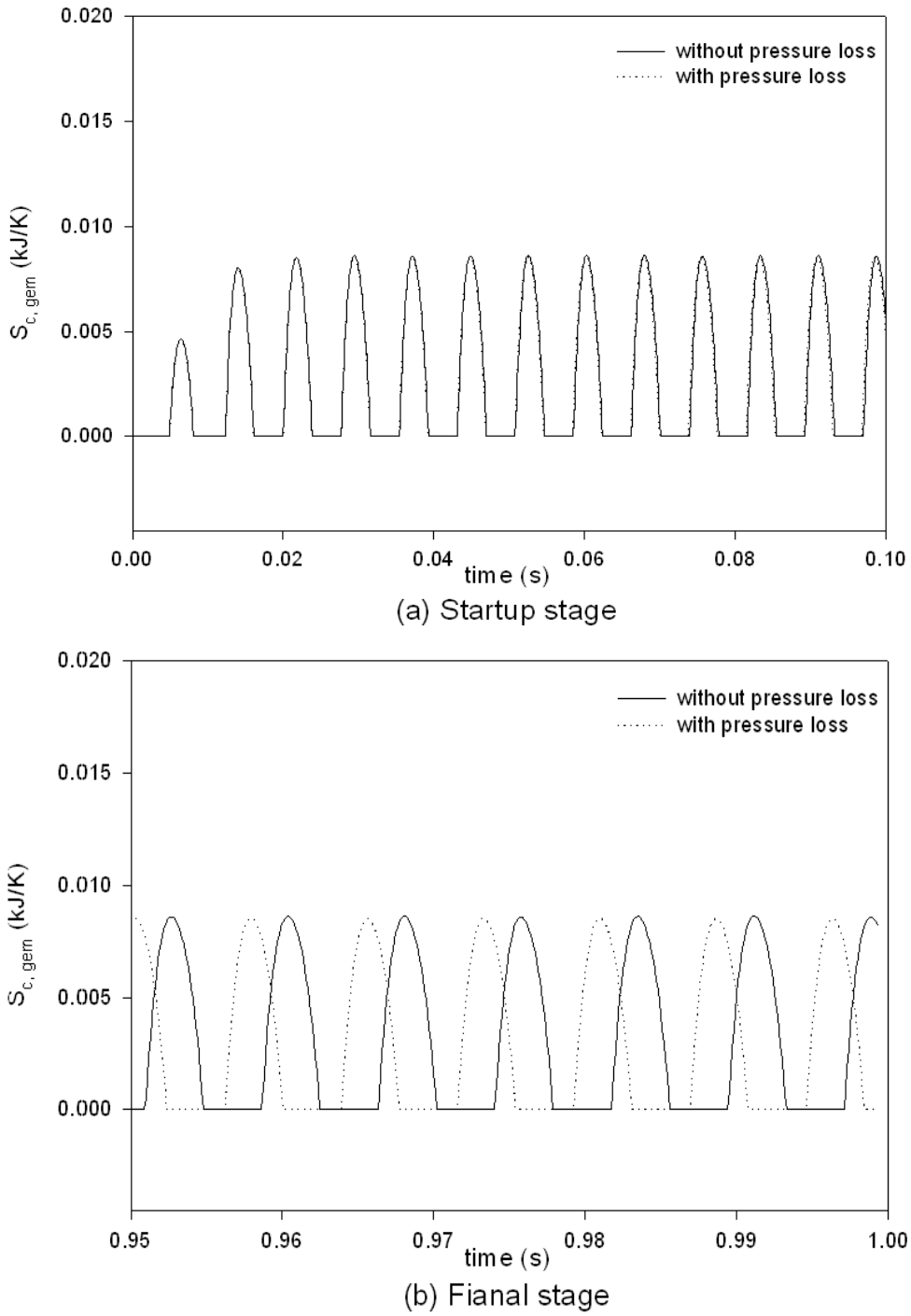

Figure 13 Entropy generation due to condensation with or without pressure loss in vapor plug 1

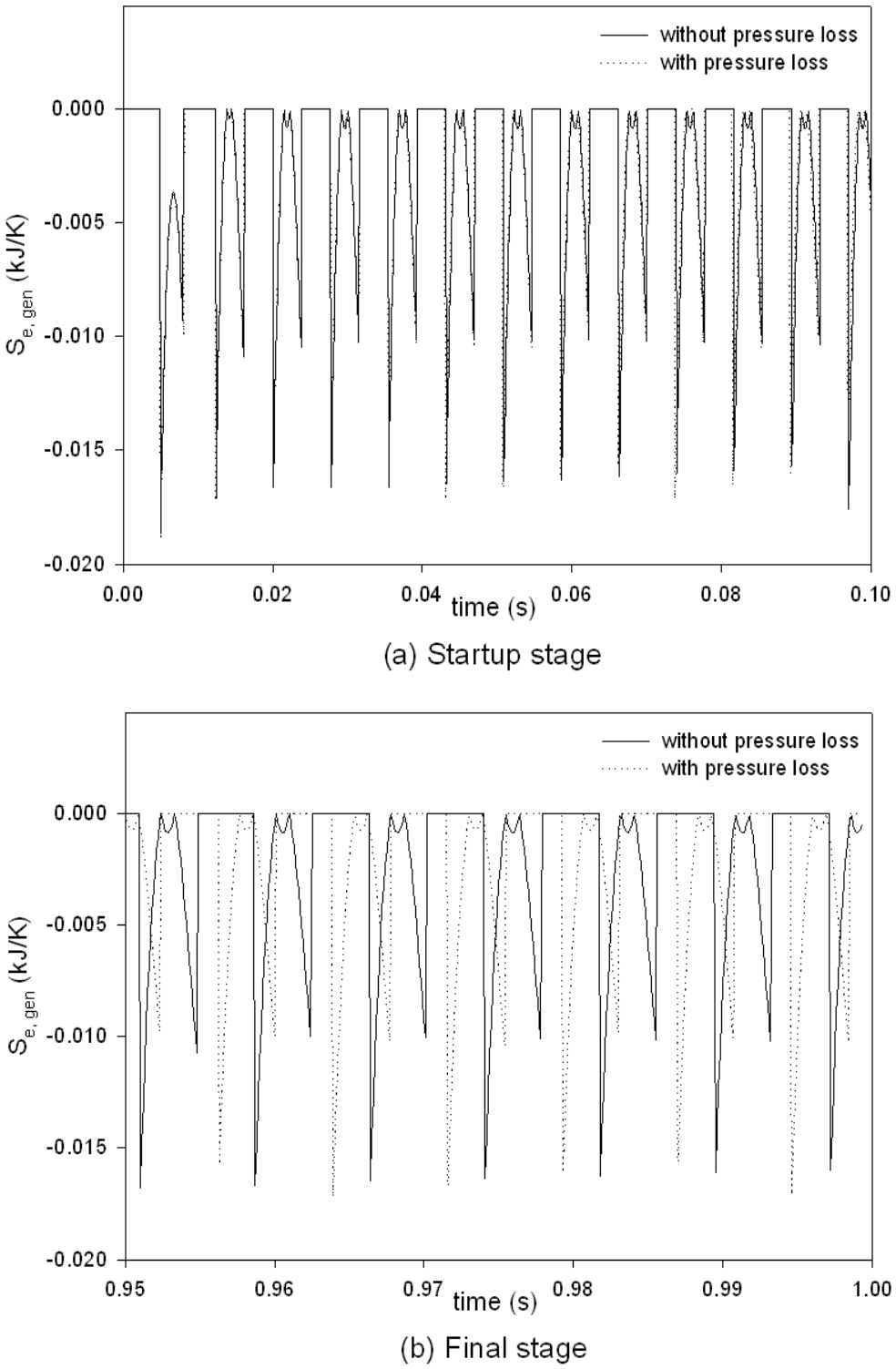

Figure 14 Entropy generation due to evaporation with or without pressure loss in vapor plug 2

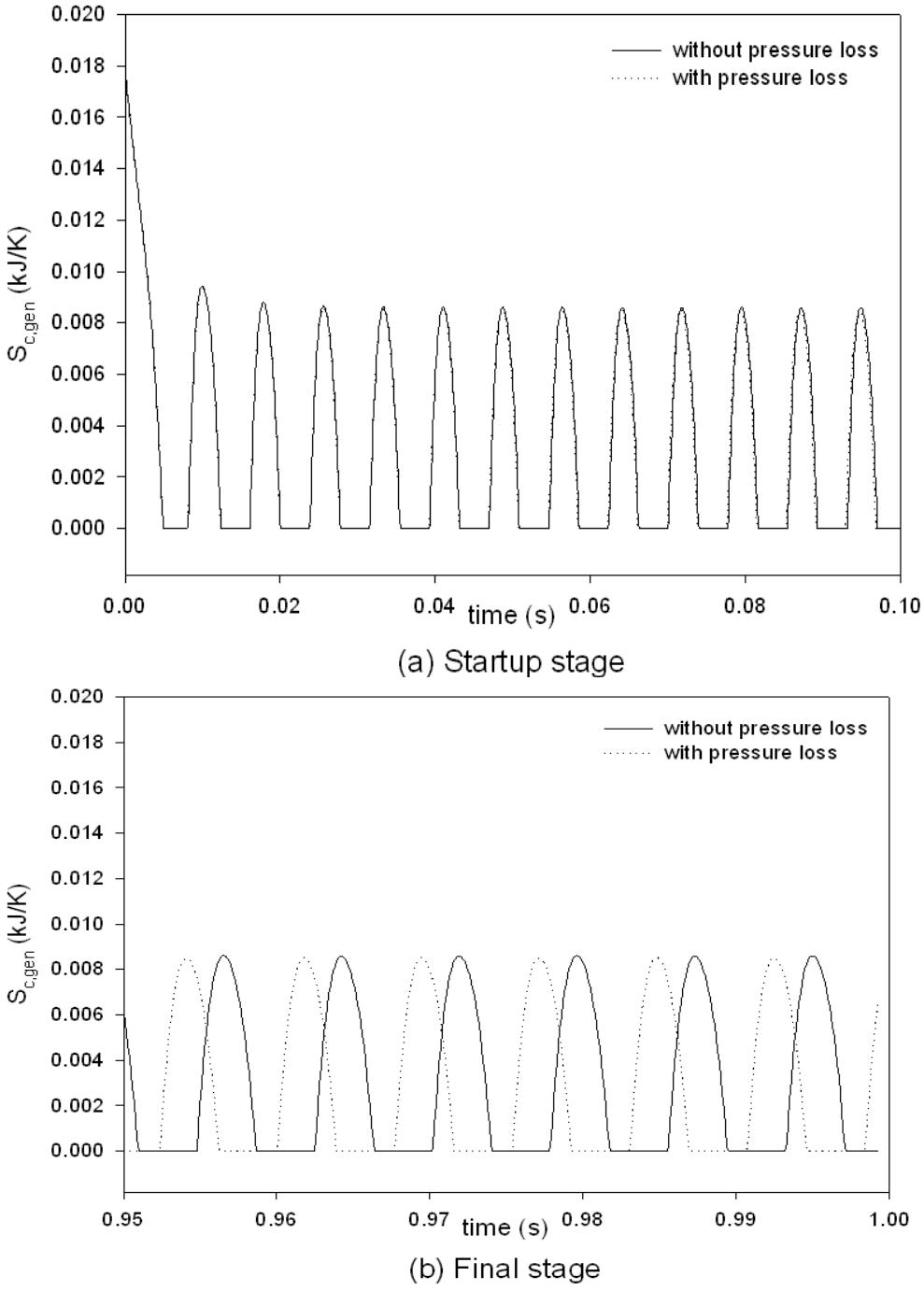

Figure 15 Entropy generation due to condensation with or without pressure loss in vapor plug 1

Figures 16 and 17 present the entropy generation due to the sensible heat of the liquid slug with or without the pressure loss in the heating section and the cooling section, respectively. Likewise as shown in Figs. 12-15, the frequencies of the entropy generation with the pressure loss are faster than those without the pressure loss in the final stage.

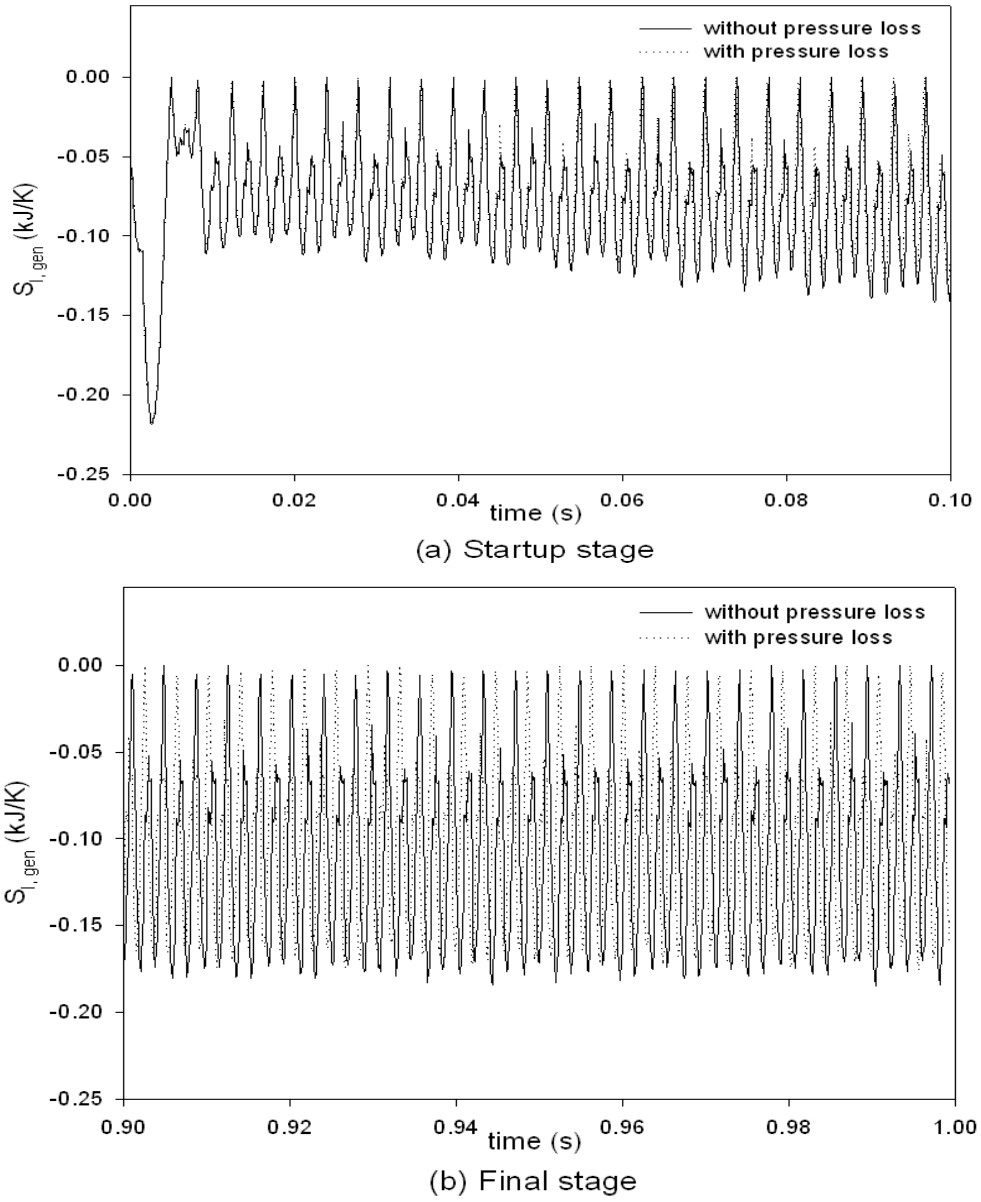

Figure 16 Entropy generation due to sensible heat into liquid slug with or without pressure loss

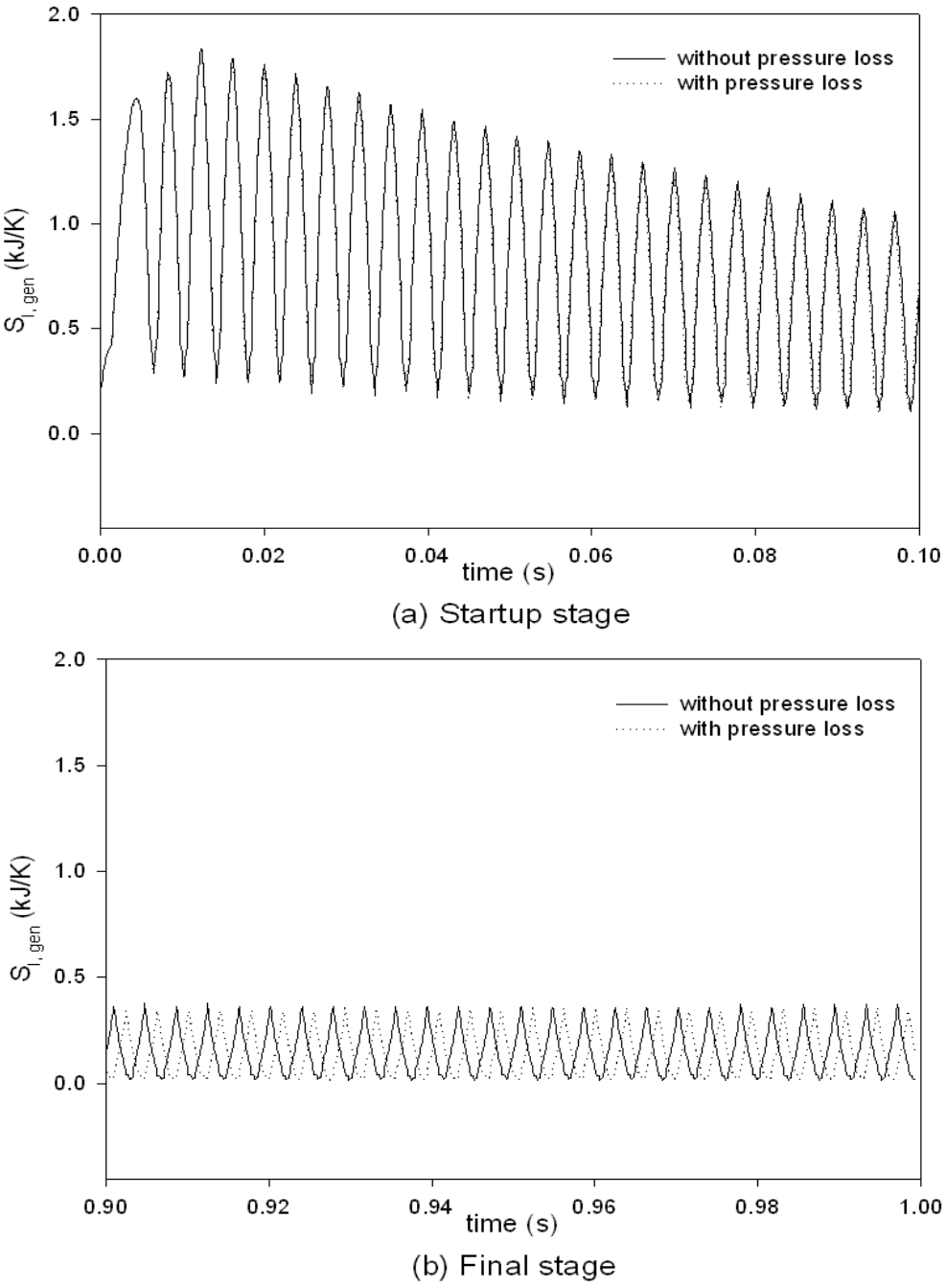

Figure 17 Entropy generation due to sensible heat out of liquid slug with or without pressure loss

Figure 18 shows the entropy generation due to the friction of the liquid slug with or without the pressure loss at the bend. The entropy generation with the pressure loss is higher than that without the pressure loss. However, the difference of the entropy generations due to the friction is small. Therefore, the friction can be ignored in the entropy generation. Figure 19

presents the above mentioned entropy generations with or without the pressure loss at the bend. The entropy generations are almost the same regardless of the pressure loss. However, the frequencies of the entropy generation with the pressure loss are quicker than those without the pressure loss at the bend.

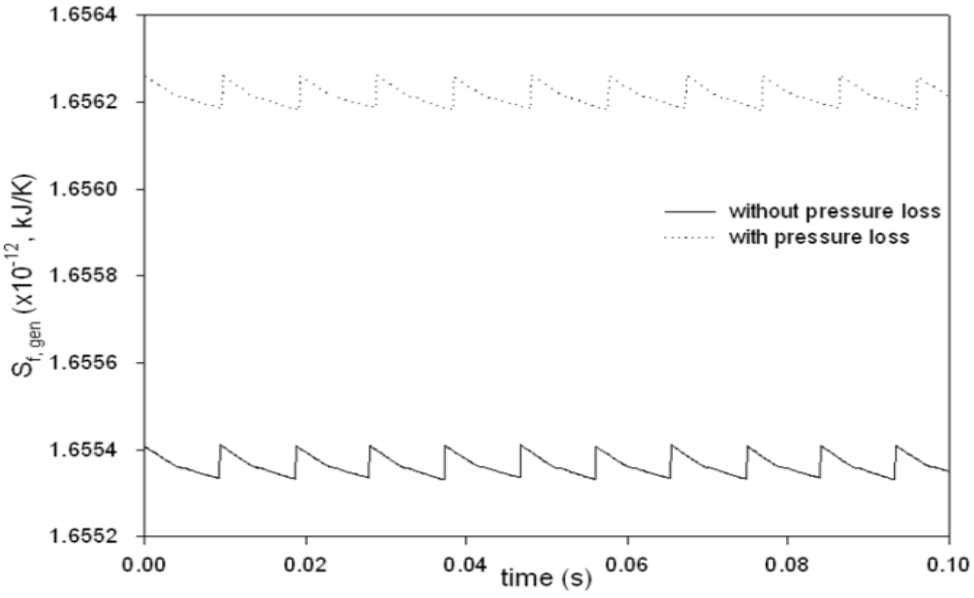

Figure 18 Entropy generation due to friction in liquid slug with or without pressure loss

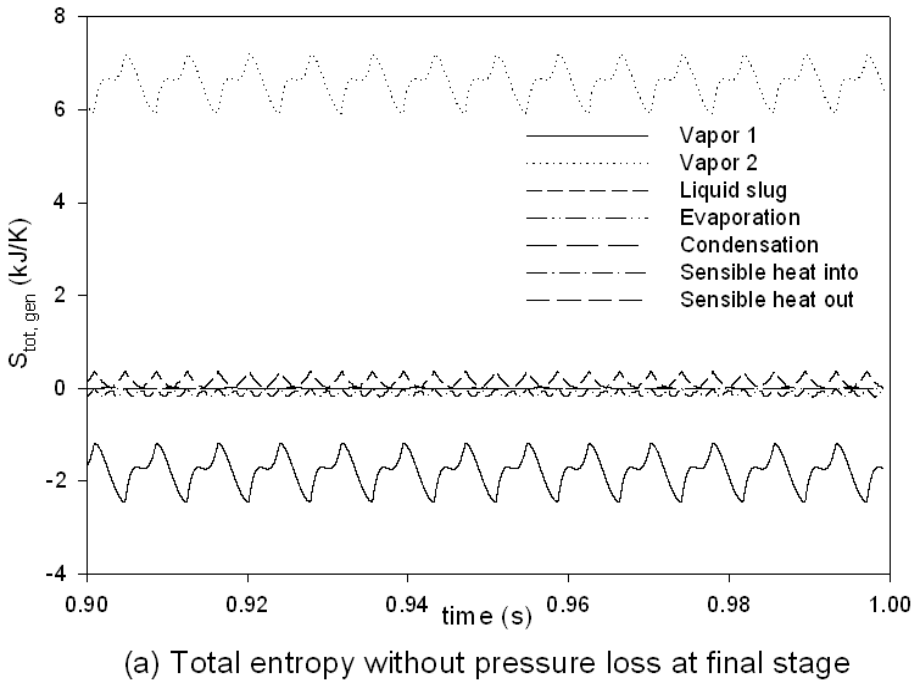

(a) Total entropy without pressure loss at final stage

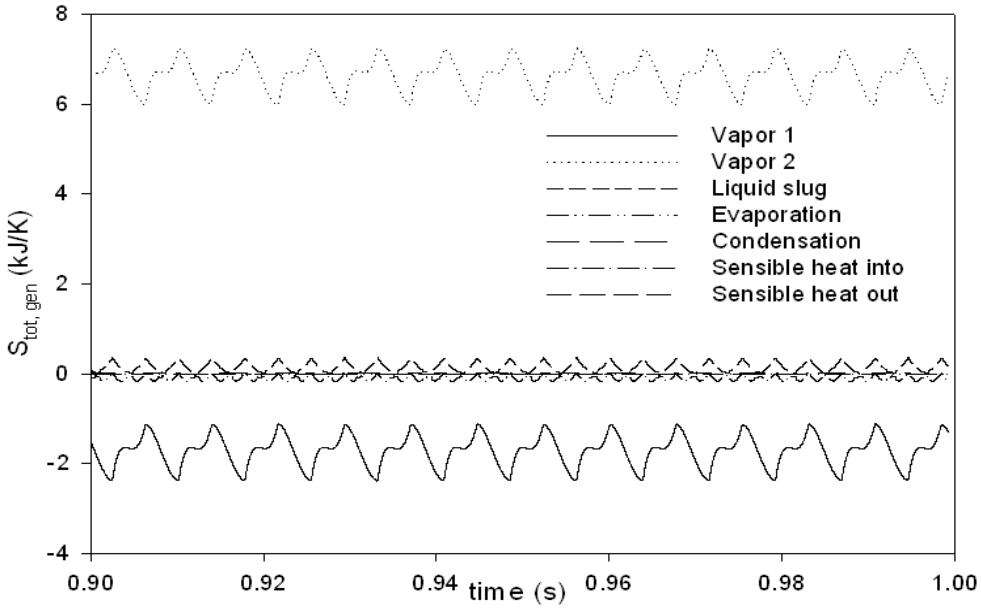

(b) Total entropy generation with pressure loss at final stage

Figure 19 Total entropy generation with or without pressure loss at bend

2.4 Conclusions

The entropy generation in the U-shaped PHP has been investigated in consideration of the initial temperatures and the pressure loss at the bend. The entropy generations are calculated from the variations of vapor mass, the liquid temperature, latent heat, sensible heat, and friction.

In result, the entropy generations are sensitively affected by the initial temperature, and the variation of the vapor mass is the main cause of the entropy generation. The amplitude of the entropy generation is irrelevant to the pressure loss at the bend. However, the frequency of the entropy generation with the pressure loss is faster than those without the pressure loss.

CHAPTER 3 Random Noise of Wall Temperature

3.1 Physical Model

3.1.1 Problem Description

Most researchers had investigated the heat transfer in PHPs based on the assumption that the heating and cooling section temperatures are constant. However, heating and cooling section temperatures are usually not constant in the real operation as it can fluctuate by changing of heating load, cooling condition or even oscillation of liquid slugs. Effects of fluctuations of heating and cooling section temperatures on the performance of a PHP are investigated in this paper. Effects of amplitude, frequency and standard deviation of the temperature fluctuations on the performance of the PHP are investigated.

3.1.2 Governing Equations and Random noise input of wall temperature for Pulsating Flow

To consider the effects of fluctuations of the wall temperatures on the performance of PHP, the following heating and cooling section temperatures are considered:

$$T_H(t) = [T_{H0} + A_H \cos(\omega t + \phi)](1 + \varepsilon_H / T_{H0}) \tag{42}$$

$$T_C(t) = [T_{C0} + A_C \cos(\omega t)](1 + \varepsilon_C / T_{C0}) \tag{43}$$

The fluctuations of wall temperatures include a periodic component and a random component. The periodic component has an amplitude of A_H or A_C and an angular frequency of ω. The phase difference between the periodic components of heating and cooling sections is ϕ. The random component is characterized by a random fluctuation ε_H or ε_C. The random fluctuation can have different patterns in graph according to mean value and standard deviation. The following normal distribution [20] is used to obtain ε_H or ε_C:

$$\varepsilon = \sigma \frac{(\sum_{i=1}^{n} RN_i) - \frac{n}{2}}{\sqrt{n/12}} \tag{44}$$

where RN_i is a random number between 0 to 1, and n is an integer.

3.2 Results and Discussion

3.2.1 Effect of random temperatures, T_H and T_C, with different amplitudes of the heating and the cooling section

The parameters used in the simulation are: L_e=0.1m, L_c=0.1m, L_p=0.2m, d=3.34mm, and $h_e = h_c = 200\,W/m^2K$. The base temperatures for heating and cooling sections are T_{H0} =393.4 K and T_{C0}=293 K, respectively. Figure 20 illustrate the changes of temperature of the heating and the cooling sections due to periodic and random fluctuations. The frequency of the periodic fluctuation was f = 9 Hz, and the standard deviations for the random fluctuation are σ_H =σ_C=2.0 K. The fluctuation of the temperatures of the heating and the cooling section increase when increasing amplitudes. Figure 21 shows the different liquid slug displacements with different A_H and A_C. As shown in Fig. 21 (a), the liquid slugs have the similar movements when the amplitude of the heating section increases; however, the period of oscillatory flow slightly increases with increasing A_H. The pattern of the graph shows the very small high-frequency fluctuations with time due to the random fluctuation of the temperature of the heating section. Figure 21 (b) presents the change of the liquid slug displacement for different A_C. The liquid slug displacements show very little difference for different amplitudes of periodic fluctuation; however, very small high-frequency fluctuations are still observed. Figure 22 presents the temperatures of the vapor plug 1 for different A_H and A_C. The maximum temperature of vapor plug 1 gradually decreases when A_H increases as shown in Fig. 22 (a). However, as A_H increases, the temperature of the vapor plug 1 is more random during evaporation than that during condensation, because A_C is equal to 0.0 for Fig. 22 (a). Figure 22 (b) shows the effect of amplitude of periodic fluctuation of the cooling section temperature on the vapor temperature. As A_C increases, the minimum vapor temperature decreases during condensation, while the vapor temperature during evaporation is not affected by A_C. Figure 23 shows the pressure of the vapor plug 1 for different amplitudes of periodic wall temperature fluctuation. The trends of vapor

pressure change with the increment of the amplitude in the heating and the cooling section are quite similar with those in Fig. 22.

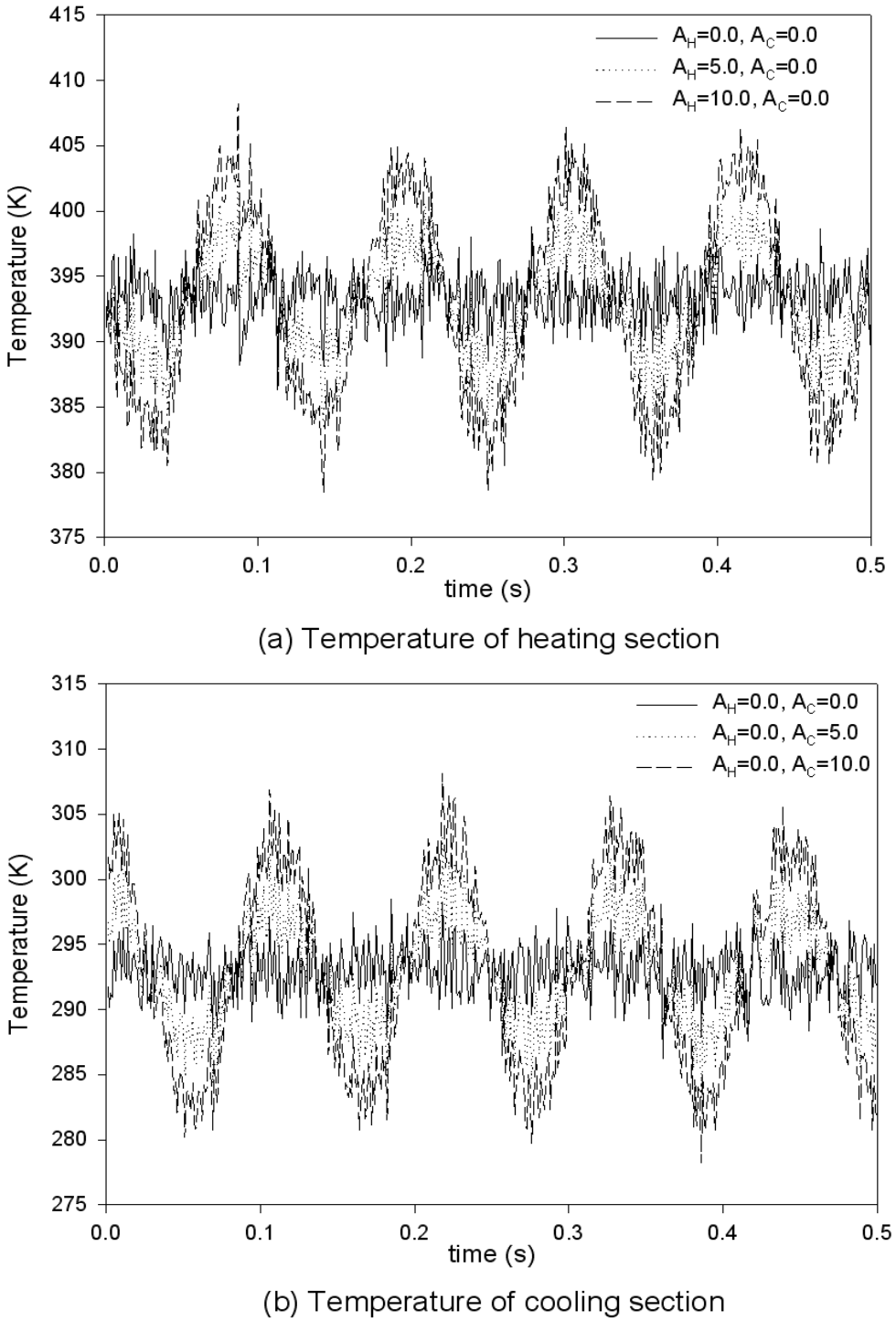

Figure 20 Fluctuation of heating and cooling section temperatures for different A_H and A_C

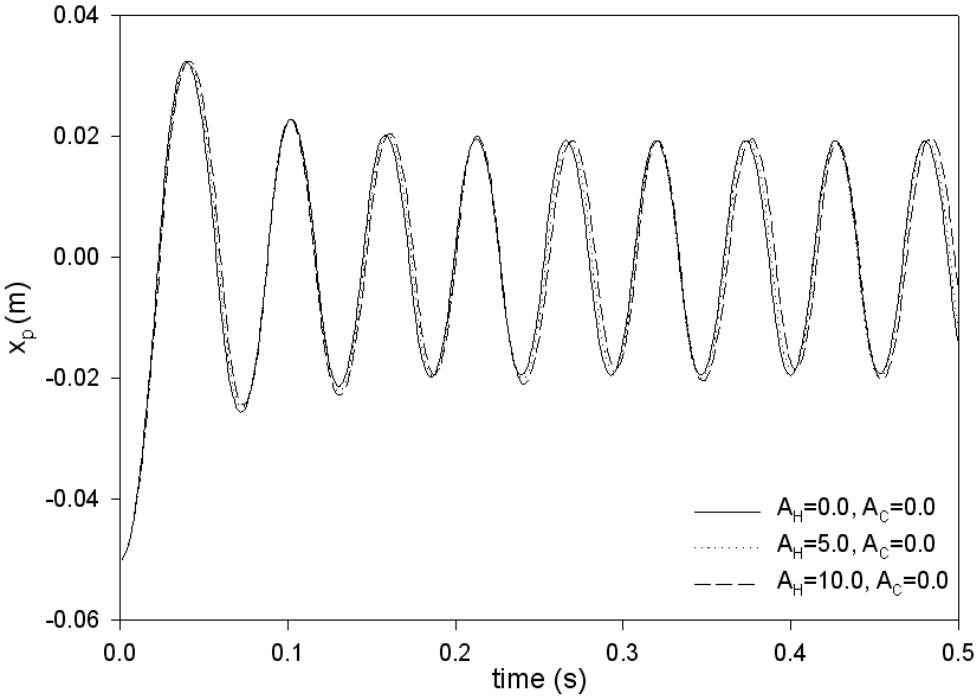

(a) Liquid slug displacement for different A_H

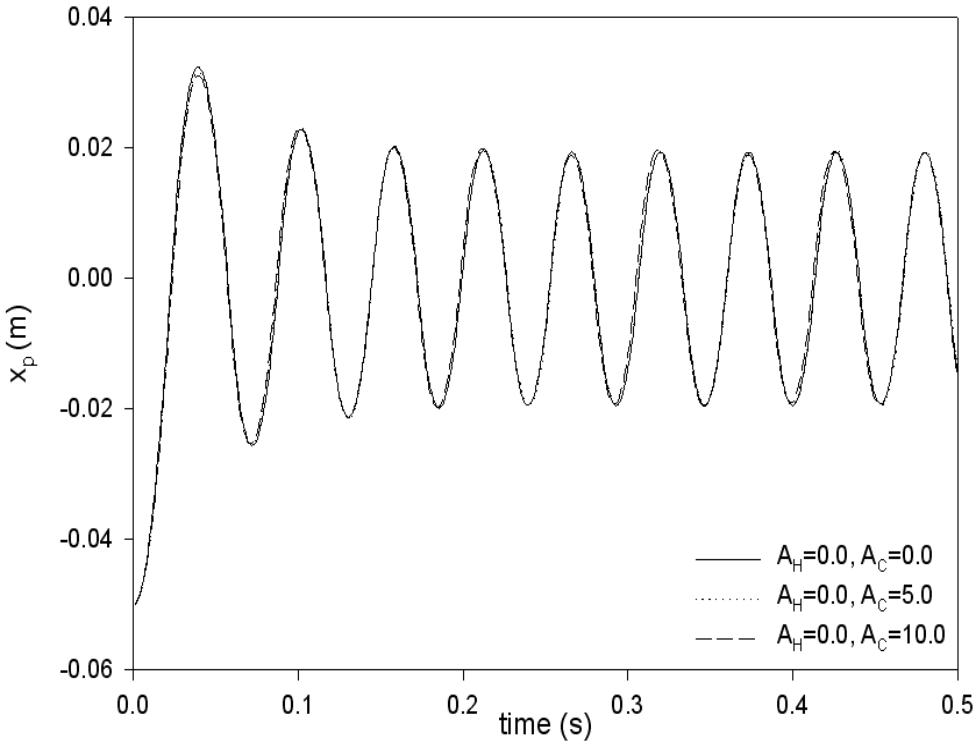

(b) Liquid slug displacement for different A_C

Figure 21 Liquid slug displacements for different A_H and A_C

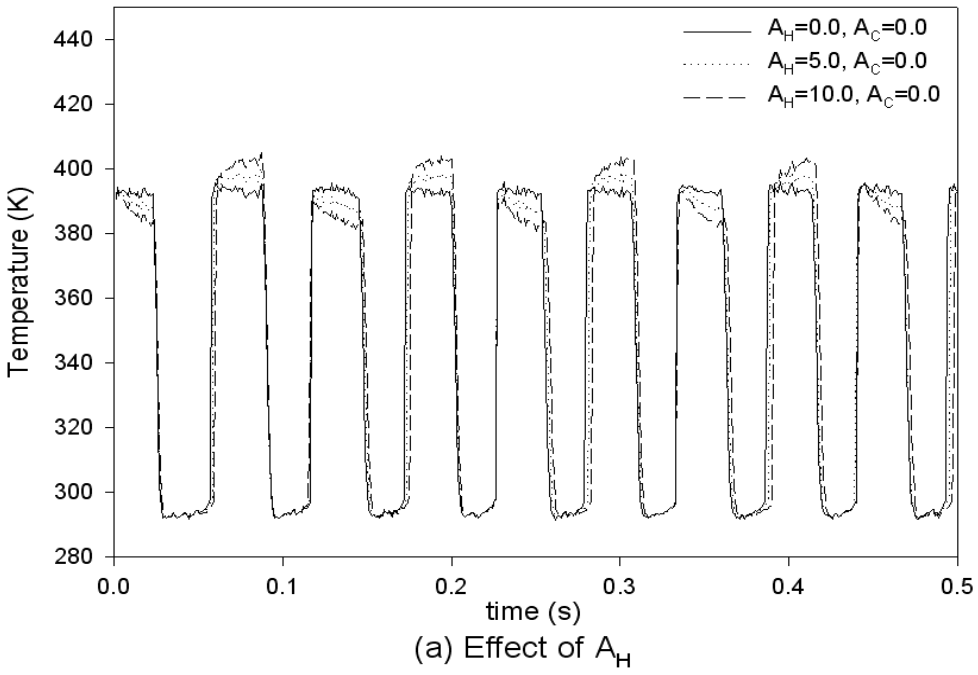

Figure 22 Temperature of vapor plug 1 for different A_H and A_C

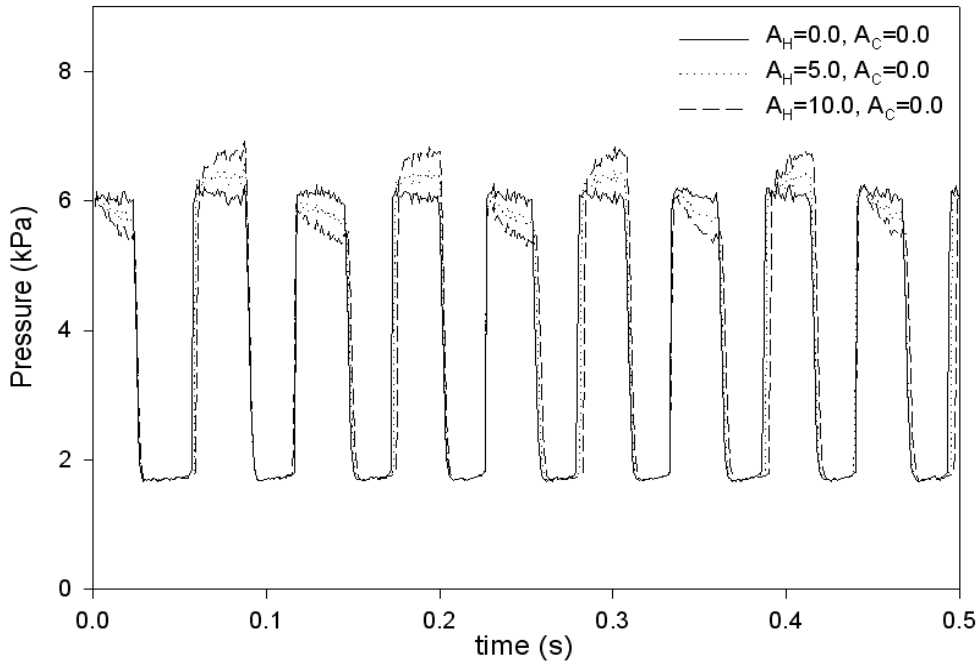

(a) Effect of A_H

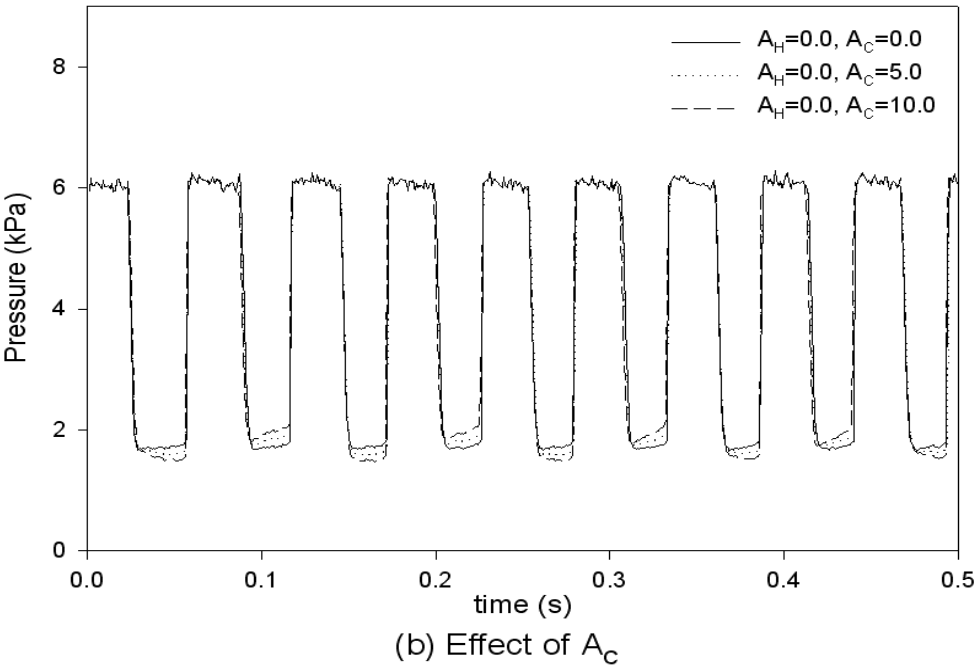

(b) Effect of A_C

Figure 23 Pressure of vapor plug 1 for different A_H and A_C

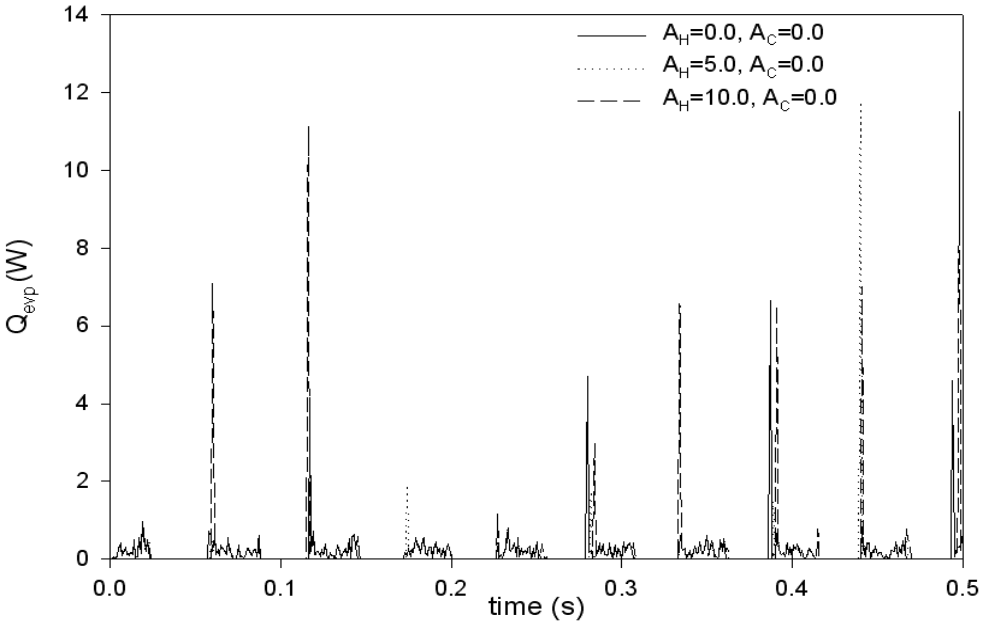

(a) Evaporation

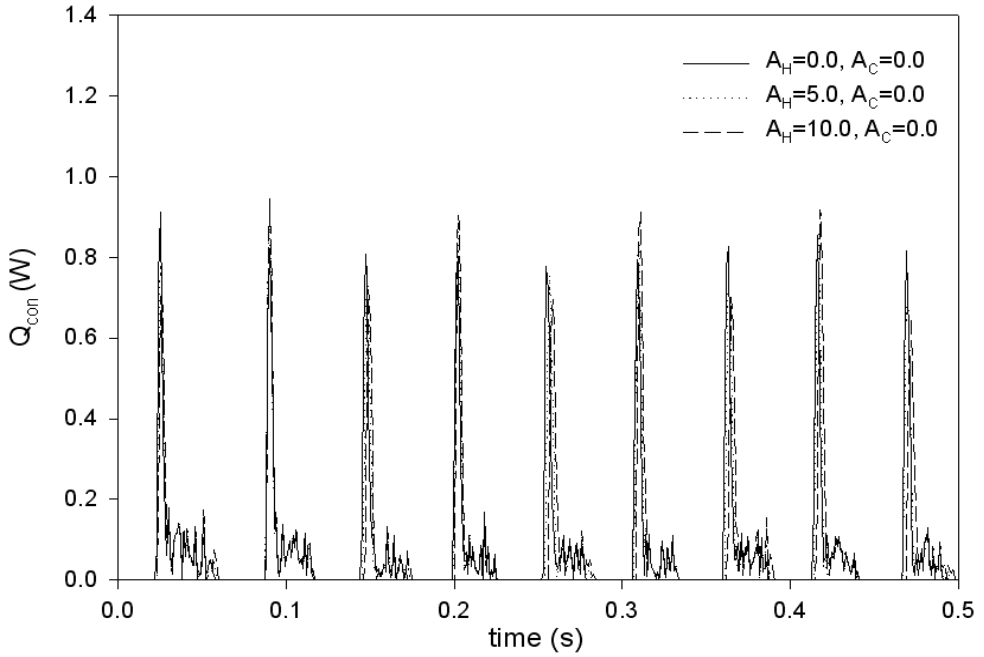

(b) Condensation

Figure 24 Latent heat transfer of vapor plug 1 for different A_H

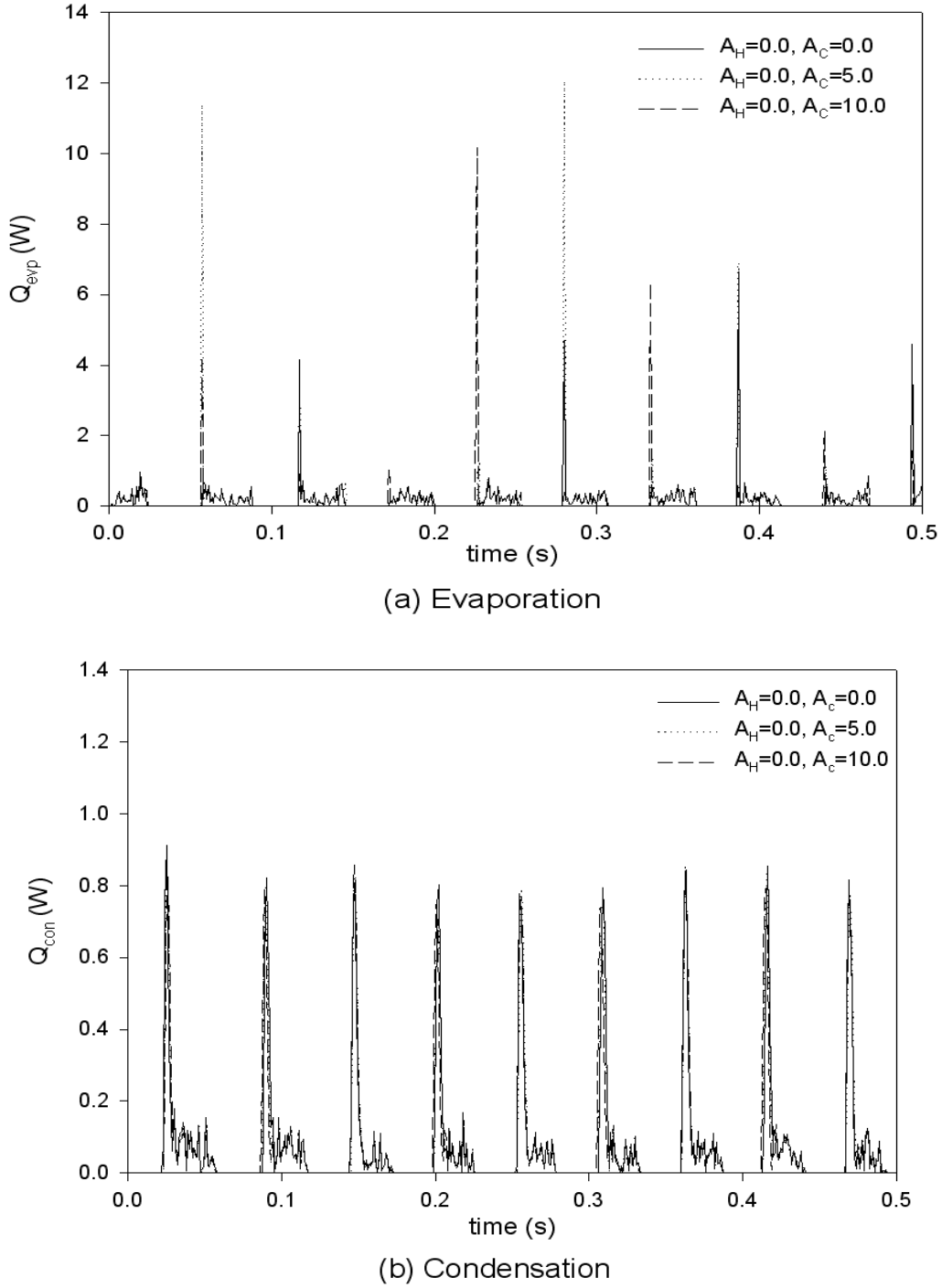

Figure 25 Latent heat transfer of vapor plug 1 for different A_C

Figure 24 (a) shows the change of latent heat in the vapor plug 1 with A_H. Although the latent heat transfer at different A_H showed different variations, its effects on the overall evaporation heat transfer is very insignificant. Figure 24 (b) shows the latent heat transfer in the

cooling section with increasing A_H, and it is shown that there is delay with increasing A_H. The latent heat transfer in the condenser section at different A_H shows the similar patterns. Figure 25 shows the latent heat transfer at the vapor plug 1 with increasing A_C. It can be seen that the patterns of Fig. 25 (a) and (b) are similar to those in Fig. 24 (a) and (b). Figure 26 and 27 present the effect of wall temperature fluctuation on the sensible heat transfer by the liquid slug. Figure 8 shows the phenomenon of the delay with increasing A_H. The sensible heat is the highest when the amplitude is equal to 0.0; however, the value of the sensible heat changes randomly as depicted in Fig. 26 (a). The sensible heat transferred out of liquid slug shows similar pattern for different A_H because the amplitude is not applied to the cooling section ($A_C = 0$) as shown in Fig. 26 (b). However, the sensible heat transferred out of the liquid slug shows delay with increasing A_H. The sensible heat transfer by liquid slug at different A_C is shown in Fig. 27. It can be seen from Fig. 27 (a) that sensible heat transfer increases with increasing A_C for most of the times. Due to the periodic components of the fluctuation, the sensible heat transfer exhibit some spikes at some instance and this behavior repeats periodically. The sensible heat transfer shows more delay with the high amplitude than the low amplitude. Figure 27 (b) has almost same pattern with Fig. 27 (a); however, the peak values of the sensible heat transferred out of the liquid slug are greater than those for sensible heat transferred into to the liquid slug. The random oscillation of the sensible heat transfer is preceded by the periodic fluctuation of the temperatures, T_H and T_C. Therefore, the fluctuations of the heating and cooling temperatures have significant effects on the performance of the PHPs.

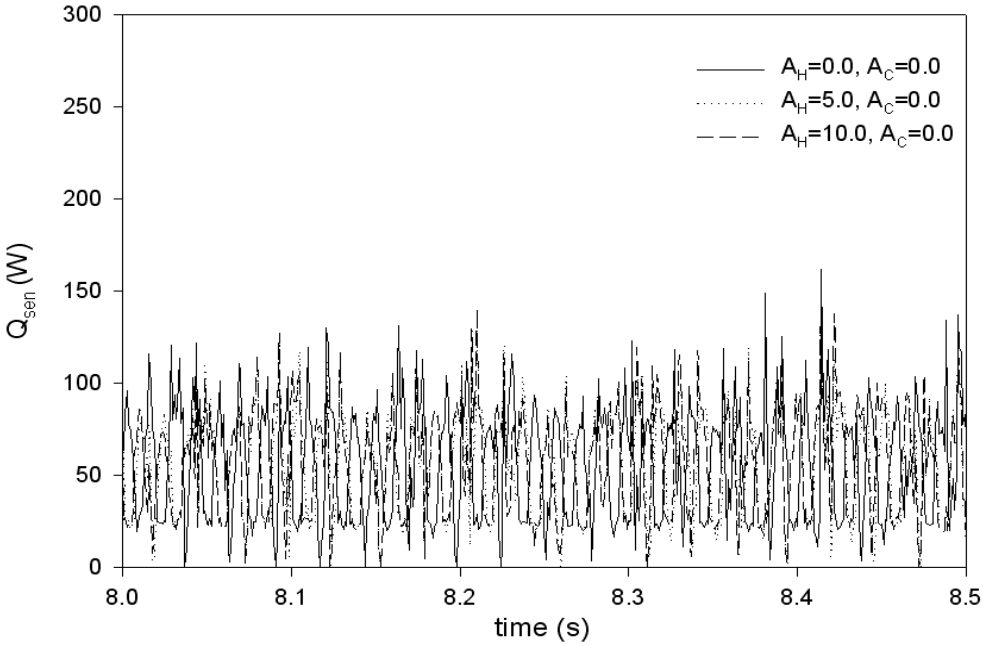

(a) Sensible heat transferred into the liquid slug

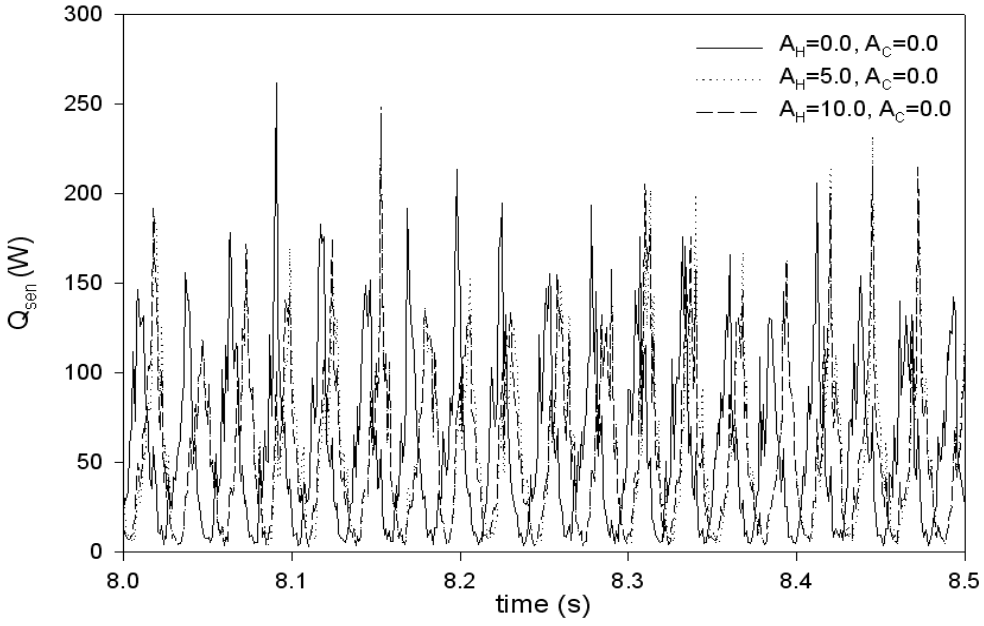

(b) Sensible heat transferred out of the liquid slug

Figure 26 Sensible heat transfer of the liquid slug for different A_H

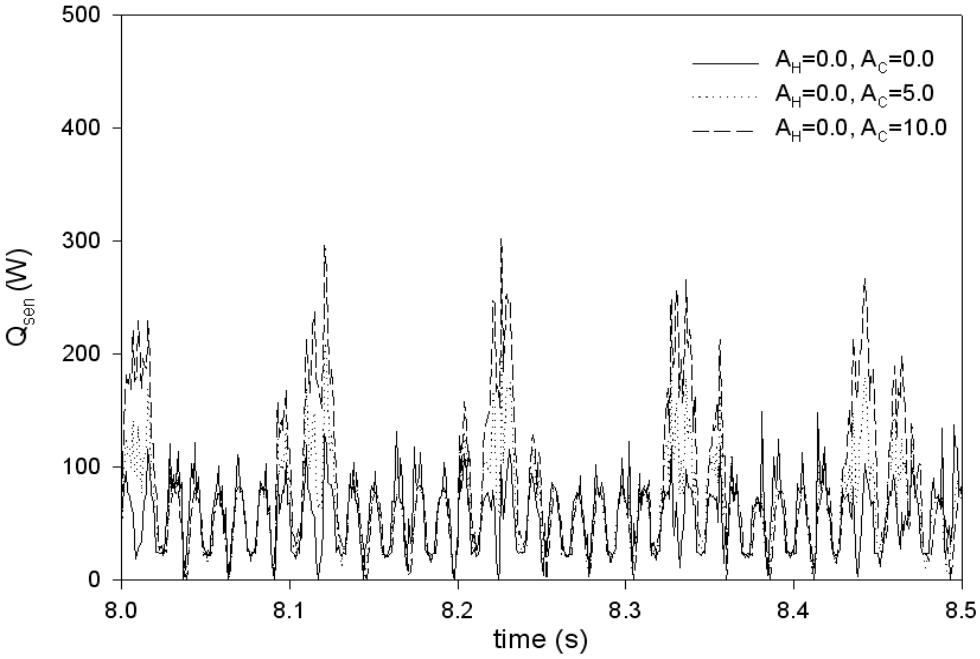

(a) Sensible heat transferred into the liquid slug

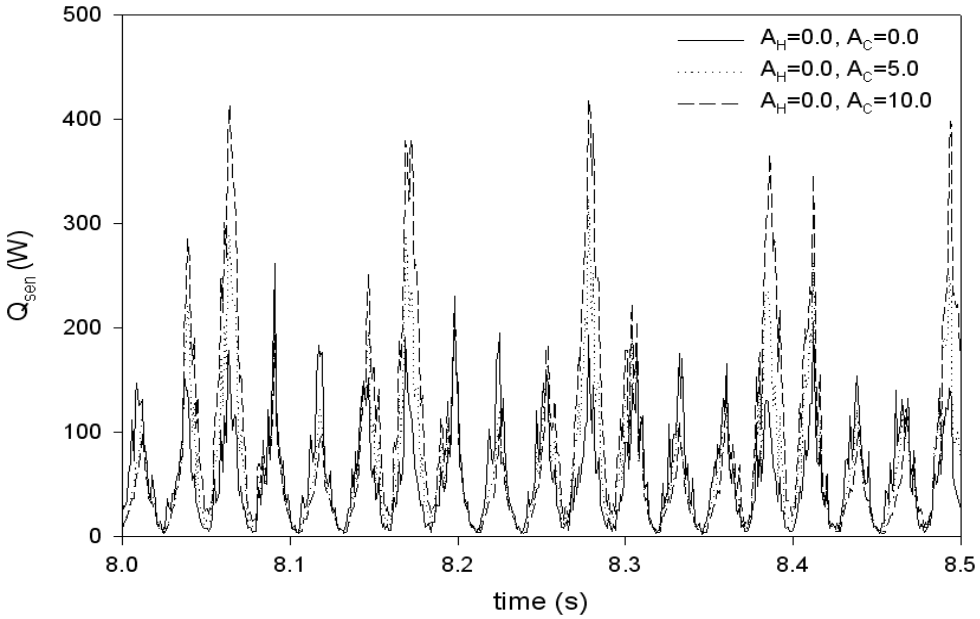

(b) Sensible heat transferred out of the liquid slug

Figure 27 Sensible heat transfer of the liquid slug for different A_C

3.2.2 Effect of random temperatures, T_H and T_C, for differnet frequency

Figures 28-32 show the effect of the frequency of the periodic component of temperature fluctuation on the performance of the U-shaped PHP. The amplitudes of the peroidic compoent

of the fluctuation are set as A_H = 10 K and A_C = 5 K, respectively. Figure 28 shows temperatures of the heating and the cooling sections for different frequencies.

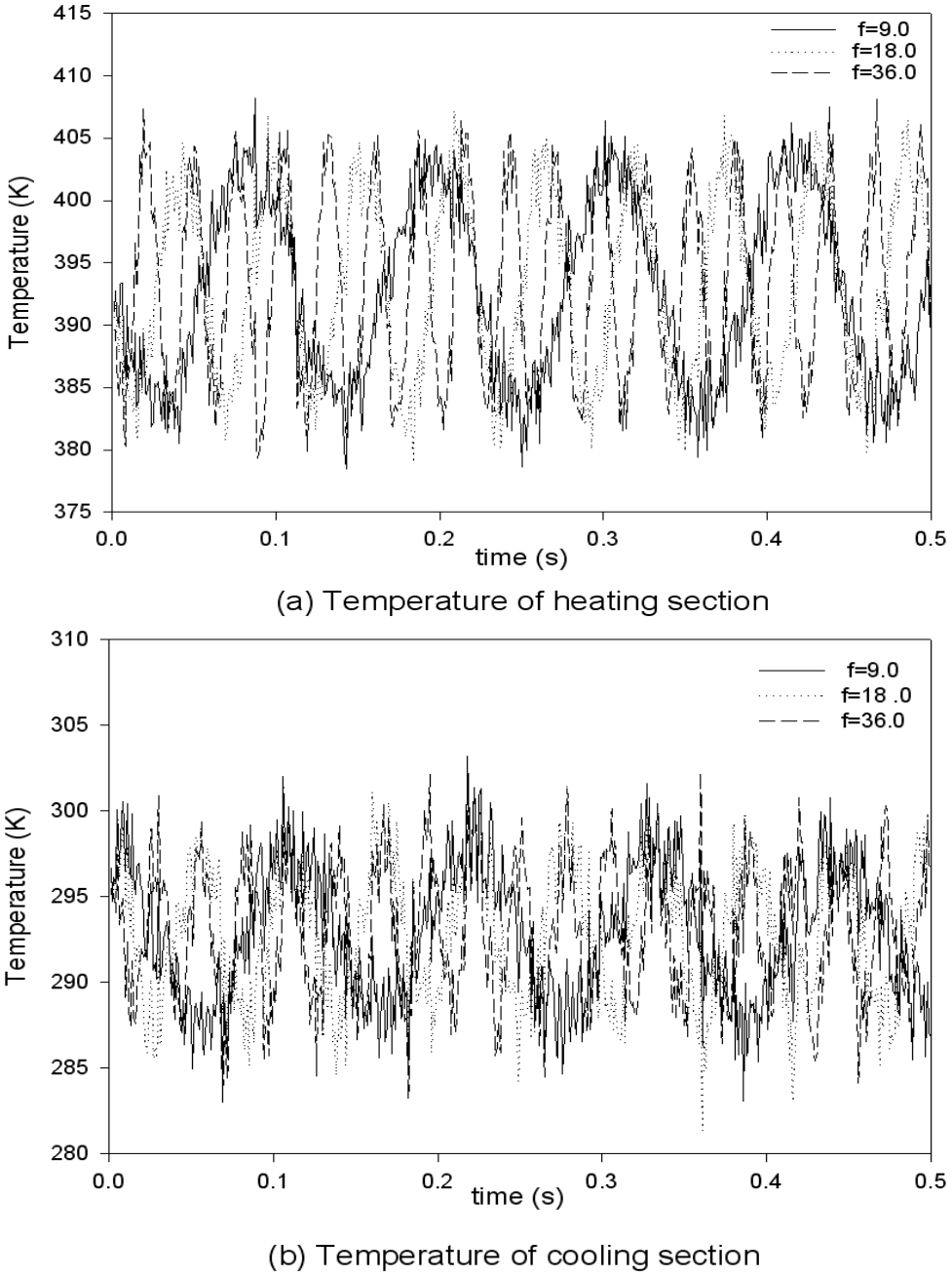

Figure 28 Temperatures of the heating and cooling section for different frequencies

Figure 29 illustrate the liquid slug displacements for different frequency of wall temperature fluctuations. The liquid slug has larger displacement with increasing frequency and the period of oscillation increases gradually.

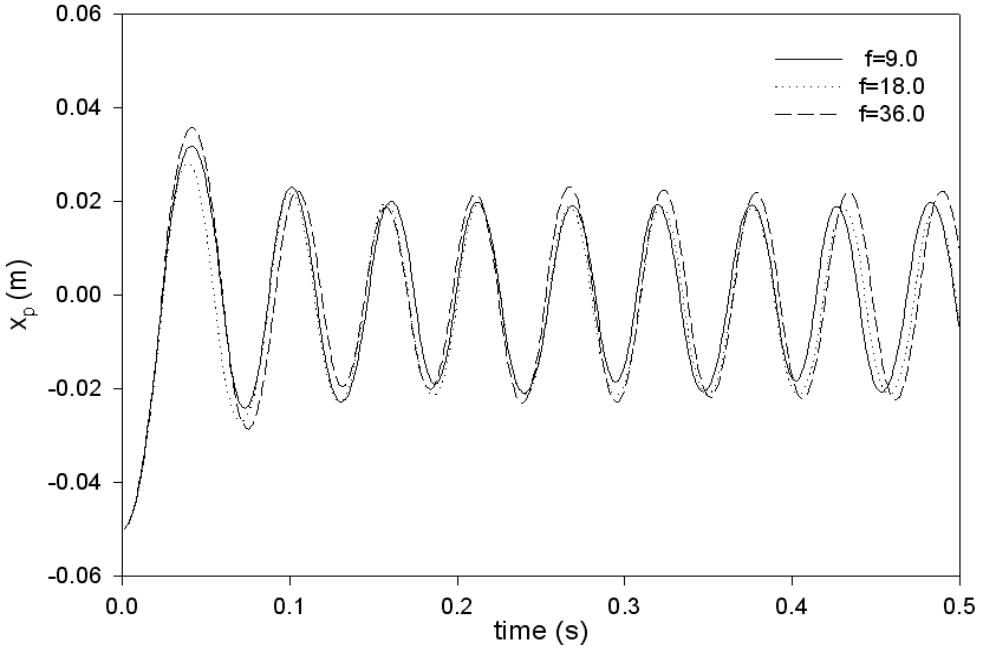

Figure 29 Liquid slug displacements for different frequencies

Figure 30 shows the temperature and pressure of vapor plug 1 for different frequencies. The magtitude of vapor temperature and pressure oscillations are different for different frequencies. The meximum (minuum) vapor temperature and pressure increase (decrease) with increasing frequency. Figure 31 shows latent heat transfer of the vapor plug 1 for differnet frequencies of the wall temeperature fluctuations. It can be seen from Fig. 31 (a) that the latent heat transfer in the heating section increases suddenly and then decreases rapidly. The peak values of evaporation heat transfer is higher when the frequency is higher. Figure 31 (b) presents quite constant pattern of the variation of the condensation heat transfer. The difference between the peak values of the latent heat transfer in the heating and the cooling sections is almost one order of magnitude. Figures 32 shows the sensible heat transfer by the liquid slug at different frequencies. It can be seen that the peak values of sensible heat transfer do not exhibit clear trend with the frequency. In other words, the maximum peak value amoung the three frequecies can be

achieved at any frequency, depending on the time. Thus, the frequency randomly affects the change and the cycle of pressures and temperatures of two vapor plugs, the displacement of the liquid slug, as well as the latent and sensible heat transfer.

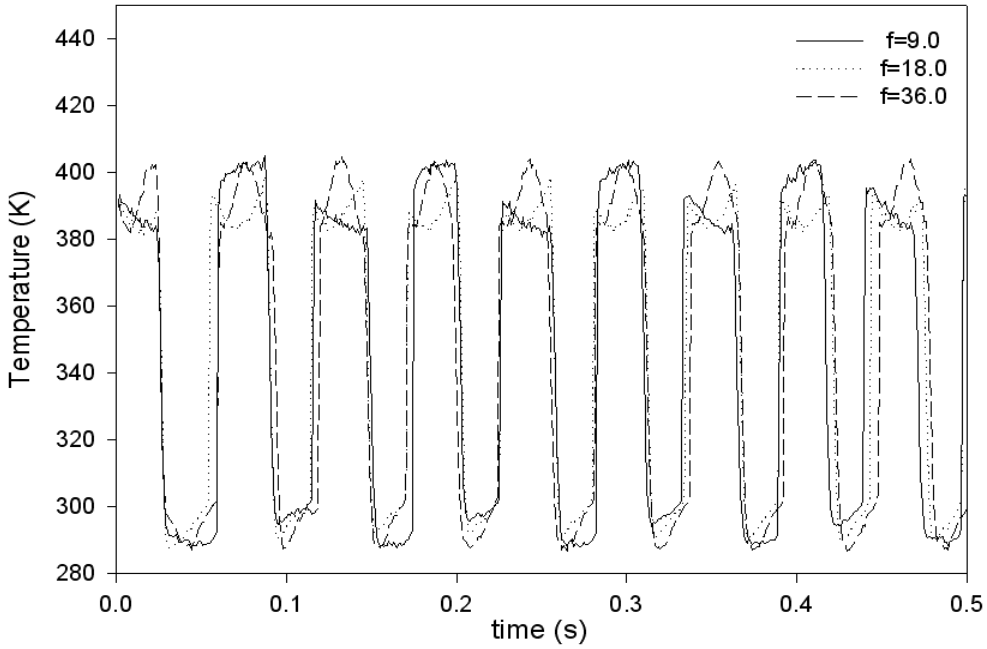

(a) Temperature

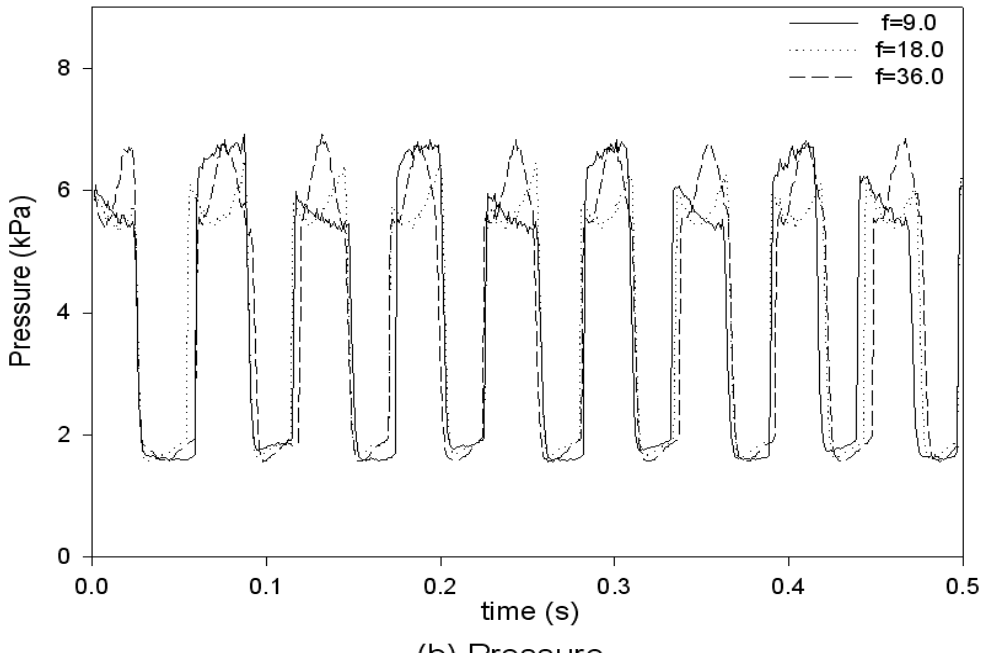

(b) Pressure

Figure 30 Temperature and pressure of vapor plug 1 for different frequencies

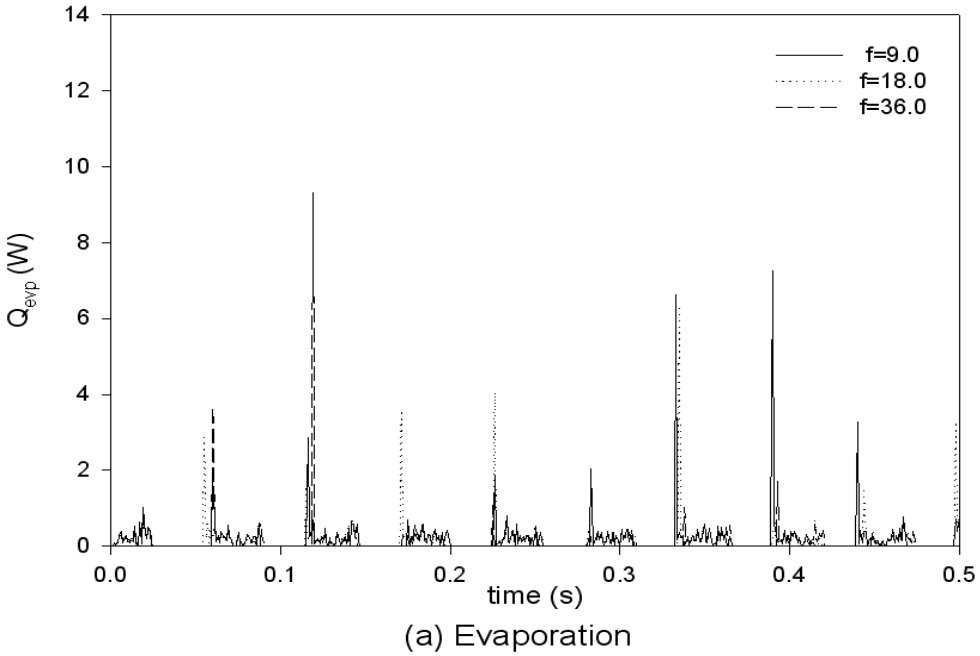

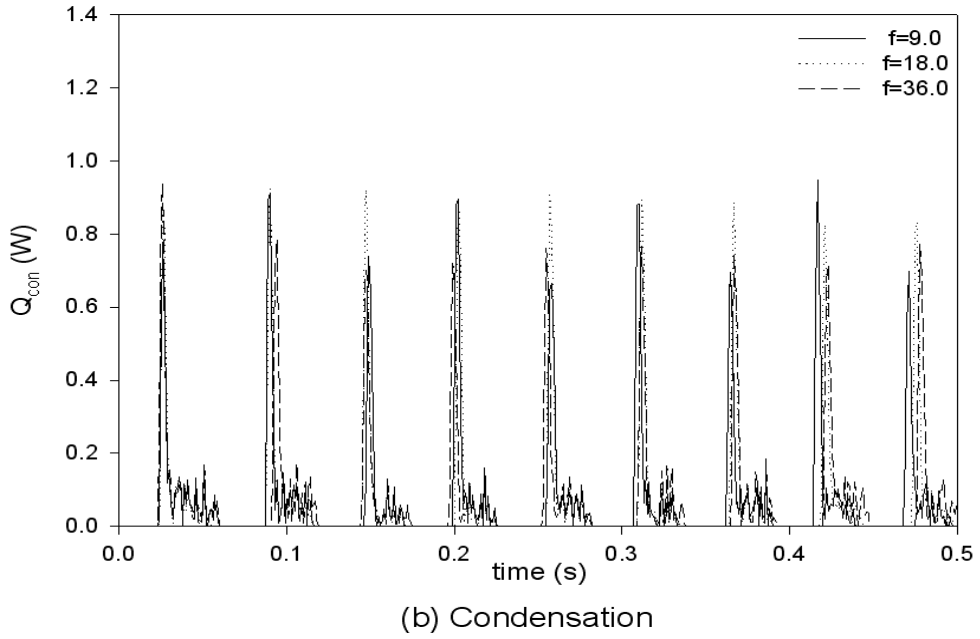

Figure 31 Latent heat transfer of vapor plug 1 for different frequencies

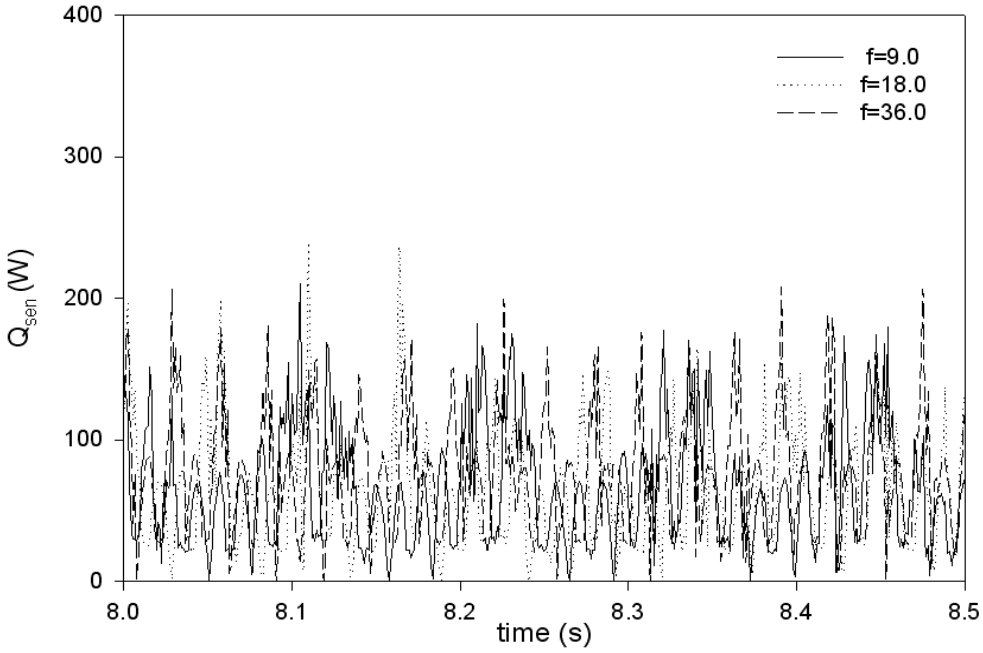

(a) Sensible heat transferred into the liquid slug

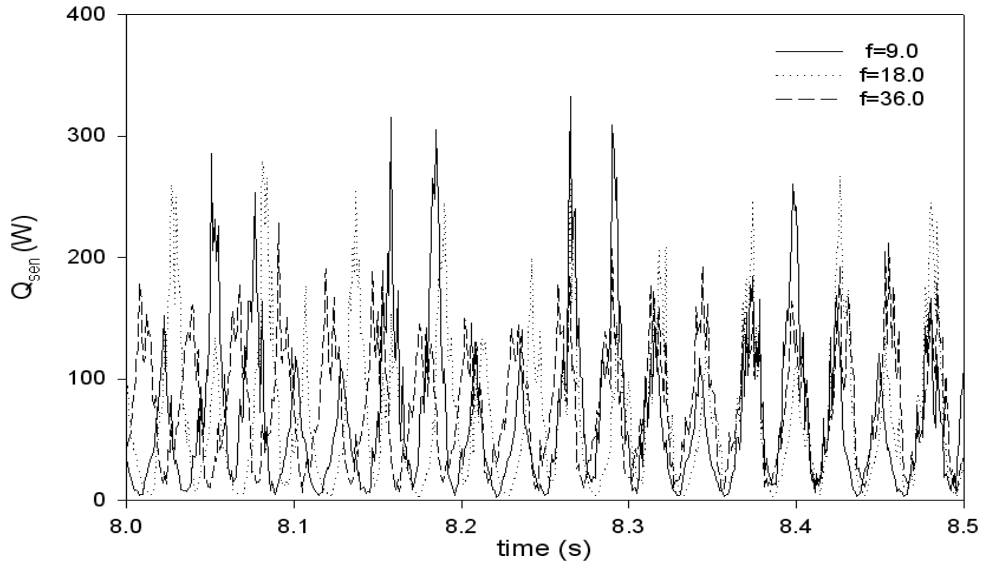

(b) Sensible heat transferred out of the liquid slug

Figure 32 Sensible heat transfer of the liquid slug for different frequencies

3.2.3 Effect of changes for different standard deviation

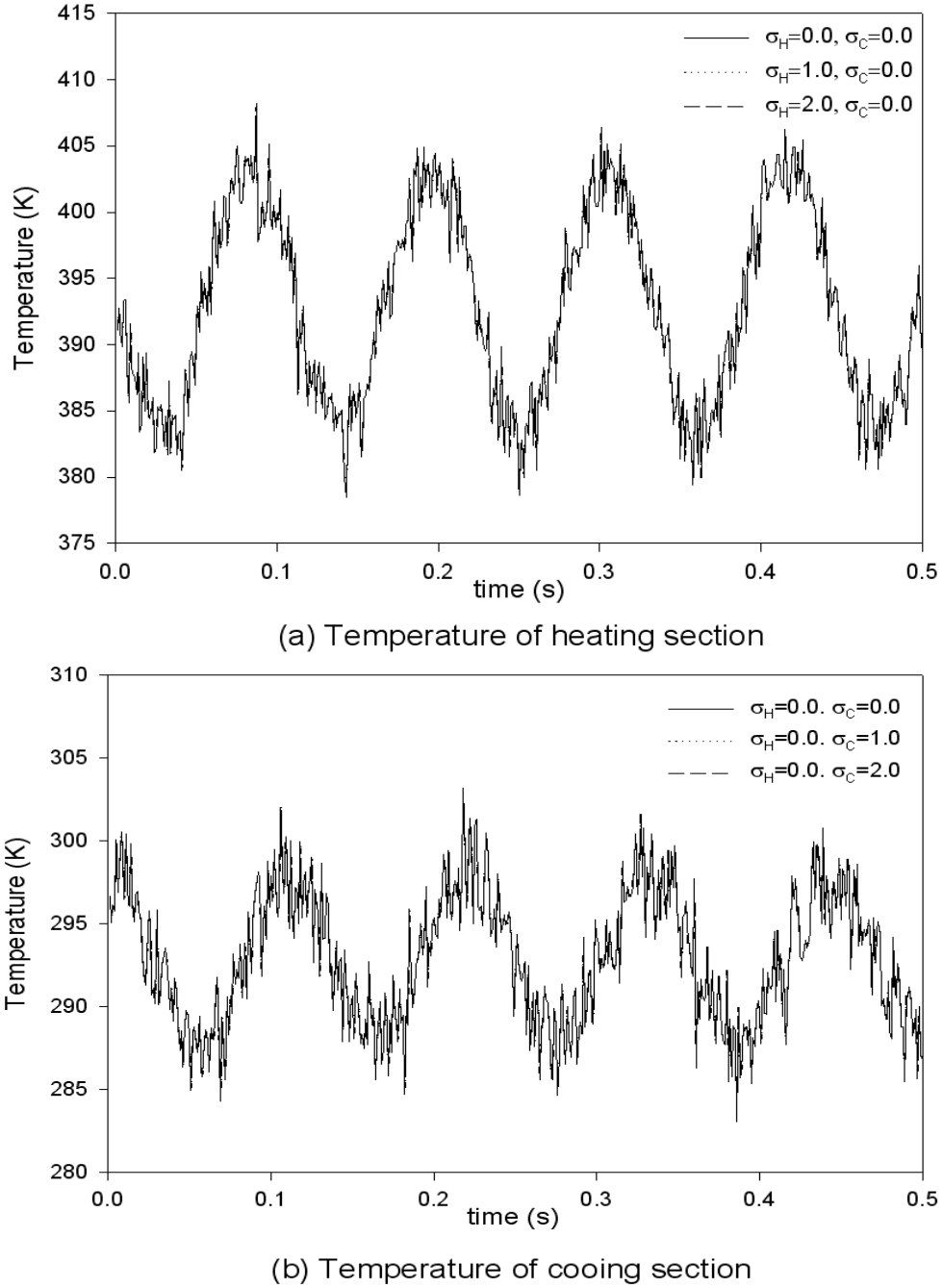

Figure 33 Temperature of heating and cooling sections for different for σ_H and σ_C

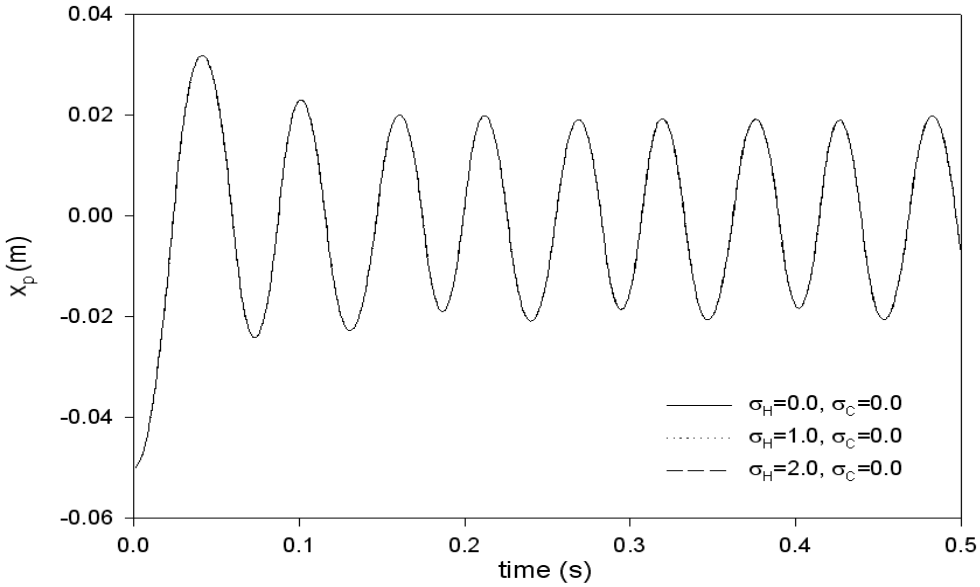

(a) Liquid slug displacement for different σ_H

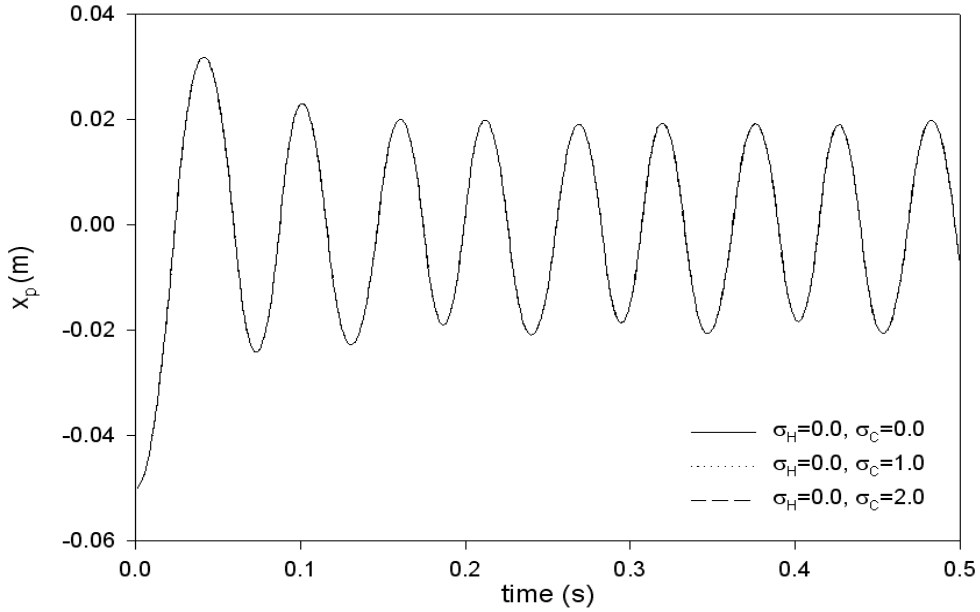

(b) Liquid slug displacement for σ_c

Figure 34 Liquid slug displacements for different for σ_H and σ_C

Effects of standard deviations of the random components of the temperature fluctuation are then studied. Figure 33 shows the temperature of the heating and the cooling sections for different σ_H and σ_C, while the frequency of the periodic component is kept at f = 9 Hz, and A_H and A_C are 10 K and 5 K, respectively. Figure 34 shows the effects of σ_H and σ_C on the

displacements of the liquid slug. It can be seen that there is not any notable effect of the standard deviations of the random components of the temperature fluctuation on the oscillatory flow. Consequently, there is also not any notable difference on vapor temperature and pressure, as well as latent and sensible heat transfer.

3.3 Conclusion

Heat transfer in the U-shaped PHP has been analyzed by applying periodic and random noises on the temperatures of the heating and the cooling sections. Effects of amplitude and frequency of the periodic component and standard deviations of the random components of the heating and cooling sections are investigated. The results showed that both amplitude and frequency of the periodic component of the temperature fluctuation have effects on the liquid slug displacements, temperatures and pressures of the two vapor plugs, as well as the latent and sensible heat transfer. The frequency of the liquid slug oscillation decreases with increasing amplitude and frequency of the periodic fluctuation of the wall temperature. However, the change of different standard deviations did not have any effect on the performance of the PHP.

CHAPTER 4 NANOFLUID EFFECT ON THE THERMAL PERFORMANCE

4.1 Physical Model

4.1.1 Problem Description

Figure 35 shows the configuration of a U-shaped pulsating heat pipe with nanofluid and its two ends sealed which are considered as the building block of a PHP. The parameters and operating conditions of this physical model is the same as in Chapter 2, except adding nanoparticles. In this study, Pure water is employed as the base fluid while Al_2O_3 with two different particle sizes i.e., 47nm and 38.4 nm is used as nanoparticle. The following assumptions are made in order to model heat transfer and fluid flow in the heat pipe [18, 30]:

(1) Shear stress at the liquid-vapor interface is negligible.

(2) Heat conduction in the liquid slug is assumed to be one-dimensional in the axial direction and exchange of heat between the liquid and wall is considered by a convective heat transfer coefficient.

(3) The liquid is incompressible and the vapor is saturated and behaves as an ideal gas.

(4) Evaporative and condensation heat transfer coefficients are assumed to be constants.

(5) The U-shaped minichannel is assumed to be a straight pipe and the effect of pressure loss in bend is considered using an empirical correlation.

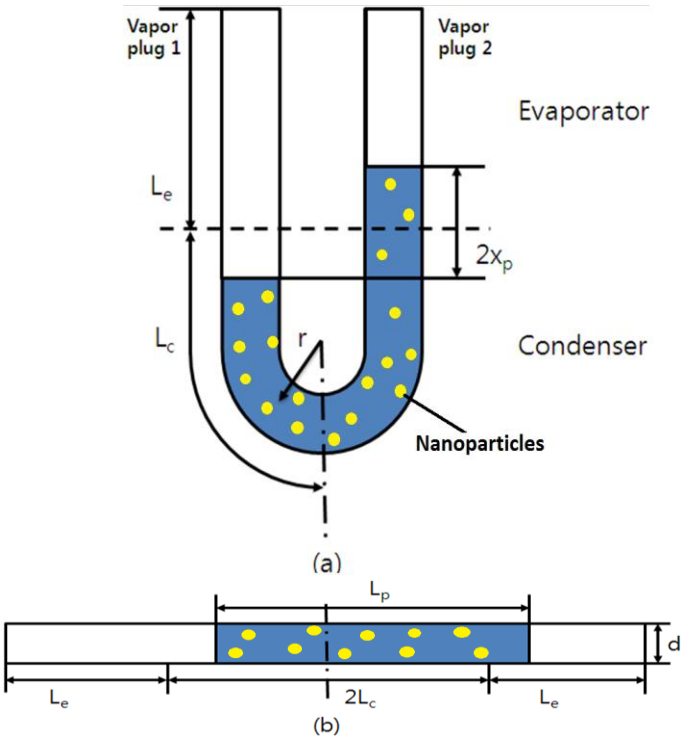

Figure 35 Configuration of U-shape pulsating heat pipe with nanofluid with adding nanofluid

4.1.2 Governing Equations for Pulsating Flow

The acceleration of the liquid slug is related with pressure, gravity and shear stress. Thus, the momentum equation is [18]:

$$AL_p\,\rho_{eff}\,\frac{d^2x_p}{dt^2}=[(p_{v1}-p_{v2})-\Delta p_b]A-2\rho_{eff}\,g\,Ax_p-\pi d\,L_p\,\tau_p \tag{45}$$

where Δp_b is the pressure loss at the bend [21]:

$$\Delta p_b=\begin{cases}K\rho_{eff}\dfrac{v_p^{\,2}}{2} & v_p>0\\ -K\rho_{eff}\dfrac{v_p^{\,2}}{2} & v_p<0\end{cases} \tag{46}$$

where K is the pressure loss coefficient, and ρ_{eff} is the effective density of nanofluid and can be calculated using the following correlation [21]:

$$\rho_{eff} = 1001.064 + 2738.6191\ \phi_p - 0.2095\ T \qquad 0 \le \phi_p \le 0.04 \qquad , \qquad 5^o \le T\left(^oC\right) \le 40^o \tag{47}$$

where ϕ_p is the volume fraction of nanoparticles and τ_ρ is the shear stress:

$$\tau_p = c_l \rho \upsilon_{eff}^{\ 2} / 2 \quad , \quad c_l = \begin{cases} 16 / \mathrm{Re}, & \mathrm{Re} < 2200 \\ 0.078\ \mathrm{Re}^{-0.2} & \mathrm{Re} > 2200 \end{cases} \tag{48}$$

The temperature and particle size dependent viscosity of nanofluid is calculated by [12]:

$$\upsilon_{eff} = \frac{1}{\rho_{eff}} \left[\begin{array}{c} -0.4491 + \frac{28.837}{T} + 0.574\,\phi_p - 0.1634\,\phi_p^{\ 2} + 23.053\,\frac{\phi_p^{\ 2}}{T^2} + 0.0132\,\phi_p^{\ 3} \\ -2354.735\,\frac{\phi_p}{T^3} + 23.498\,\frac{\phi_p^{\ 2}}{d_p^{\ 2}} - 3.0185\,\frac{\phi_p^{\ 3}}{d_p^{\ 2}} \end{array} \right] \tag{49}$$

$$1\% \le \phi_p \le 9\%\ ,\ 20 \le T\left(^oC\right) \le 70\ ,\ 13\,nm \le d_p \le 131\,nm$$

where d_p is the diameter of nanoparticles.

The energy equations of the two vapor plugs are [18]:

$$\frac{d(m_{v1} c_v T_{v1})}{dt} = c_p T_{v1} \frac{dm_{v1}}{dt} - p_{v1} \frac{\pi}{4} d^2 \frac{dx_p}{dt} \tag{50}$$

$$\frac{d(m_{v2} c_v T_{v2})}{dt} = c_p T_{v2} \frac{dm_{v2}}{dt} + p_{v2} \frac{\pi}{4} d^2 \frac{dx_p}{dt} \tag{51}$$

The vapor plug can be assumed to be an ideal gas. Thus, the equation of state can be presented by:

$$p_{v1}(L_e + x_p)\frac{\pi}{4} d^2 = m_{v1} R T_{v1} \tag{52}$$

$$p_{v2}(L_e - x_p)\frac{\pi}{4} d^2 = m_{v2} R T_{v2} \tag{53}$$

Considering the initial conditions, the masses and the temperatures of the two vapor plugs can be obtained:

$$m_{v1} = \frac{\pi d^2 p_0}{4RT_0}\left(\frac{p_{v1}}{p_0}\right)^{\frac{1}{\gamma}}(L_e + x_p) \tag{54}$$

$$m_{v2} = \frac{\pi d^2 p_0}{4RT_0}\left(\frac{p_{v2}}{p_0}\right)^{\frac{1}{\gamma}}(L_e - x_p) \tag{55}$$

$$T_{v1} = T_0\left(\frac{p_{v1}}{p_0}\right)^{\frac{(\gamma-1)}{\gamma}} \tag{56}$$

$$T_{v2} = T_0\left(\frac{p_{v2}}{p_0}\right)^{\frac{(\gamma-1)}{\gamma}} \tag{57}$$

where T_0 and P_0 are the initial temperature and the pressure, respectively.

4.1.3 Latent and sensible heat transfer

The heat transfer in the PHP represents that the heat transported from the evaporator section to the condenser section. There are two types of the heat transfer in the PHP. One is the latent heat transfer due to the phase change of the working fluid, and the other is the sensible heat transfer because of the heat transfer between the PHP wall and the liquid slug. The heat transfer rates in the two vapors are related with the mass flux, and can be obtained by:

$$Q_{in,v1} = \dot{m}_{evp,v1} h_{lv} \tag{58}$$

$$Q_{out,v1} = \dot{m}_{con,v1} h_{lv} \tag{59}$$

$$Q_{in,v2} = \dot{m}_{evp,v2} h_{lv} \tag{60}$$

$$Q_{out,v2} = \dot{m}_{con,v2} h_{lv} \tag{61}$$

The temperature distribution of the liquid slug can be obtained by solving the energy equation:

$$\frac{\rho_{eff} C_{p,eff}}{k_{eff}} \frac{dT_l}{dt} = \frac{d^2 T_l}{dx_p^2} - \frac{h_{lsen} \pi d}{k_{eff} A} (T_l - T_w) \tag{62}$$

The specific heat of nanofluid can be calculated using the following equation [22]:

$$C_{p,eff} = \frac{1}{\rho_{eff}} \left[(1-\phi_p) \rho_f C_{p,f} + \phi_p \rho_p C_{p,p} \right] \tag{63}$$

where C_p is specific heat and indices of p and f refer to nanoparticles and the base fluid. The thermal conductivity of Al_2O_3-water nanofluid is function of temperature, volume fraction and nanoparticle's diameter, effective viscosity of nanofluid as well as dynamic viscosity of water [21]:

$$\frac{k_{eff}}{k_f} = \left\{ \begin{array}{c} 0.9843 + 0.398 \, \phi_p^{\,0.7383} \left(\frac{1}{d_p(nm)} \right)^{0.2246} \left(\frac{\mu_{eff}(T)}{\mu_f(T)} \right)^{0.0235} \\ -3.9517 \frac{\phi_p}{T} + 34.034 \frac{\phi_p^{\,2}}{T^3} + 32.509 \frac{\phi_p}{T^2} \end{array} \right\} \tag{64}$$

$$1\% \le \phi_p \le 10\% \ , \ 20^o C \le T(^o C) \le 70^o C \ , \ 11\, nm \le d_p \le 150\, nm$$

where k_f is thermal conductivity of base fluid. The initial and boundary conditions for Eq. (62) are:

$$T = T_0, \ \ t = 0, \ \ 0 < x_p < L_p \tag{65}$$

$$T = T_{v1}, \ \ x_p = 0 \tag{66}$$

$$T = T_{v2}, \ \ x_p = L_p \tag{67}$$

The wall temperature of the tube can be either T_e or T_c, depending on the displacement of the liquid slug, i.e.,

When $x_p > 0$

$$T_w = \begin{cases} T_c & 0 < x_l < L_p - x_p \\ T_e & L_p - x_p < x_l < L_p \end{cases} \tag{68}$$

When $x_p < 0$

$$T_w = \begin{cases} T_c & 0 < x_l < |x_p| \\ T_e & |x_p| < x_l < L_p \end{cases} \tag{69}$$

The sensible heat transferred in and out of the liquid slug can be obtained by integrating the heat transfer over the length of the liquid slug [26]:

$$Q_{in,s,l} = \begin{cases} \int_{L_p - x_p}^{L_p} \pi dh(T_e - T_l) dx_l, \ x_p > 0 \\ \int_0^{|x_p|} \pi dh(T_e - T_l) dx_l, \ x_p < 0 \end{cases} \tag{70}$$

$$Q_{out,s,l} = \begin{cases} \int_0^{-x_p} \pi dh(T_l - T_c) dx_l, \ x_p > 0 \\ \int_{|x_p|}^{L_p} \pi dh(T_l - T_c) dx_l, \ x_p < 0 \end{cases} \tag{71}$$

where the sensible heat transfer coefficient can be obtained from $h = Nuk_l / d$ [18].

4.2 Numerical Procedure

The iteration method and the implicit finite difference method are used to solve the governing equations of the vapor plugs and the liquid slug. Also, the heat conduction in liquid is solved by Tridiagonal Matrix Algorithm (TDMA). The numerical procedures are as follows:

1) Temperatures of the two vapor plugs, T_{v1} and T_{v2}, are assumed, and the thermal and physical properties of the nanofluid are calculated according to T_l.

2) The vapor pressures, p_{v1} and p_{v2}, are solved by Eqs. (56) and (57).

3) The displacement of the liquid slug, x_p, is calculated by Eq. (45).

4) The new masses of the two vapor plugs, m_{v1} and m_{v2}, are obtained by accounting for the change of the vapor masses from Eqs. (54) and (55).

5) The pressures of the two vapor plugs, p_{v1} and p_{v2}, are calculated by Eqs. (52) and (53).

6) T_{v1} and T_{v2} are solved by Eqs. (56) and (57).

7) T_{v1} and T_{v2} are compared, which are obtained in step 6, with the assumed values in the step 1. If the differences meet the small tolerance, go to the step 8; otherwise, the above procedures are repeated the steps 2-6 until a converged solution is obtained.

8) The temperature distribution of the liquid slug is solved by Eq. (62) and then the sensible heat is calculated by Eqs. (70) and (71).

9) The latent heat is obtained by Eqs. (58)-(61).

4.3 Results and Discussion

The variations of liquid slug location, vapor pressure and vapor temperature with time for different volume fractions of nanoparticles as well as pure water are shown in Figs. 36-38. As can be seen from Fig. 36, using nanofluid will cause the frequency of the oscillation decreases while the amplitude is approximately same for all cases studied. With increasing the volume fraction, the phase is much more delayed while the change of amplitude of the liquid slug displacement is so small. Figure 37 shows the comparison of vapor plug temperatures in three different volume fractions as well as that for the case of pure water. Similar to the trend of liquid slug displacement, there is a delay in the phase of the vapor temperature with adding nanoparticle to working fluid. The frequency of the temperature oscillation is decreased as volume fraction increases. Comparison of the pressure variations of the vapor plugs for different volume fraction is shown in Fig. 38. It can be seen that the vapor pressure oscillates due to thin film evaporation and condensation, which makes the operation of PHP possible. Steady oscillation is established after t = 0.2 s. The vapor plug pressures in all cases exhibited the similar trend as the vapor plug temperatures. Therefore, one can conclude that as volume fraction

increases, the frequencies of displacement are decreased, while the amplitude, vapor plug temperature and pressure are nearly constant.

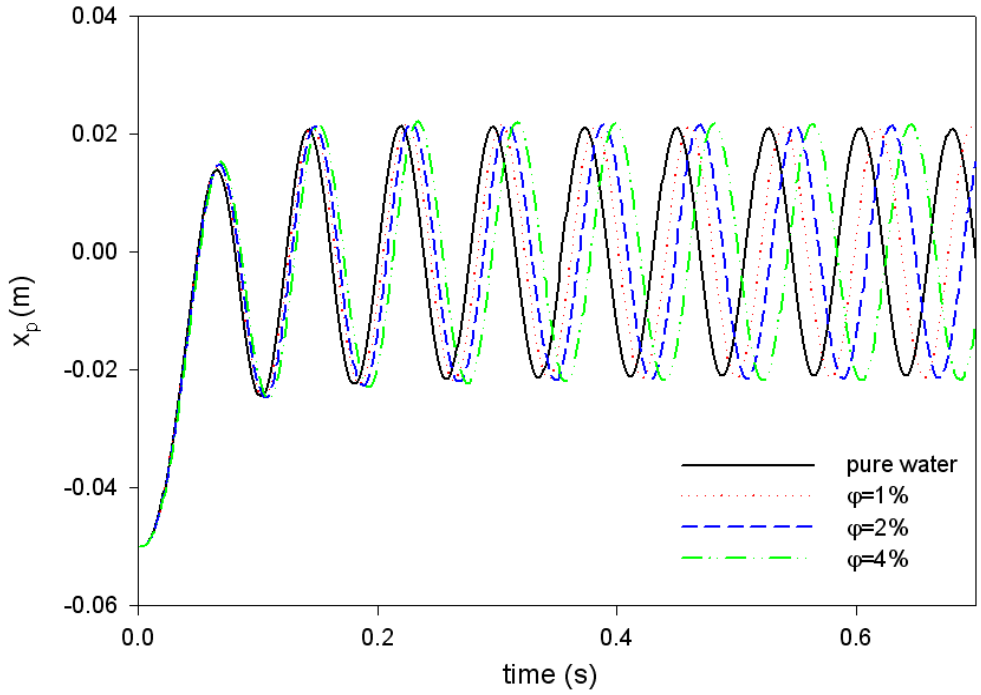

Figure 36 Effect of nanoparticles on liquid slug displacement for d_p=38.4 nm

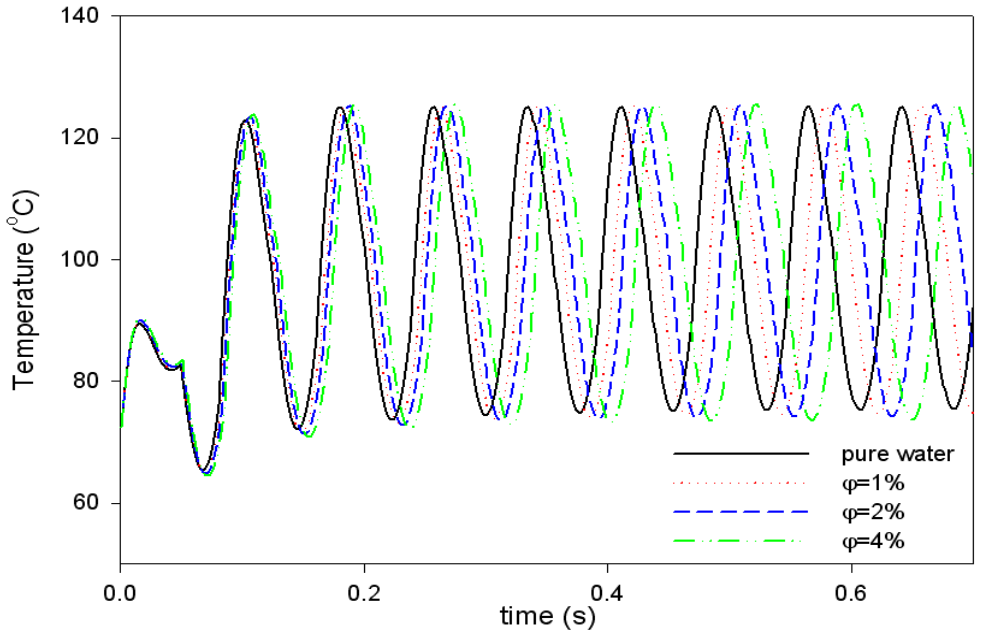

(a) Vapor plug 1

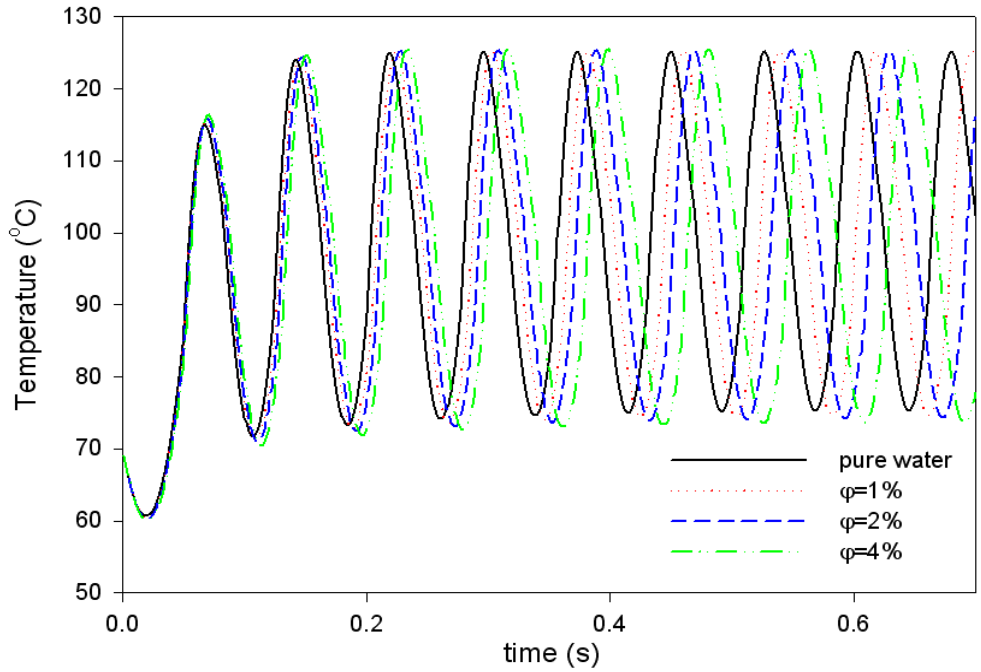

(b) Vapor plug 2

Figure 37 Effect of nanoparticles on temperature of two vapor plugs for d_p= 38.4 nm

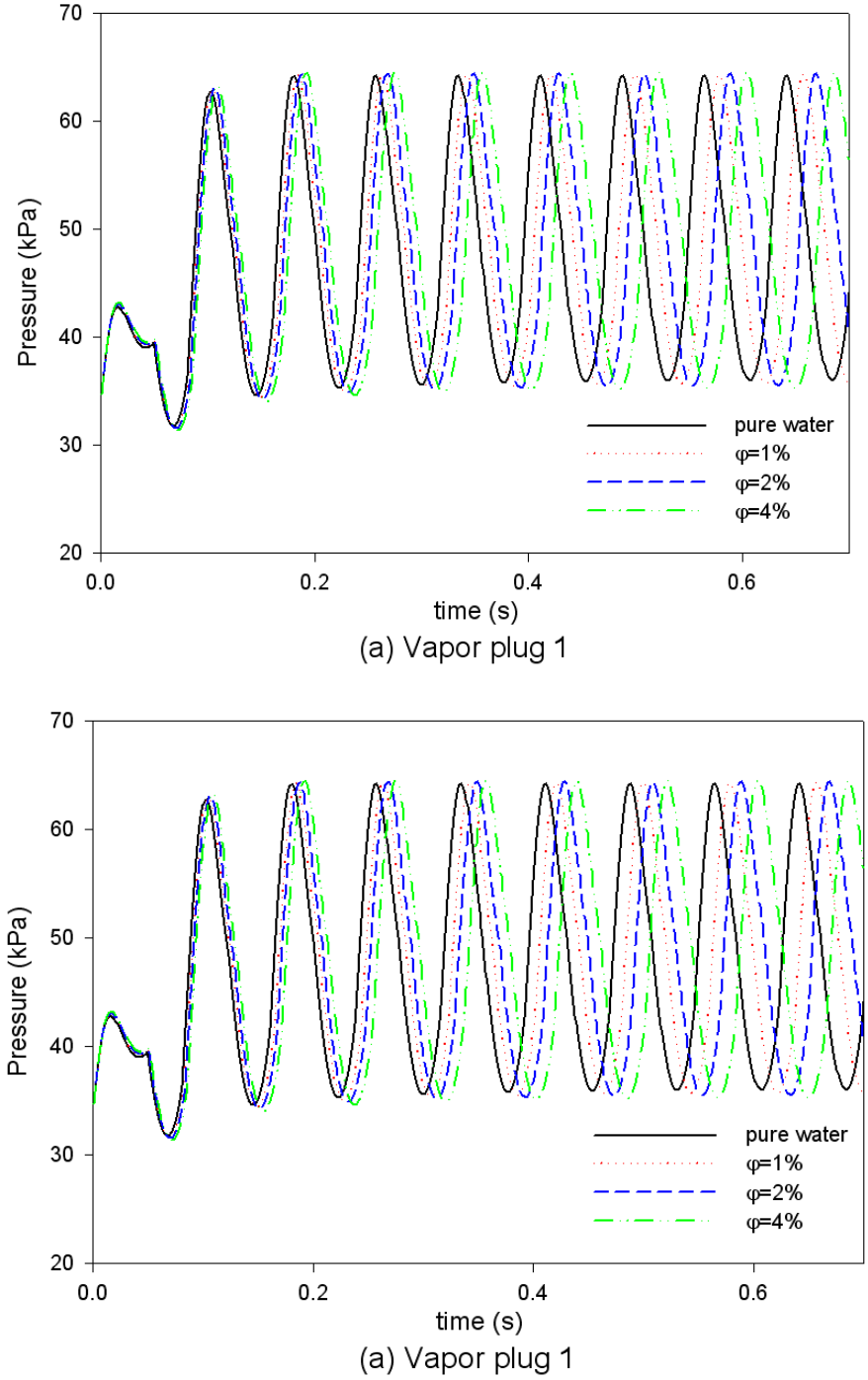

Figure 38 Effect of nanoparticles on pressure of two vapor plugs for d_p=38.4 nm

Figure 39 shows the comparison of sensible heat transfer transferred into and out of the liquid slug for different volume fractions of nanoparticles as well as for pure water. There is a delay of the phase and a strong enhancement of sensible heat transfer in and out of the liquid slug

when using nanofluid instead of pure water as working fluid. The phase delay in sensible heat transfer is due to higher viscosity and mass of nanofluid compared to pure water which cause the velocity of liquid slug decrease so we observe a phase delay in sensible heat transfer. The enhancement in sensible heat transfer is due to enhanced thermophysical properties of nanofluid, especially thermal conductivity. With increasing volume fraction of nanoparticles, the thermal conductivity of nanofluid increases, which leads to enhancement in sensible heat transfer. Due to enhanced oscillatory motion of the liquid slug, the total sensible heat transfer rate is increased from 38.99 W for pure water case to 69.42 W for nanofluid case with volume fraction of 4%. At this point, it is important to mention that the influence of nanoparticles elucidates two opposing effects on the heat transfer coefficient and total thermal resistance: an undesirable effect promoted by high level of viscosity experienced at high volume fractions of nanoparticles and a favorable effect that is driven by the presence of high thermal conductivity of nanoparticles. In other words, the addition of nanoparticles to the base fluid enhances the heat conduction and with increasing particle volume fraction for a given particle size, the enhancement increases. The enhancement of the heat conduction should increase the convective heat transfer coefficient. However, the nanofluid viscosity increases with increasing particle volume fraction, which should result in a reduction in velocity and convection and consequently lowers convective heat transfer coefficient. As shown clearly in Fig. 39, increasing nanoparticle volume fraction cause thermal performance enhancement. This indicates that under the condition of this work, the positive effect of the thermal conduction enhancement outweighs the negative effect of viscosity enhancement. The comparison of latent heat transfer of vapor plugs for different cases is shown in Figs. 40 and 41. It is seen that the delay of the phase of the oscillation also results the delay of the phase of evaporation heat transfer but the amplitude of condensation heat transfer does not increase much.

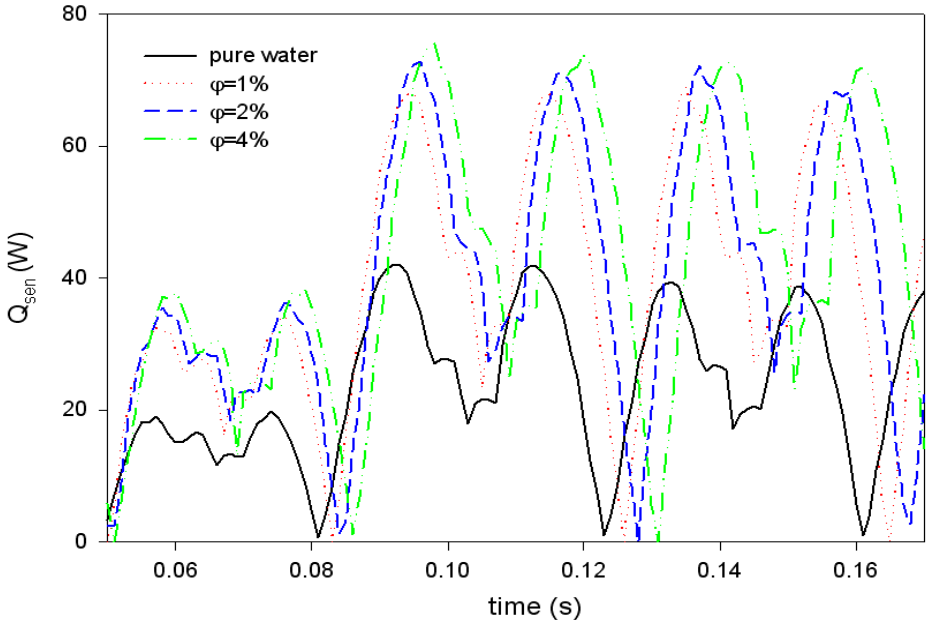

(a) Sensible heat transferred into the liquid slug

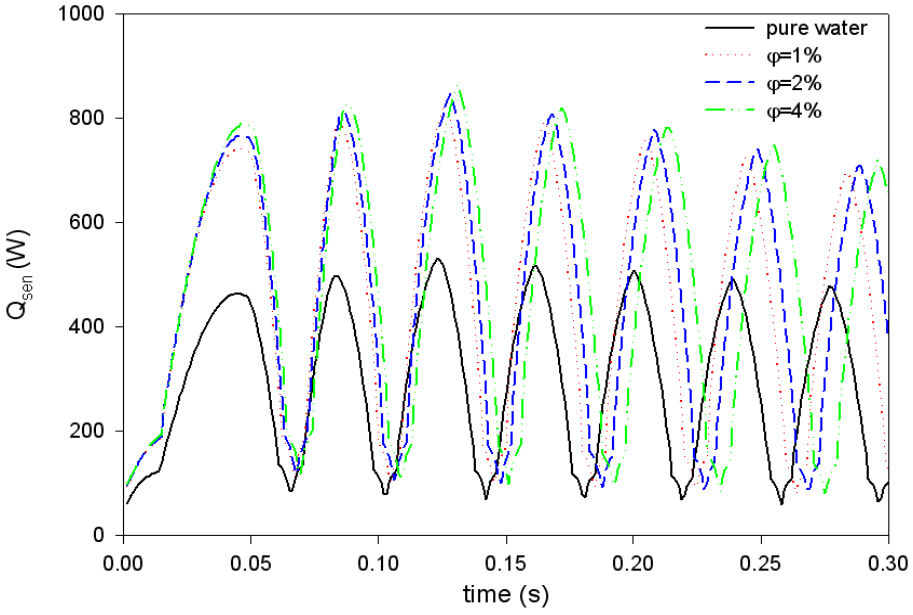

(b) Sensible heat transferred out of the liquid slug

Figure 39 Effect of nanoparticle on sensible heat transferred into the liquid slug for d_p = 38.4 nm

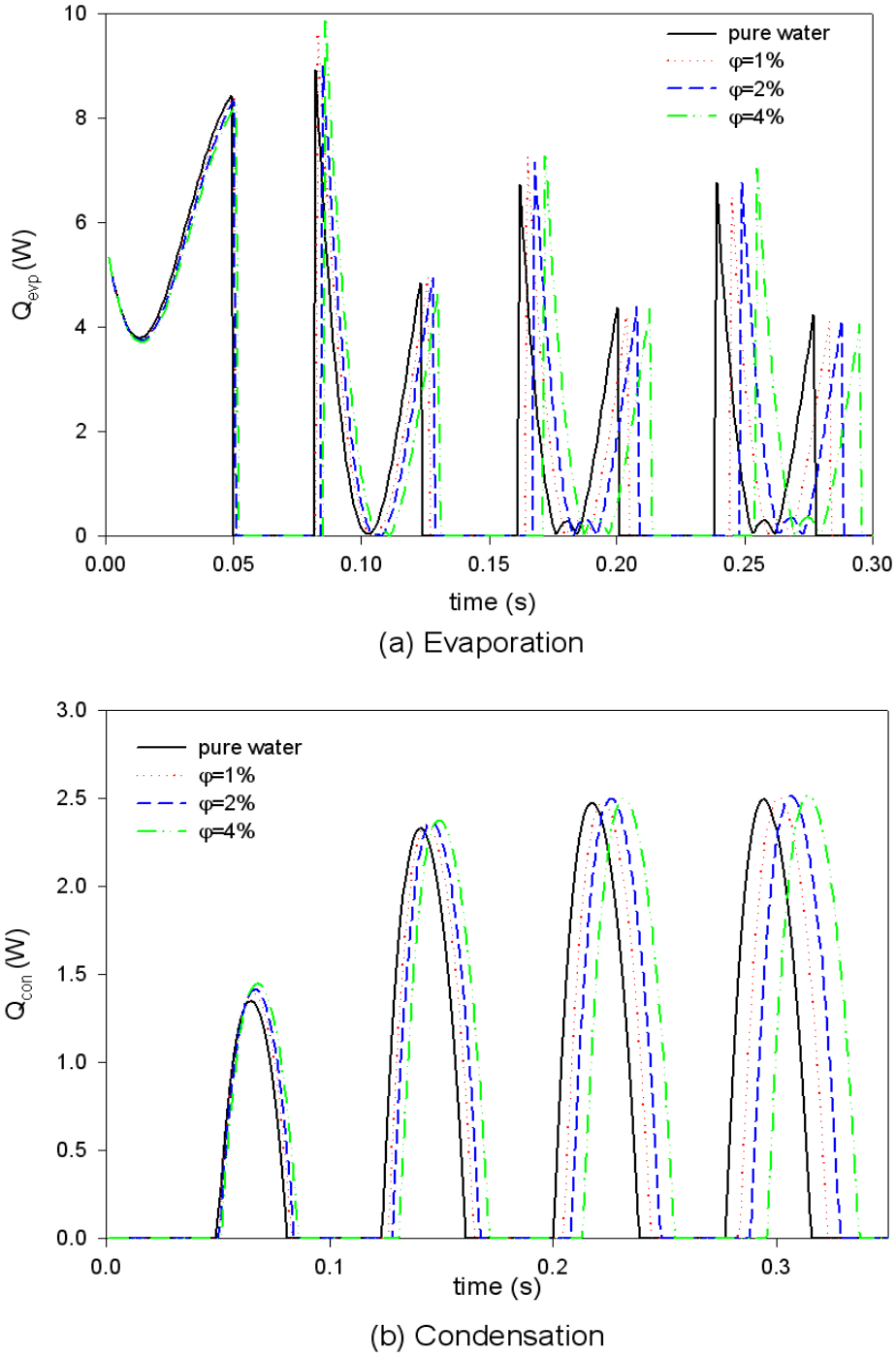

Figure 40 Effect of nanoparticles on latent heat of vapor plug 1 for different volume fraction at d_p = 38.4 nm

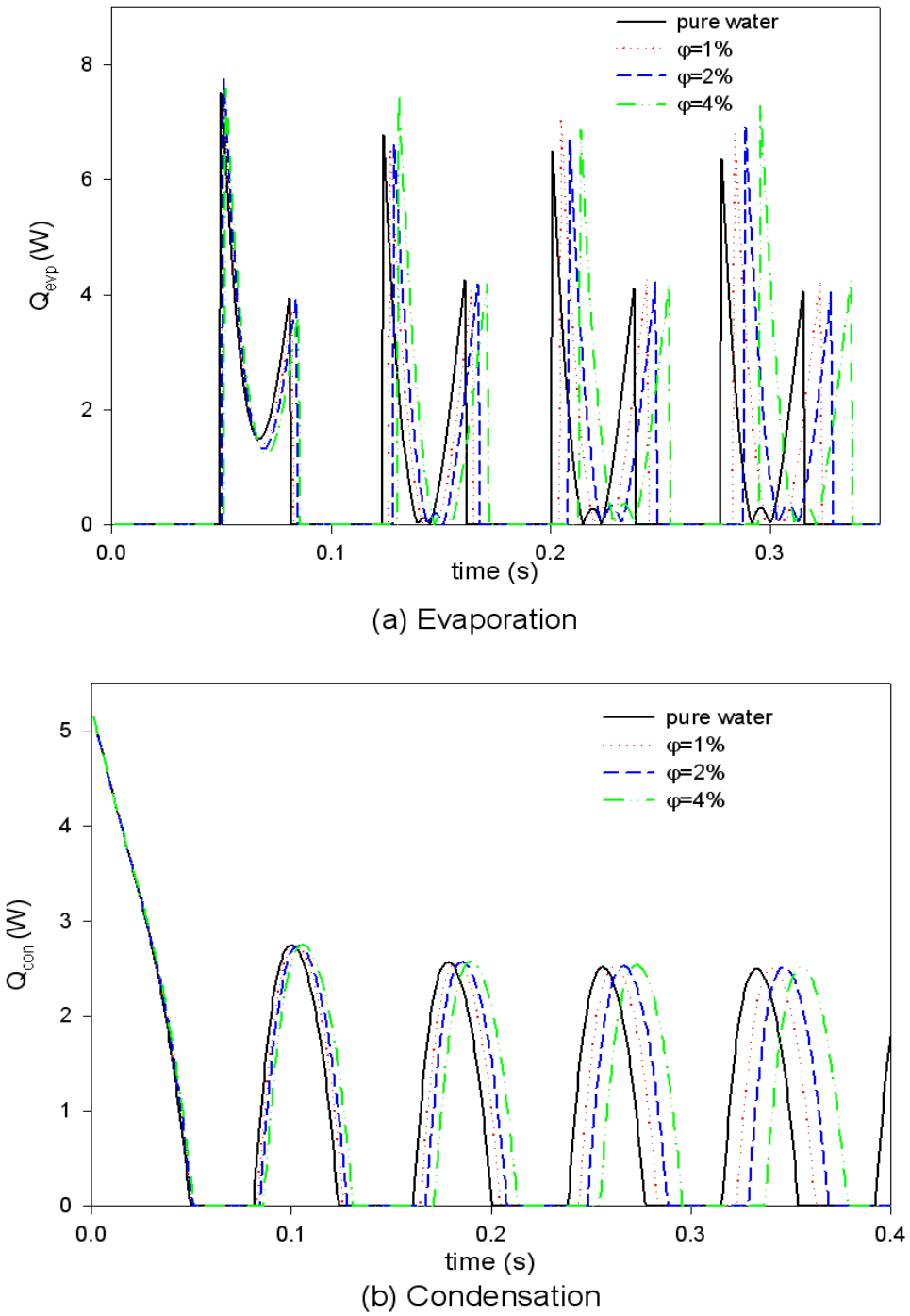

Figure 41 Effect of nanoparticles on latent heat of vapor plug 2 for different volume fraction at d_p = 38.4 nm

The effect of nanoparticles diameter on the performance of PHP is studied next. Figure 42 shows the comparison of the displacement for two different particles diameter i.e., 38.4 and 47.0

nm. As can be seen, at other conditions being equal, the amplitude of oscillation is nearly constant while the frequency of the oscillation increases when the particle size increases. It can be seen that, the change of amplitude of the liquid slug displacement is not significant and the phase is much more advanced for d_p = 38.4 nm. Figure 43 shows the comparison of vapor plugs temperatures for two different nanoparticle diameters. With decreasing nanoparticle size, the amplitude of temperature oscillation is constant while the phase of oscillation advances. Figure 44 shows the comparison of the pressure variations of the vapor plugs for different particles diameters. The vapor plug pressures in different nanoparticle size exhibited the similar trend as the vapor plug temperatures.

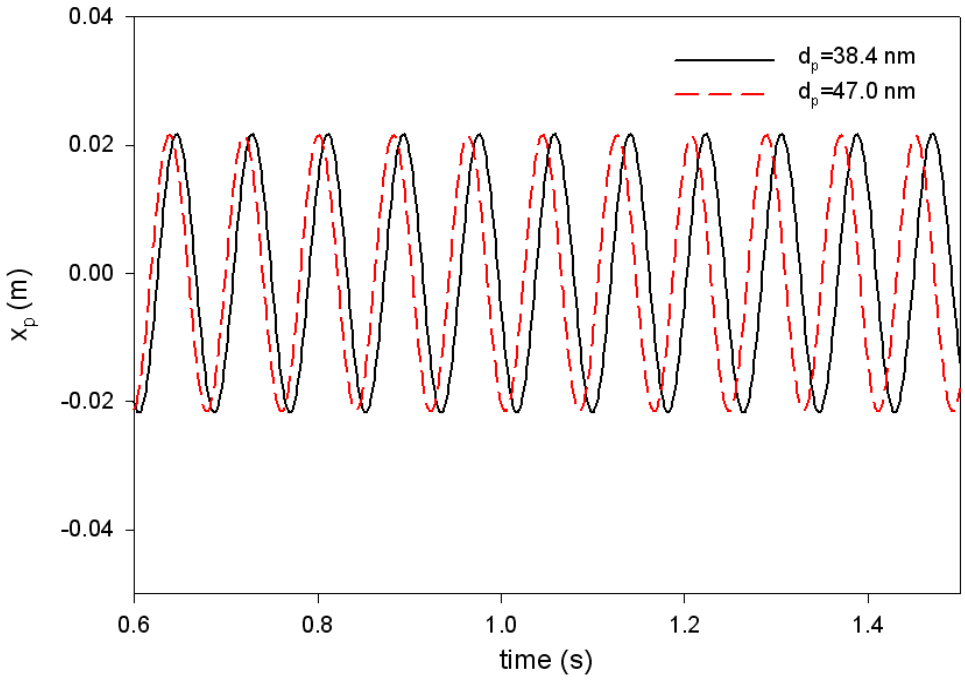

Figure 42 Effect of nanoparticle size on liquid slug displacement for volume fraction of 4%

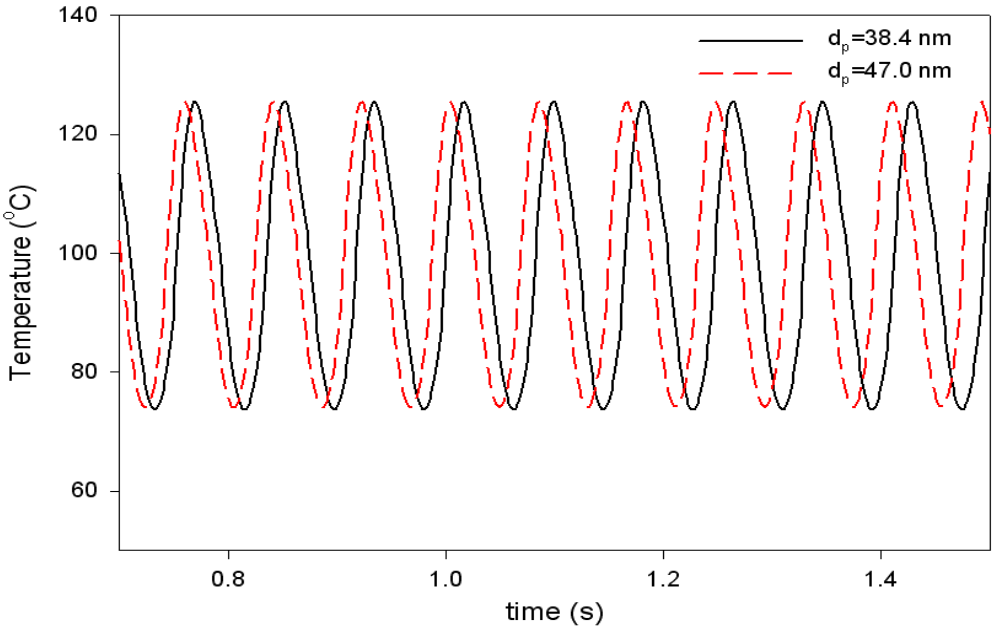

(a) Vapor plug 1

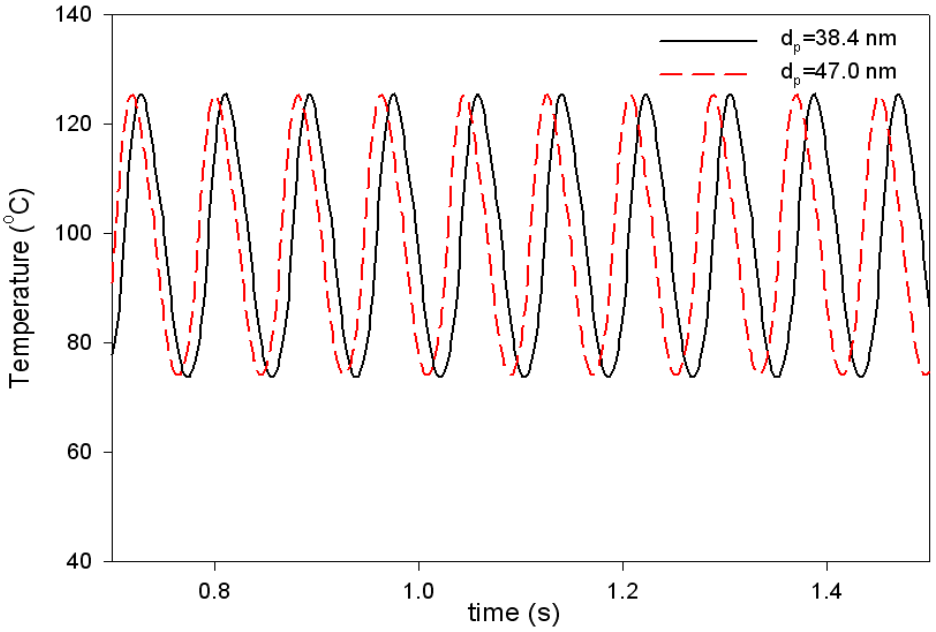

(b) Vapor plug 2

Fig.43 Effect of nanoparticle size on temperature of vapor plugs for volume fraction of 4%

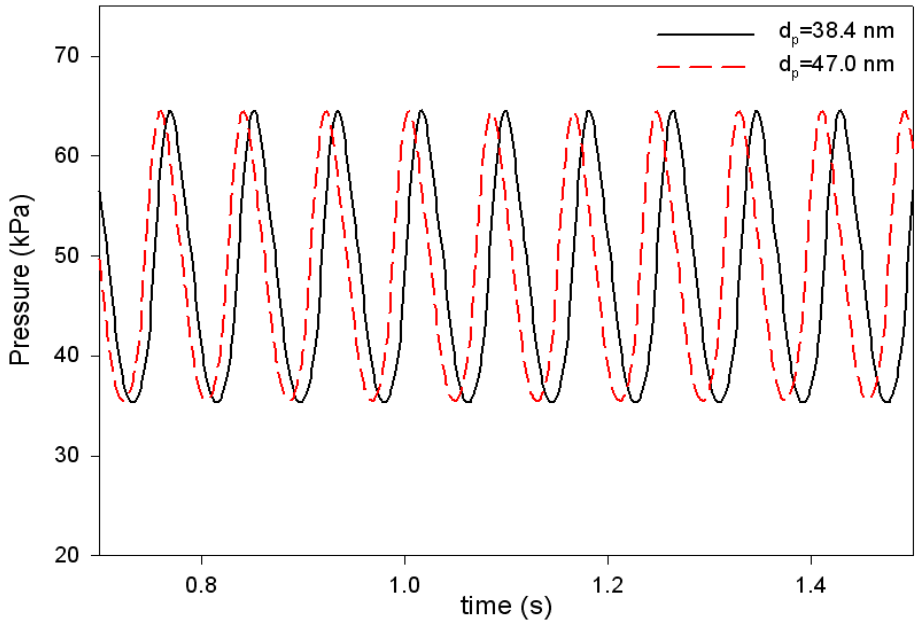

(a) Vapor plug 1

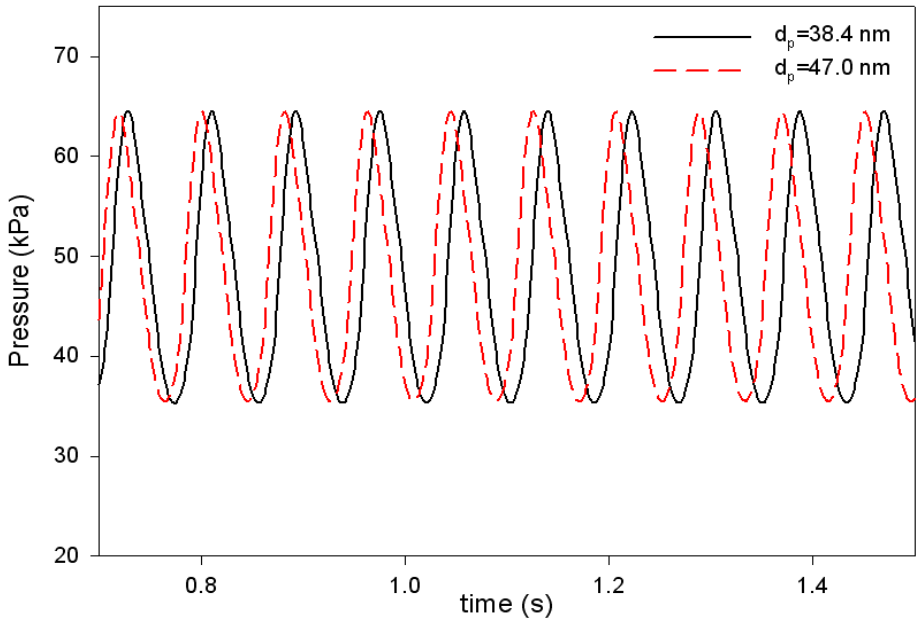

(b) Vapor plug 2

Figure 44 Effect of nanoparticle size on pressure of vapor plugs for volume fraction of 4%

Figure 45 shows the comparison of the sensible heat transfer for different nanoparticle diameters. With decreasing the nanoparticle diameter the phase of sensible heat transfer advances because of lower velocity of liquid plug for smaller particle diameter. Furthermore, it

can be seen that there is an increase of the sensible heat transfer when the size of nanoparticles decreases. This is due to the fact that smaller size nanoparticles lead to higher effective thermal conductivity of nanofluid. This is due to aggregation of nanoparticles and stronger Brownian motion at smaller nanoparticles diameters, which lead to higher thermal conductivity of nanofluids [24, 25]. At this point, it should be noted that the Brownian motion is one of the main mechanisms of thermal conductivity enhancement and with decreasing the particles diameter, the effect of Brownian motion increases due to improvement of micro-convection around nanoparticles. Secondly, the formation of solid-like liquid layers around nanoparticles is another mechanism of enhancement of thermal conductivity. With decreasing particles diameter, the specific area of nanoparticles increases which results in enhancement in thermal conductivity due to nanolayers. Another reason for higher thermal conductivity of Al_2O_3 water nanofluid for smaller size nanoparticles is that the thermal energy transfer is dependent on surface area and smaller particles of same volume fraction provide more surface area for the transfer of thermal energy. Understanding the effects of which mechanism or mechanisms might be stronger for the results presented in this paper will require significant future work. Therefore, for Al_2O_3 water nanofluid with decreasing the size of nanoparticles the effect of aggregation, nanolayer formations, Brownian motion and energy transfer increase which lead to enhancement of thermal conductivity and consequently heat transfer coefficient [22]. Figures 46 and 47 show the comparison of latent heat transfer for different nanoparticle diameters. The latent heat transfer is constant for different particle diameters while there is a delay between two nanoparticle sizes. The effect of nanoparticle diameter and volume fraction on total heat transport rate and contribution of latent and sensible heat transfer of PHP is presented in Table 1. From this table, it can be concluded that nanofluid plays a major role in increasing the heat transfer rate. With increasing the volume fraction and decreasing nanoparticles size, the sensible heat transfers increases. As mentioned earlier, these enhancements are due to enhancement in thermophysical properties of the nanofluid.

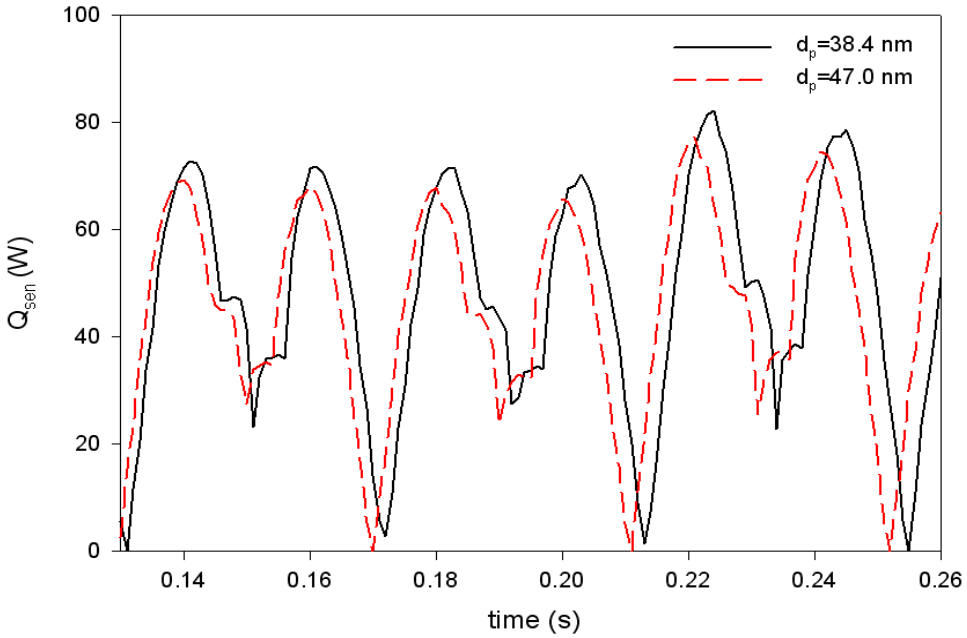

(a) Sensible heat transferred into the liquid slug

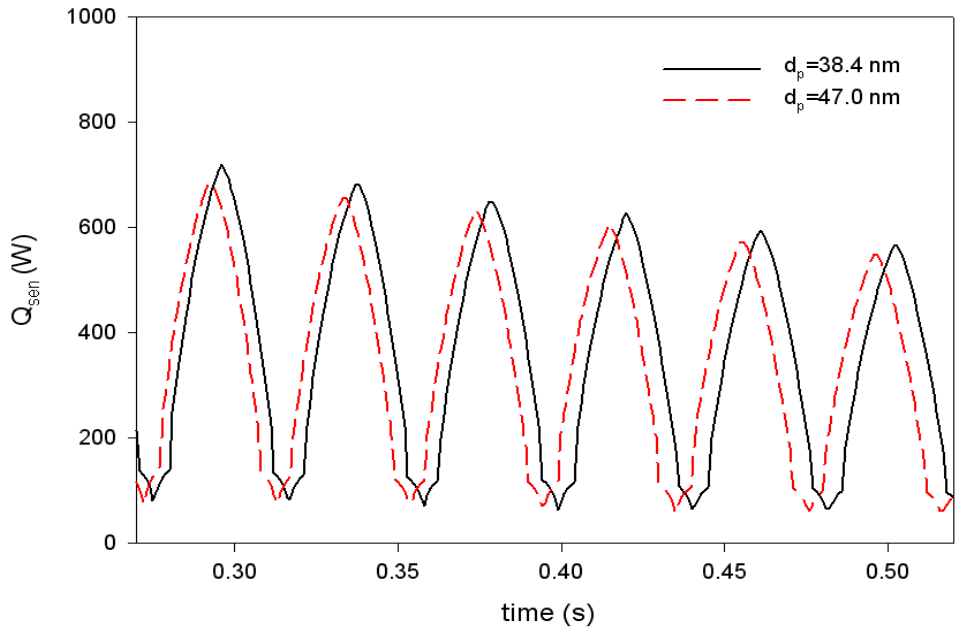

(b) Sensible heat transferred out of the liquid slug

Figure 45 Effect of nanoparticle size on sensible heat of the liquid slug

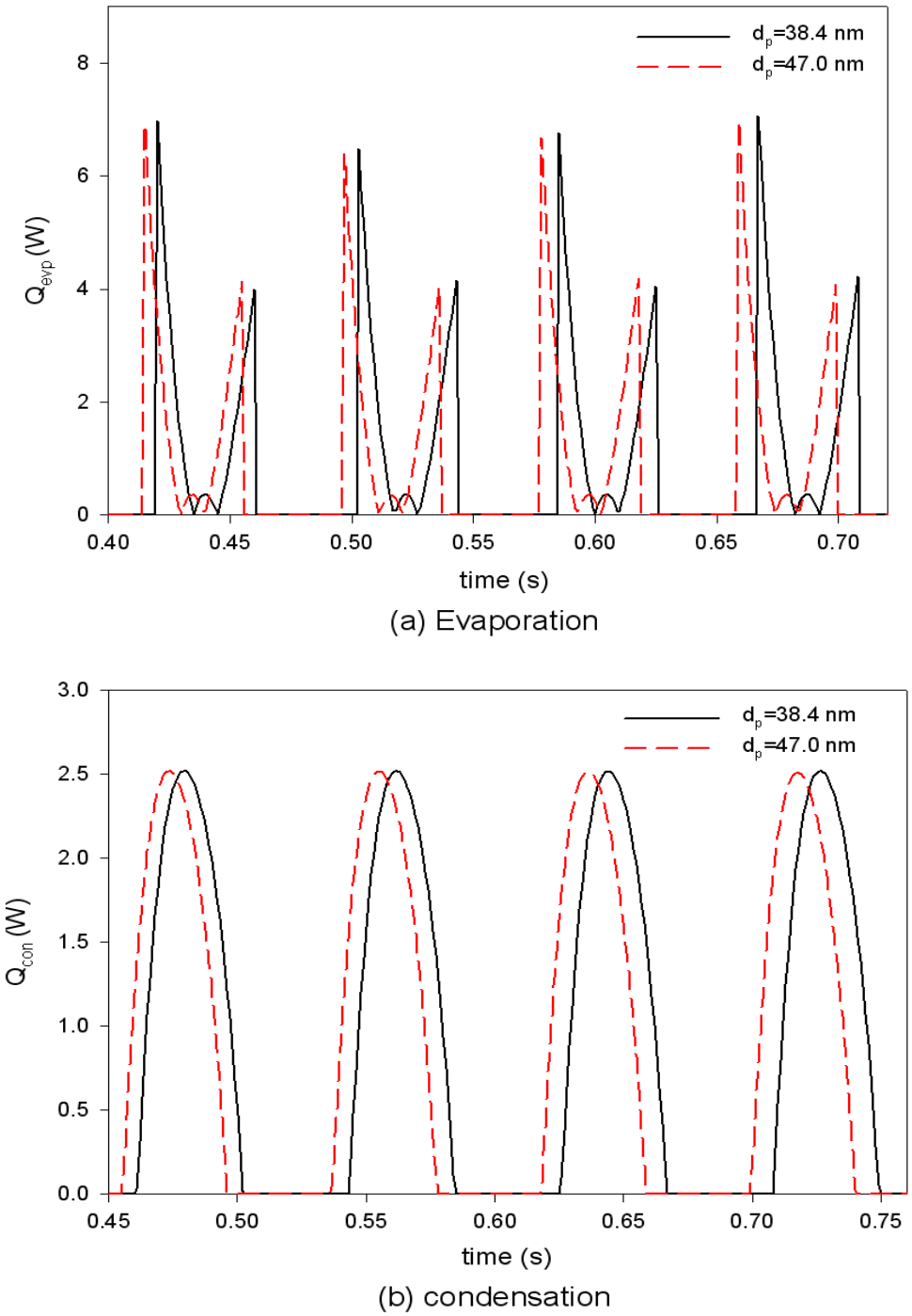

Figure 46 Effect of nanoparticle size on latent heat vapor plug 1

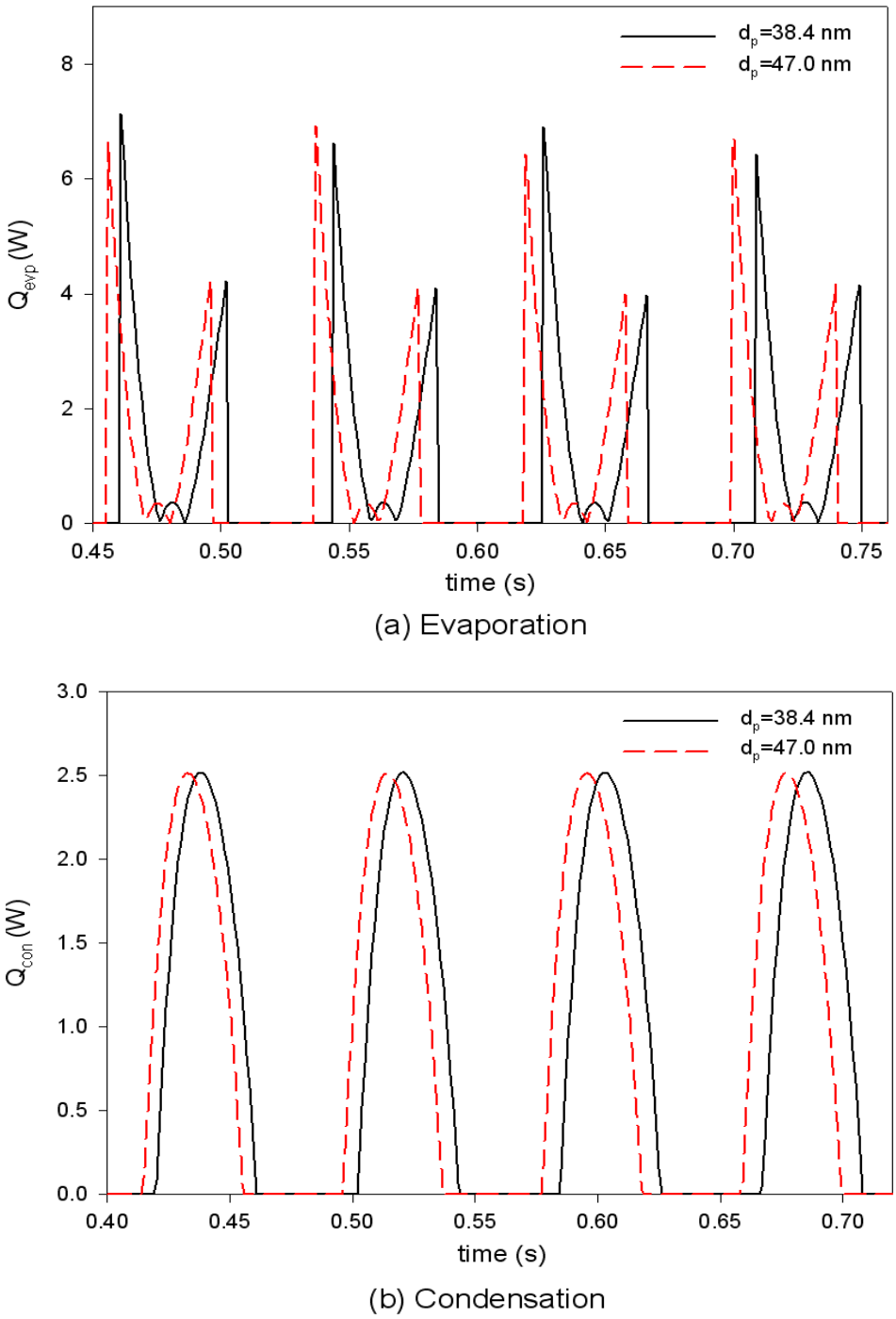

Figure 47 Effect of nanoparticle size on latent heat of vapor plug 2

Table 1. Total heat transport rate and contribution of latent and sensible heat transfer

dp (nm)	φ	$\overline{Q_{evp}}$	$\overline{Q_{h,s}}$	$\overline{Q_t}$	$\overline{Q_{h,s}}/\overline{Q_t}$
38.4	0	0.917	38.985	39.902	97.701
	1	0.927	64.203	65.130	98.577
	2	0.929	66.897	67.827	98.630
	4	0.940	69.415	70.355	98.662
47	0	0.917	38.985	39.902	97.701
	1	0.923	60.207	61.131	98.489
	2	0.926	61.899	62.825	98.525
	4	0.934	65.404	66.399	98.592

4.4 Conclusion

Nanofluid effects on oscillatory flow and heat transfer of a pulsating heat pipe are investigated by comparing displacement of liquid slug, temperature and pressure of vapor plugs, as well as latent and sensible heat transfer. It is concluded that nanofluid has significant effect on thermal performance of the system and with increasing the volume fraction the enhancement intensifies. Furthermore, the size of nanoparticles influences the magnitude of sensible heat and smaller nanoparticles leads to larger sensible heats. With increasing the particle size, the amplitude of oscillation is nearly constant while the frequency of the oscillation increases.

CHAPTER 5 CONCLUSIONS

The entropy generations are calculated from the variations of vapor mass, the liquid temperature, latent heat, sensible heat, and friction. In result, the entropy generations are sensitively affected by the initial temperature, and the variation of the vapor mass is the main cause of the entropy generation. The amplitude of the entropy generation is irrelevant to the pressure loss at the bend. However, the frequency of the entropy generation with the pressure loss is faster than those without the pressure loss.

Effects of amplitude and frequency of the periodic component and standard deviations of the random components of the heating and cooling sections are investigated. The results showed that both amplitude and frequency of the periodic component of the temperature fluctuation have effects on the liquid slug displacements, temperatures and pressures of the two vapor plugs, as well as the latent and sensible heat transfer. The frequency of the liquid slug oscillation decreases with increasing amplitude and frequency of the periodic fluctuation of the wall temperature. However, the change of different standard deviations did not have any effect on the performance of the PHP.

Nanofluid effects on oscillatory flow and heat transfer of an oscillating heat pipe are fully investigated by comparing displacement of liquid slug, temperature and pressure of vapor plugs, as well as latent and sensible heat transfer. It is concluded that nanofluid has significant effect on thermal performance of the system and with increasing the volume fraction the enhancement intensifies. Furthermore, the size of nanoparticles influences the magnitude of sensible heat and smaller nanoparticles leads to larger sensible heats. With increasing the particle size, the amplitude of oscillation is nearly constant while the frequency of the oscillation increases.

REFERENCES

[1] H. Akachi, "Looped Capillary Heat Pipes", Japanese Patent, No. Hei697147, 1994.

[2] L. Trefethen, "On the Surface Tension Pumping of Liquids or a Possible Role of the Candlewick in Space Exploration". G. E. Tech. Info., Serial No. 615 D114, 1962

[3] G. Grover, T. Cotter and G. Erikson, "Structure of Very High Thermal Conductance". J. Appl. Phys., Vol. 35, pp. 1990-1991, 1964

[4] G. Grover, "Evaporation-Condensation Heat Transfer Device". U.S. Patent 3229759, 1966

[5] I. B. Leefer, "Nuclear Thermionic Energy Converter", Proc. 4th Int. Heat Pipe conf., London, UK, pp. 725-734, 1966

[6] F. J. Judge, "RCA Test Thermal Energy Pipe". J. Missile and Rockets, pp. 36-38, 1966

[7] T. R. Dobson, and M. T. Harms, "Lumped Parameter Analysis of Closed and Open Oscillatory Heat Pipe, Proc". 11th Int. Heat Pipe Conf., Tokyo, Japan, pp. 12-16, 1999

[8] Q. Cai, R. Chen and L. C. Chen, "An Investigation of Evaporation, Boiling and Heat Transport Performance in Pulsating Heat Pipe". Proc. ASME Int. Mechanical Engineering Congress & Exposition, New Orleans, Louisiana, USA, 2002

[9] M. Hosoda, S. Nishio, and R. Shirakashi, "Meandering Closed Loop Heat Transport Tube (Propagation Phenomena of Vapor Plug)", Proc. 5th ASME/JSME Joint thermal Engineering Conf., AJTE99-6306, San Diego, California, USA, pp. 1-6, 1999

[10] Y. Zhang and A. Faghri, "Heat Transfer in a Pulsating Heat Pipe with Open End", International Journal of Heat and Mass Transfer, vol. 45, pp. 755–764, 2002.

[11] M. Groll and S. Khandekar, "Pulsating Heat Pipe: Progress and Prospects", Proc. Int. Conf. on Energy and the Environment, 1, Shanghai, China, pp. 723-730, 2003

[12] S. Rittidech, W. Dangeton and S. Soponroimarit, "Closed-Ended Oscillating Heat-Pipe (CEOHP) Air-Preheater for Energy Thrift in a Dryer", Applied Energy, vol. 81, pp. 198–208, 2005.

[13] S. Kim, Y. Zhang and J. Choi, "Entropy Generation during Thermally-Induced Oscillatory Flow in a U-Shaped Minichannel," Heat Transfer Research, Accepted, 2012.

[14] H. Khalkhali, A. Faghri and Z. J. Zuo, "Entropy Generation in a Heat pipe system". Applied Thermal Engineering, 19, pp. 1027-1043, 1999

[15] T. I. Al-Zaharnah, "Entropy Analysis in Pipe Flow Subjected to External Heating". Entropy, 5, pp. 391-403, 2003

[16] T. I. Al-Zaharnah and S. B. Yilbas, "Thermal Analysis in Pipe Flow: Influence of Variable Viscosity on Entropy Generation". Entropy, pp. 344-363, 2004

[17] Z. A. Sahin and R. Ben-Mansour, "Entropy Generation in Laminar Fluid Flow through a Circular Pipe". Entropy, 5(5), pp. 404-416, 2003

[18] W. Shao and Y. Zhang, "Thermally-Induced Oscillatory Flow and Heat Transfer in a U-shaped Minichannel". Journal of Enhanced Heat Transfer, 18(3), pp. 177-190, 2011

[19] M. W. Rohsenow, P. J. Hartnett and N. E. Ganic, Handbook of Heat Transfer Fundamentals. 2nd ed., McGraw-Hill, New York, Chap. 7, 1985

[20] Xu, Shiliang, FORTRAN Programs, Tsing Hua University Express, Beijing, 1995

[21] K. Khanafer and K. Vafai, "A critical synthesis of thermophysical characteristics of nanofluids," International Journal of Heat and Mass Transfer 54 4410–4428, 2011

[22] H.R Seyf and M.Feizbakhshi, "Computational analysis of nanofluid effects on convective heat transfer enhancement of micro-pin-fin heat sinks," International Journal of Thermal Sciences, 58, 168-179, 2012

[23] W.M. Kays, M.E. Crawford and B., Weigand, Convective Heat Transfer, 4th ed., McGraw-Hill, New York, Chap. 8, 2005

[24]. J. Koo and C. Kleinstreuer, "A new thermal conductivity model for nanofluids", Journal of Nanoparticle Research 6, 577e588, 2004

[25] R.S. Vajjha and D.K. Das, "Experimental determination of thermal conductivity of three nanofluids and development of new correlations", International Journal of Heat and Mass Transfer 52 4675-4682, 2009

[26] R. L. Hamilton and O. K. Crosser, "Thermal Conductivity of Heterogeneous Two Component Systems", I & EC Fundamentals, Vol. 1, pp. 187– 191, 1962

[27] J. C. Maxwell, A Treatise on Electricity and Magnetism, 2nd ed., Oxford University Press, Cambridge, UK, 1904

[28] S. P. Jang and S. U. S. Choi, "The Role of Brownian Motion in the Enhanced Thermal Conductivity of Nanofluids", Appl. Phys. Lett., 84, pp. 4316–4318, 2004

[29] L. Godson, B. Raja, D. Lal and S. Wongwises, "Enhancement of heat transfer using nanofluids e an overview", Renewable and Sustainable Energy Reviews 14 629-641, 2010

[30] H.R. Seyf, B. Nikaaein, 2012, Analysis of Brownian motion and particle size effects on the thermal behavior and cooling performance of microchannel heat sinks, International Journal of Thermal Sciences, 58, 36-44.

PUBLICATIONS

[1] S. Kim, Y. Zhang and J. Choi, "Entropy Generation during Thermally-Induced Oscillatory Flow in a U-Shaped Minichannel," Heat Transfer Research, Accepted, 2012.